ABSTRACT

Title of Document: ENERGY BALANCE, WATER BALANCE, AND PLANT DYNAMICS OF A SLOPED, THIN EXTENSIVE GREEN ROOF INSTALLED IN THE MID-ATLANTIC REGION OF THE UNITED STATES

Scott William Tjaden, Master of Science, 2014

Directed By: Associate Professor, Dr. David Tilley, Department of Environmental Science and Technology

Vegetated extensive green roofs can reduce peak runoff amounts during rain events. As the desire to install green roofs expands beyond roofs with little slope to those with steeper slopes, often found on residential homes, there is a need to understand how slope affects runoff. *WaterShed,* the University of Maryland's winning entry in the 2011 U.S. Department of Energy Solar Decathlon competition, is used as an applied research site where studies like the runoff analysis can be completed, while helping to promote and demonstrate environmental sustainability and energy consumption efficiency. Instrumentation installed on the roof will allow high-resolution data analysis, producing hydrographs. The research has related the sloped green roof to different moisture holding capacities throughout the different elevations, resulting in a unique energy balance for the installed green roof. The thin substrate did not significantly contribute to overall runoff reduction, rather it helped to reduce the overall peak runoff and elongate the runoff lag after a rain event. This living technology's performance over time in a new application to sloped roofs is crucial both to ensure regulatory standards are met and to provide feedback for future improvements to the design and technology itself.

ENERGY BALANCE, WATER BALANCE, AND PLANT DYNAMICS OF A SLOPED, THIN EXTENSIVE GREEN ROOF INSTALLED IN THE MID-ATLANTIC REGION OF THE UNITED STATES

By

Scott William Tjaden

Thesis submitted to the Faculty of the Graduate School of the
University of Maryland, College Park, in partial fulfillment
of the requirements for the degree of
Master of Science
2014

Advisory Committee:

Associate Professor, Dr. David Tilley, Chair

Associate Professor, Dr. Kaye Brubaker

Professor, Dr. John Lea-Cox

Dedication

I dedicate this research to my late grandfather, Robert L. Tjaden Sr., and to my ever-supporting parents, Robert and Linda Tjaden, and to my brother, Bobby Tjaden. They've taught me many life lessons that I base my own everyday life, and have provided endless support, love, and encouragement to me over the years. They've all helped me couple my love for nature and thinking creatively!

Acknowledgements

I would like to thank Pepco for its support during my Master's program, and continued support of applied research, educational outreach, and community engagement at the *WaterShed* Sustainability Center. I would like to thank Rob Stewart, specifically, who has provided care and guidance throughout the development of the Pepco WaterShed Sustainability Center.

I would like to thank my graduate advisor and mentor, Dr. David Tilley, for his support and encouragement of my ambitious projects and goals during my time at Maryland. I hope these projects live on, and I look forward to future collaborations!

I would like to thank Veronkia Zhiteneva, Isabel Enerson, and Rhea Thompson for their assistance in the reconstruction and equipment installation at the *WaterShed* house.

I would also like to thank the original student team that constructed WaterShed and the supporters who helped the construction of the *WaterShed* project be a success for the Solar Decathlon competition. These supporters include but are not limited to the Department of Energy, National Renewable Energy Laboratory, Pepco Holdings Inc., The School of Architecture Planning, and Preservation, The A. James Clark School of Engineering, The College of Agriculture and Natural Resources, Maryland Sustainability Fund, Maryland Water Resources Research Center, Maryland Custom Builders, Inc., and Whiting-Turner. Additional Sponsors can be found at: http://2011.solarteam.org/sponsors

Table of Contents

List of Tables

List of Figures

1. Introduction

As population size continues to increase, natural resources are growing scarcer as a result of unsustainable consumption. Continuous development and redevelopment contributes significantly to environmental impacts both directly and indirectly. Because of land development the natural flow of rainwater is obstructed as a result of increased installation of impervious surfaces (e.g., concrete, asphalt, and conventional rooftops) with relatively low albedo values, elevating surface reflecting value (Hilten, 2005), and high thermal conductivity, while urban areas suffer from the urban heat island effect (Wolf and Lundholm, 2008). Indirectly, the carbon footprint increases because the construction and operation of buildings create a high demand for energy relative to pre development periods.

While development is constantly occurring, a strategic integration of natural systems and the built environment is needed. Standards based on energy and water efficiency within and around buildings have been developed, through leadership from federally funded programs like Energy Star (U.S. Environmental Protection Agency, 2014), along with private programs including LEED (Leadership in Energy and Environmental Design) (Kubba, 2010) . These standards help to reduce the overall impact on the environment directly and indirectly, based on many influential factors, including: improved building envelope and mechanical performance, energy modeling performance (Kubba, 2010), and returning the hydrologic flow to predevelopment standards (MDE, 2000). While the design of these programs encourage initial installation of systems like green roofs, the overall performance is not evaluated over time, giving programs like Living Building Challenge an advantage to site specific performance and validation (McLennan, 2008).

Green roofs are an example of a technology that can help to mitigate both directly and indirectly the influences of our built environment. Green roofs provide a thermal mass given the soil substrate in which the plants are growing, while allowing rainwater to be stored in the media and consumed over time. Given the soil substrate that can retain stormwater, many areas, including some in Maryland, are recognizing this technology as a best management practice (BMP) while providing incentives for its adoption through tax rebates or rain tax reductions. The rain tax charges residential properties a set dollar value per area of impervious surface, trying to encourage the installation of Low Impact Development (LID) technologies. Currently, in Montgomery County, residential properties are eligible for up to $2,500 in tax rebates, on top of their reduced runoff tax, for installation of approved stormwater techniques, including green roofs, rain barrels, and porous asphalt, to help manage stormwater within the Chesapeake Bay watershed (Montgomery County Government, 2014). Manuals like the *Maryland 2000 Stormwater Management Design Manual* (MDE, 2000) help to provide specific design criteria for areas within the state of Maryland. Programs like this were implemented because of the U.S. Environmental Protection Agency's (EPA) mandate to reduce pollutants in the waterways to help improve Chesapeake Bay health (Chesapeake Program, 2014). Within the state of Maryland, House Bill 987, Stormwater Management – Watershed Protection and Restoration Program, was passed in 2012 in hopes of persuading local counties or municipalities to encourage residents to undertake protection and restoration efforts (Hucker, 2012). As more counties adopt programs for their residents to participate in, performance analysis of the various systems installed are crucial to ensure federal money is spent appropriately.

2. Green Roof Literature Review

2.1 Water Benefits

Green roofs are a form of bio-retention, which is implemented to mimic predevelopment hydrology, while improving the quality of water before it is discharged (He and Davis, 2011). The implementation of BMPs has a positive impact on the ecosystem; the goal is to maintain groundwater recharge and base flow, increase surface and groundwater pollution removal, protect waterways with erosion control, and reduce peak flow during storm events (Davis et al., 2009). Primary design elements taken into consideration for bio-retention systems include media depth and composition, underlay configuration, rainfall characteristics (including depth, duration, and intensity), vegetation, and local climate conditions (Davis et al., 2009).

Vegetation processes are one of the most influential performance variables, as they help to manage stormwater once it is absorbed in the substrate and is used through various plant processes. Different plants use water at different rates, primarily through evapotranspiration (ET), which is the movement of water vapor from the substrate by way of transpiration through the stomata of the plant's leaf (Zotarelli et al., 2013). These plant processes that contribute to ET depend directly on available energy (water movement and physical transformation of water to vapor energy requirement), water, surrounding conditions (i.e., solar radiation, air temperature, humidity, wind speed), and crop characteristics (Allen, Pereria, & Raes, 1998). These plant functions can be determined by the resources and environmental conditions presented to the plant (Perini et al., 2011), along with plant metabolism rates. Traditionally green roofs are planted with sedum due to their physiological and morphological adaptations present.

2.2 Energy Regulation

Green roofs provide numerous ecosystem services while directly influencing how energy is consumed and transferred within the roof as a whole (Oberndorfer et al., 2007). The thermal benefit of a green roof helps to regulate interior temperature, reducing the amount of energy needed to condition the space, dependent upon original insulation values of roof structure (D'Orazio, Di Perna, and Di Giuseppe, 2012). Vegetated roofs can be used in warm climates, by reducing the solar radiation absorption, or in cool climates, by adding a soil thermal mass layer depending on the overall thickness of substrate (Zinzi and Agnoli, 2012). Many variables contribute to this benefit, including, but not limited to, pre-existing insulation values of the structure, thickness of the green roof growing media, regional climate, and ratio of overall footprint of green roof to building size/height. Previous studies have concluded that during the summer the energy savings in cooling the interior of a noninsulated building with a green roof compared to the same building with a standard roof ranged from 15-49%, while for an insulated building the energy savings ranged from 6-33% (Santamouris et al., 2007). Ongoing research will provide a better understanding of how energy and thermal transfer are influenced by green roofs, given the site conditions, green roof types, and geographical location.

2.3 Thin and Sloped Influences

If the application of green roofs is spreading to residential settings, analyzing the performance of a sloped green roof is important given the average residential roof pitch is between 10 and 36 degrees. Commonly, a green roof system is applied to commercial flat roofs because of ease of installation and maintenance. Both for new and retrofitting construction, flat or sloped roofs can be converted into green roofs, particularly with thin,

extensive lightweight systems due to the lower structural support load requirements of the building (Carter and Butler, 2008). The average extensive green roof that is currently installed has a media depth typically between 4 and 6 inches (Hathaway, Hunt, and Jennings 2008), while intensive green roofs can range above 6 inches to several feet depending on desired plant selections. For a green roof installation on a steeper pitch, the roof would have to have additional structural supports, parapets or a grid pattern within the substrate, to support the downward force of the green roof materials. Because the instillation of lighter systems is intended for a wider application of buildings, the performance of the sloped roof is not yet determined; performance is extrapolated from the performance of flat roofs.

With the combination of a lighter, thin system and the varying slopes of residential homes, additional analysis of the water and energy performance is needed for existing residential applications. Analysis can provide valuable feedback to the industry, along with providing homeowners information about how the systems perform depending on the variables present. Performance data for new technologies and installation types are critical to state and local initiatives, providing feedback to increase performance analysis**.**

2.4 Vegetation Review

Most of the green roof systems installed are planted with *Sedum*, a succulent stonecrop that can handle times with adequate water stored within the substrate as well as periods of drought. The various types of *Sedum* perform differently (Cook-Patton and Bauerle, 2012). Specific *Sedum* varieties are usually chosen for local conditions, while plants self-select over time, and have seasonal year-to-year variations in color and biomass. It's important to see how the green roof systems are affected as growing conditions are influenced by slope and reduced substrate thickness. The different *Sedum* varieties respond differently to

the various micro-zones created within the system. Plant selection is crucial for this application, as the thin soil will promote periodic drought and rapid fluctuations of moisture within the soil media (Wolf and Lundholm, 2008). These processes in which plants consume water depend also on their physiology, which commonly include C3 and C4 plants that consume water and exchange gas within the stomata during the day when sunlight is available (Oberndorfer et al., 2007), while Crassulacean acid metabolism (CAM) physiology causes the plant to conserve water during the day and exchange gases within the stomata at night (Durhman, Rowe, and Rugh, 2006).

Sedum are CAM plants, plants able to adapt to water availability by fixing and re-assimilating CO_2 during nighttime (Cushman and Borland, 2002), while some have the ability to cycle to C3 during times of high available water. Understanding how the plants within the green roof system utilize water is crucial to determining the overall water and energy budget of the roof; thus the CAM physiology of the different species used for green roofs can help lead to more accurate representation of water and energy flows within green roof systems (Starry, 2013).

2.5 Research Objectives and Hypothesis

The overall goal of this research is to quantify the water and energy balances of a thin green roof system applied to a sloped roof in the mid-Atlantic region**.** I hypothesized that the performance throughout the elevation of the sloped roof will differ, with the lowest available water at the top and highest availability close to the bottom. As a result the different water availabilities will influence the plant processes. I proposed the analysis of standard ET modeling techniques (e.g., Penman-Monteith ET model) and compared them to measured conditions for a thin, sloped installed green roof. I hypothesized that the relationship between

the water and energy balances will help to quantify overall energy transfers within the system, influencing building performance. The information gathered will help validate the performance of the system, quantifying retention rates and reduced peak flow during rain events, while contributing valuable data to evapotranspiration models traditionally used for green roof applications.

2.5 Plan of Study

In the case of this research project a model residential home named *WaterShed* has a sloped roof with a thin substrate green roof. The roof was instrumented with sensors to monitor the energy and water fluxes during a 3-month period. Two different methods are to be used for determining ET, ET potential (ET_P), and ET actual (ET_A). The modeled ET is considered ET_P, as it is predicting ET given, site/surface conditions, and quantity of water the plants are utilizing. The ET_A is derived from the substrate moisture sensors between rain events, using the soil depletion method, with the assumption that inputs and outputs are zero and with the result that any loss in water is caused by ET. The change between substrate moisture measurements will equal change in substrate moisture and can be directly compared to the potential ET model. These ET measurements can then be used as variables within the water and energy budget for the roof to determine balances within the system.

3. Materials and Methods

3.1 Site Description

The green roof studied was on the south module of a sustainable house, *WaterShed*, built by a team of students and faculty from the University of Maryland for the U.S. Department of Energy's 2011 Solar Decathlon competition (Gensler, 2011). In addition to hosting a thin, sloped green roof, the championship house was designed to be energy self-sufficient, producing more energy than it consumed by using 9.2 kW of solar panels, and to manage its stormwater with an integrated system of green roof, constructed wetlands, large cisterns, and rain garden. Currently, Pepco, the regional power utility, owns the house and operates it as an educational sustainability center in Rockville, MD. *WaterShed*'s green roof is unique given its slope, thin growing medium, and northern orientation (Figure 3.1).

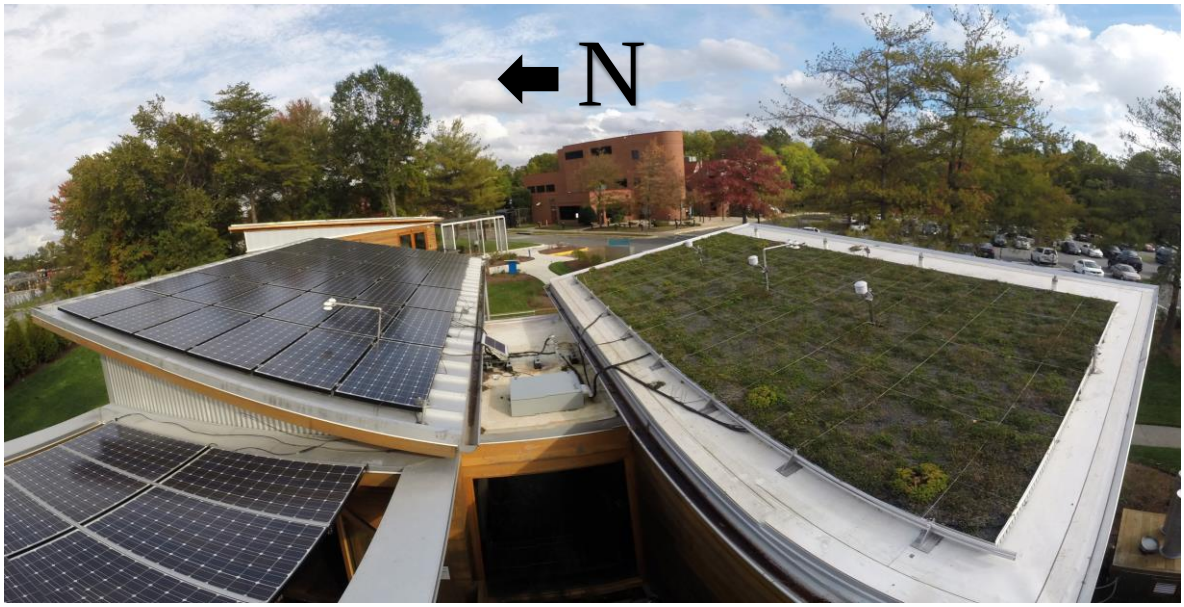

Figure 3.1 *WaterShed*'s green roof and PV panel layout.

Orientation and layout of *WaterShed*'s roof. These butterfly-shaped roofs help to concentrate water towards the center for rainwater storage.

The green roof is composed of a thin soil tray system, purchased from LiveRoof®, with an average soil depth of 2-1/2 in, weighing approximately 15–17 lbs/ft^2 (fully saturated). The 100% recycled polypropylene trays are 2 ft. long by 1 ft. wide and 1-3/4 in tall with an interlocking design allowing for easy installation. The substrate consists of 84.5% engineered shale, 4.5% sand, and 11% compost by dry weight. The original plant selection included *Sedum album* 'Coral Carpet,' *Sedum spurium* 'Dragon's Blood,' *Sedum spurium* 'Tricolor,' *Sedum reflexum* 'Blue Spruce,' *Sedum rupestre* 'Angelina,' and *Sedum sexangular 'Utah.'* Appendix A provides supplementary information for each of these sedum varieties. These sedum are a type of stonecrop within the *Crassulaceae* family ranging in shape, color, and growing preferences. The green roof covers 312 ft^2 (29 m^2) of the south (north-facing) module, while the north module (south-facing) is covered with about 400 ft^2 of solar panels (Figure 3.1). The green roof has a slope of 10 degrees and is waterproofed with white Thermoplastic Polyolefin (TPO) membrane, while the solar panel roof has a slope of 12.8 degrees, waterproofed with a standing seam metal roof.

Since the north-facing roof held the green roof, which is dependent upon sunlight, a solar incidence model (Figure 3.2) was prepared to ensure adequate sunlight would be available to the

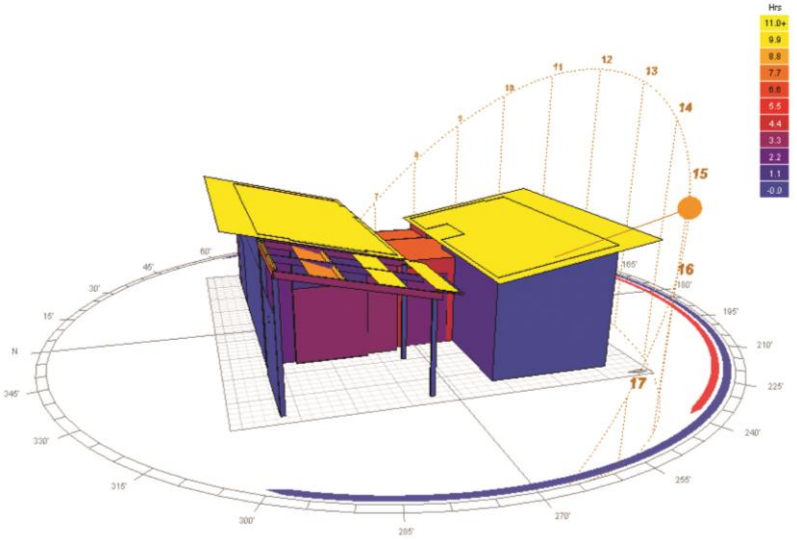

Figure 3.2 Solar incidence study of WaterShed.

Solar incidence for entire building given the orientation of WaterShed. Yellow colors indicate 11+ hours of sunlight, while dark blue represents reduced exposure.

green roof system. Figure 3.2 also shows this model given the average orientation within the sky throughout the day with early fall orientation shown. This initial analysis was crucial to ensure the slope and orientation for the house was suitable to have the green roof on this slightly sloped northern-facing roof, given the change in orientation of the sun throughout the seasons. As the sun drops in the horizon during winter months the roof will receive less direct sun exposure, while summer exposure will be more direct because of the sun's higher orientation in the sky.

The green roof sits on top of a TPO white membrane material, which has a border ranging from 15–20 inches between the vegetation and edge of the roof. This influences the runoff quantities caused by no retention (white roof) and undetermined retention (green roof). The underlying interior structure was designed to achieve the greatest energy efficiency through a complex layering of natural and engineered materials (Figure 3.3). This integration

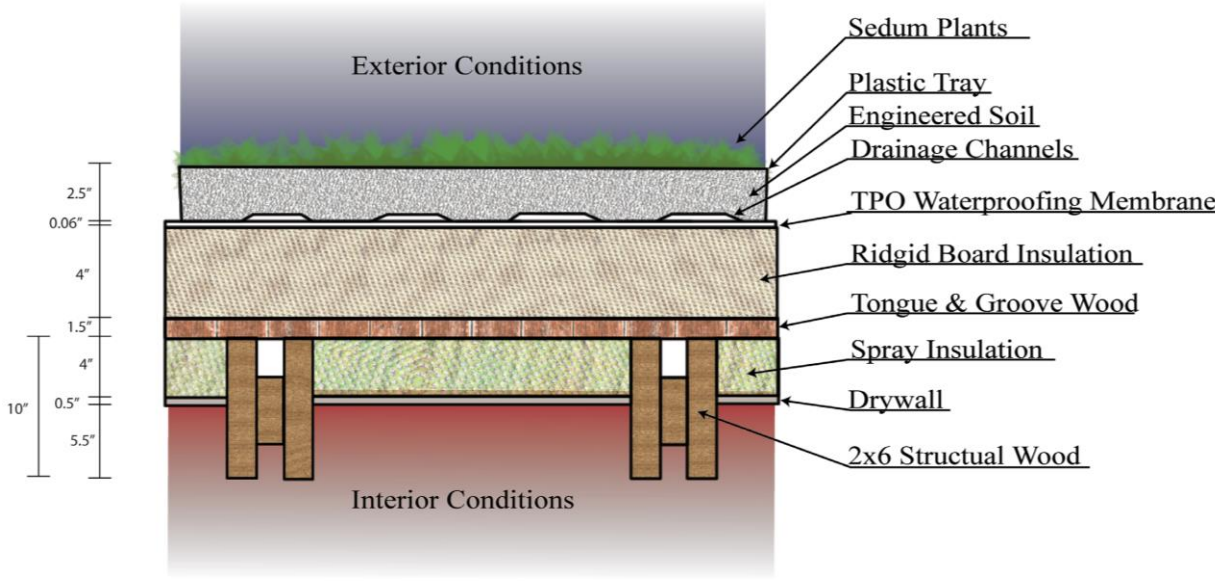

Figure 3.3 Layers within *WaterShed*'s roof.

WaterShed's unique structure and insulation have a combined insulation value of R-40+ in the walls, along with R-50 in the roof and floor.

R-Value units: $h \cdot ft^2 \cdot °F/Btu$

of different materials produces an insulation value of R-04 in the roof cavities. Currently, traditional American residential construction calls for R-30 in the roof (Northern American Insitution, 2014), while older homes can be substantially lower in R-value. Within Montgomery County, currently, the code requires all new residential homes to have an R-19 value in the floors, R-20 in the walls, and R-49 in the ceilings (Montgomery County Government, 2012).

Sensors were installed throughout *WaterShed* to help validate the performance of the various interior and exterior systems. Specifically, within the green roof, moisture and temperature sensors were installed to provide data for the moisture gradient moving up the sloped elevations of roof, temperature gradient through the layers of roof materials, and temperature of the surrounding exposed white roof. Overall data are collected from the dataloggers every 15 minutes, with varying sub-scan intervals. These sub-scans are averaged or totaled within the 15-minute window to provide the collected data. Of the 241 new data points installed on *WaterShed*, 183 were installed specifically in the green roof and are shown in Figures 3.4 through 3.7. These various zones were installed strategically to provide slope moisture and temperature data zones throughout the elevation of slope and the various layers of the roof. Supplementary information on the sensors used, broken up by the various systems, can be found in Tables B.1 through B.6 in the Appendix.

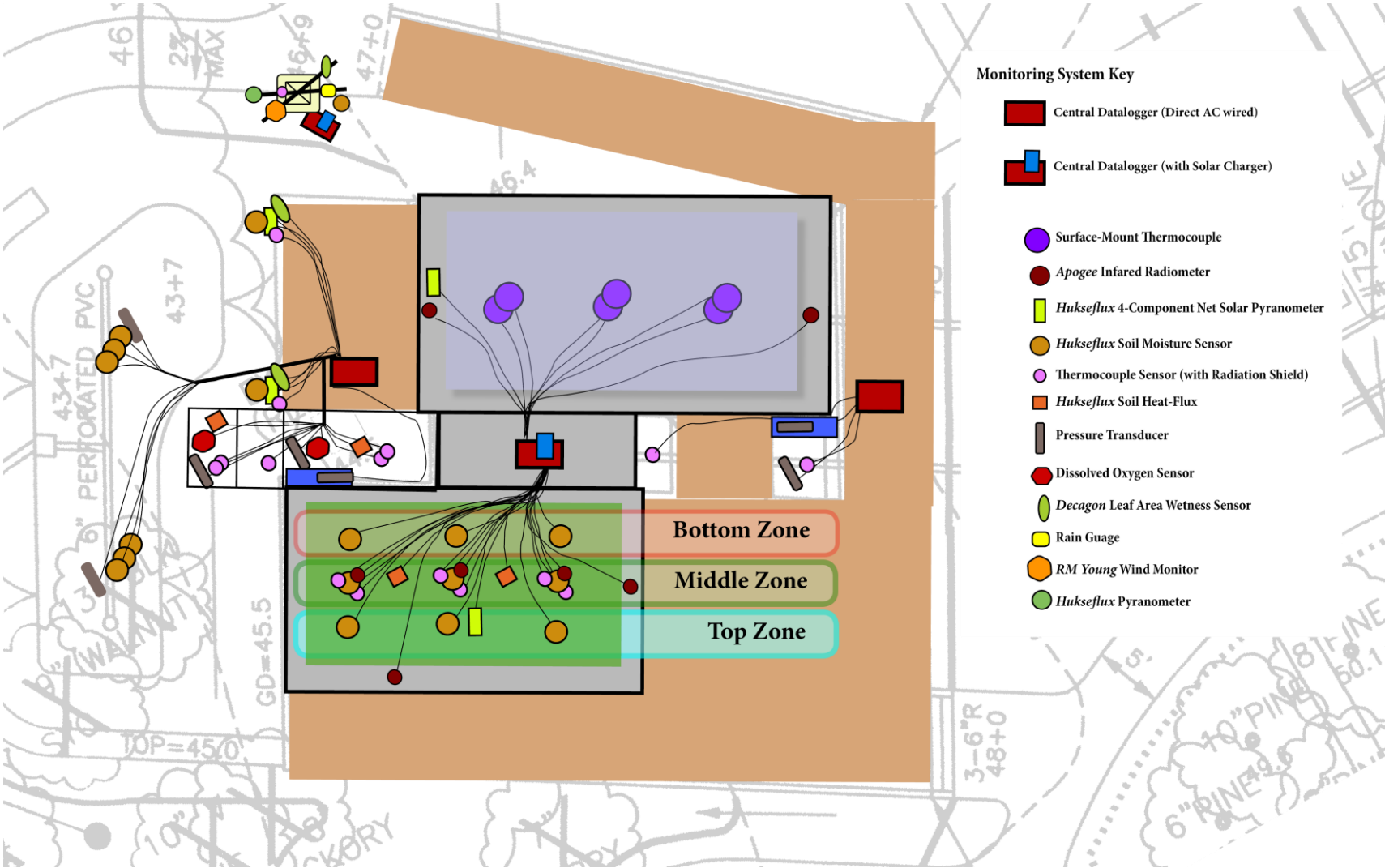

Figure 3.4 General sensor layout on the exterior of *WaterShed*. The different zones noted are explained in Figures 3.5-3.7

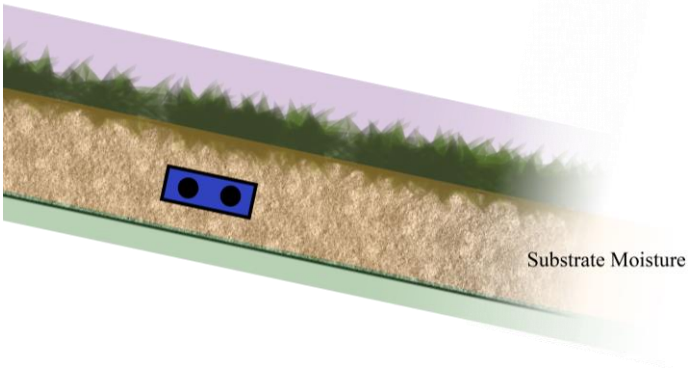

Figure 3.5 Top/bottom zone.

Consists of a soil *Water Content Reflectometer*, measuring volumetric water content (VWC) and temperature of the substrate. The sensor is installed approximately 1.5 in below surface of substrate with probes parallel to the roof and perpendicular to the slope.

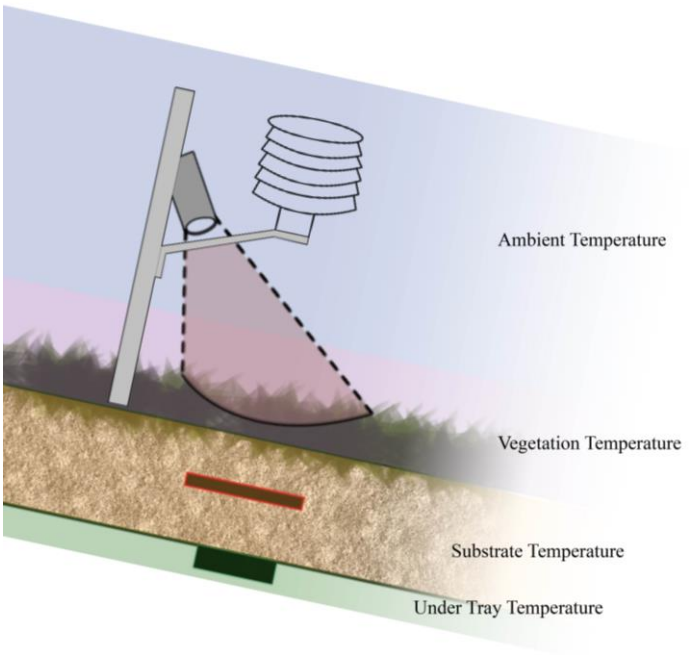

Figure 3.6 Middle zone.

Various levels through the layers of the green roof:

- Thermocouple with radiation shield—measuring ambient temperature (approximately 15 in off surface)
- Apogee infrared radiometer—measuring vegetation temperature (elevated approximately 13 in off surface)
- Water content reflectometer—measuring VWC and temperature of substrate
- Thermocouple—measuring under-tray temperature (directly under tray).

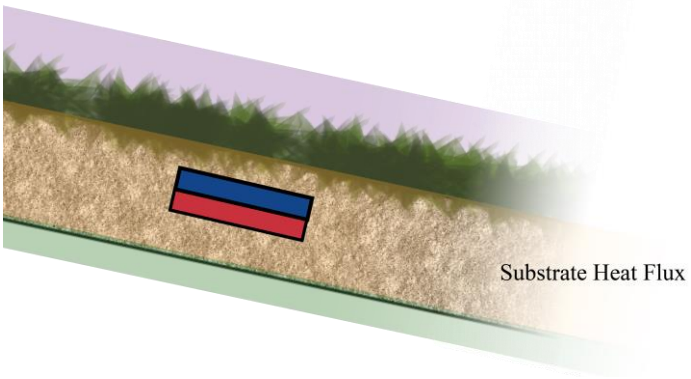

Figure 3.7 Middle zone.

Consists of a soil heat flux sensor—measuring energy transfer though the substrate. The sensor is installed approximately 1.5 in below surface (located in the middle zone)

3.2 Water Balance Measurements

Water balances, or water budgets, are established to determine the various fluxes of water within a system. These budgets can be applied to any system that handles water, ranging from an engineered system inside a building to a living system in nature. For this application at *WaterShed* a water budget will be applied to the green roof system, helping to quantify the changes in stored water over time.

The water stored and utilized by the green roof is extremely important, but can be influenced in many different ways depending on weather, plant conditions, and given site characteristics. Retention of rainwater helps to reduce the quantity of runoff during peak flow and runoff quantities of rain events, while also helping to improve water quality. Sensors were installed within the green roof to help quantify the capacity, during and after a storm, while also relying on a designed flume box. Figure 3.8 shows the cables under between the tray system.

Figure 3.8 Green roof sensor integration.

Live roof systems have an interlocking tray mechanism that enables the installed trays to overlap, preventing movement or uplift from wind. Sensor cables were positioned underneath the tray to reduce disturbance to green roof performance.

Equation Background

For a green roof analysis, the general water budget can be broken down to Equation 1.

$$P - RO - ET \pm \Delta SW = 0 \qquad \textbf{(Eq. 1)}$$

At the *WaterShed* site precipitation (*P)* was measured with the onsite high accuracy *Hydrological Services TB4* rain gauge. This allows the precipitation data to be used as a reference point for when the system is receiving an input (rain). Otherwise, during times of no precipitation the variables *P* and *RO* can be eliminated. *RO* is discussed in the next section. This leaves ET and ΔSW during times when no precipitation is present, allowing ET to be directly measured by the change within the substrate moisture over time.

The runoff variable of the green roof is crucial in determining reduced peak flow and total runoff retention volume, while helping to determine when the green roof substrate is losing moisture caused by runoff or ET. This runoff data will provide feedback for other variables and can be used as a benchmark point. The runoff flowing to the gutters can be measured in two different ways. The first uses designed flume boxes attached to the down spouts of the gutter, which record the rainwater flow coming off each roof (which is discussed in the following section). The other method uses the volumetric water content sensors within the substrate of the green roof, while looking at the soil depletion from the previous time stamp and upscaling the change of the volume to the entire roof. When the change in soil depletion is positive it is losing moisture, while negative numbers result in a moisture gain. With this being said, during a rain event the change would be negative and at the end of recorded precipitation the rate would switch quickly positive as the soil media is starting to decrease in soil moisture**.** Because of

limited retention space within the roof, the retention rate will depend on rain characteristics (e.g., intensity, duration), while also being dependent on antecedent conditions.

Since the green roof is not covering the entire north-facing roof, the white roof contributes directly to runoff, due to no retention (Figure 3.9), followed by the green roof contributing to runoff (Figure 3.10). Equations B.1-5 in Appendix B interpret the calculations for the volume upscaled to *WaterShed*'s roof footprint. During the time immediately after the rain stops the total north-facing roof has an elongated runoff timeframe caused by the short-term retention of the soil substrate of the green roof (Figure 3.11). During this time the precipitation is zero, the decreasing rate of soil moisture (ΔSW) can resemble measured runoff until a deflection point in the rate of decrease is reached. After this point the

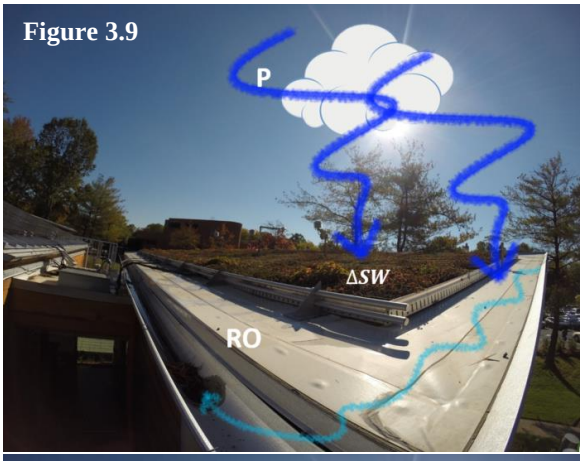

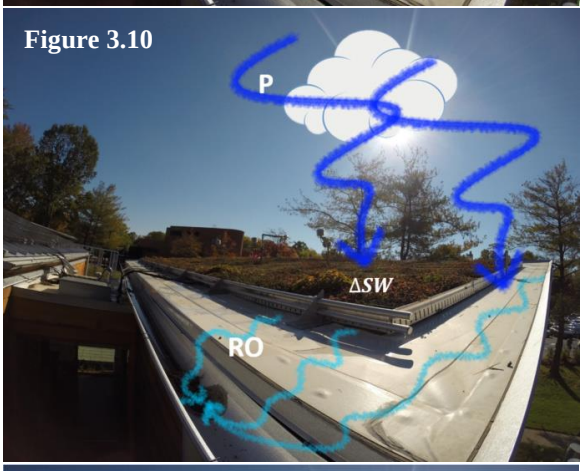

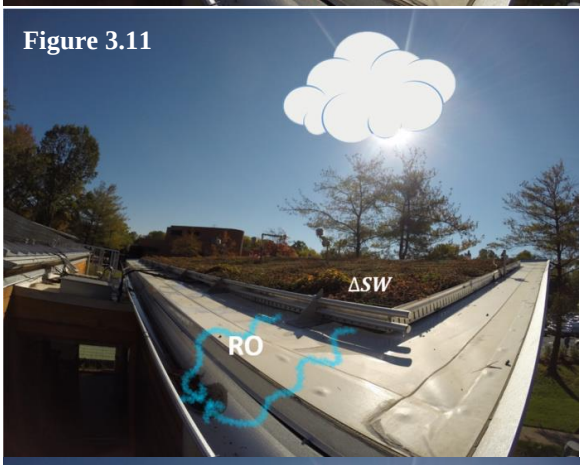

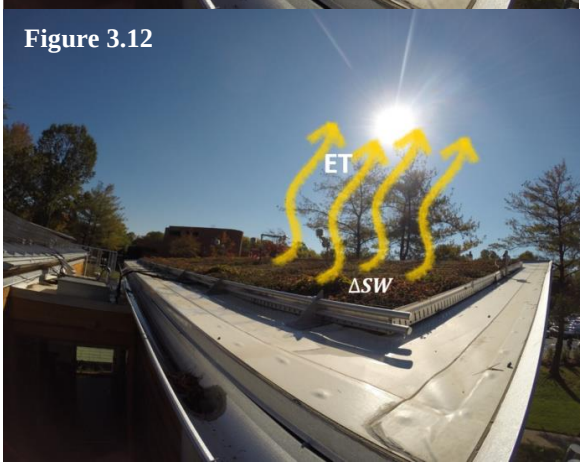

Figure 3.9 Animation of roof performance during initial rainfall. Runoff only from surrounding white roof.

Figure 3.10 Runoff from direct runoff and green roof.

Figure 3.11 Runoff from only green roof after precipitation stops

Figure 3.12 Animation of ET occurring

water pores will drain under gravity, contributing to overall runoff *(RO)*, eventually reaching field capacity. This deflection point indicates when the roof has released all the stored water to runoff in the gutter vs. the vegetation utilizing the water through the ET process (Figure 3.12). Until the slope of the change in storage reaches a deflection point, change in storage is still treated as runoff, but after that point *RO* can be eliminated. Traditionally, an average threshold was established that was based on time or on subjectively analyzing slope to quantify runoff periods. These methods can result in under and over prediction of ET rates and runoff volumes.

When observing the soil depletion over time (Figure D.5 in Appendix), we can notice diurnal fluctuations along with responses to precipitation events. When it rains the change in substrate moisture has a negative value. During times when the value is positive the moisture can either be considered runoff (i.e., draining out of the substrate) or be utilized by the plants drawing moisture out of the system (Figure 3.13). Occurrences when the change in substrate is negative during times when no precipitation is present include condensation (dew) forming on plants during night hours, resulting in added moisture to the system.

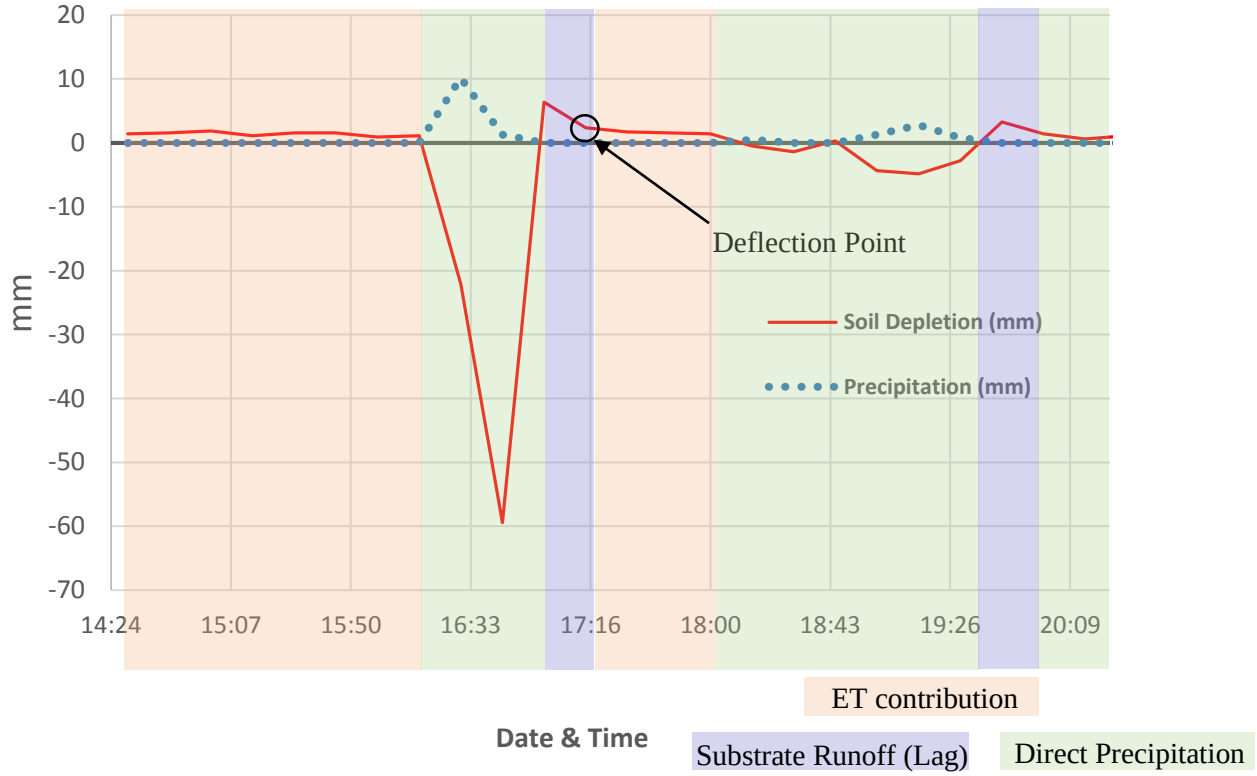

Figure 3.13 Hydrograph in comparison to change in moisture of green roof substrate September 2, 2014, rain event.

During times of precipitation, change in substrate becomes negative, as moisture is being absorbed into the growing media, and, immediately after precipitation stops, this change becomes positive because of drainage and of eventual contribution from ET.

Figure 3.13 shows how the readings will switch to positive immediately after a storm as short-term storage drains out into the gutter system. During times when precipitation is present and during the threshold set after the storms, the change in soil moisture is considered runoff and is not used. During rain events the soil depletion method can be an indicator of how much water is falling on the roof. This increasingly negative correlation represents a higher rate of rainfall given the positive change in volumetric water content. The change in VWC within the substrate was used to populate the soil depletion numbers, converted to millimeter to compare to total precipitation (mm) during the 15 minute interval.

Runoff Flumes for WaterShed

In order to get an accurate reading for the runoff from the respective roofs a runoff flume was developed to record large and small quantities of rainwater flowing off the roof. A 100 year storm was used as the max flow, given a rainfall of 7.2 inches for the Rockville, MD, area (MDE, 2000). The purpose of the flume is to determine quantities of water coming off the roof to determine peak flow reduction, overall runoff lag period after the rain stops, and total rainfall reduction, while providing an accurate time stamp following the termination of a runoff to confirm fluctuations in the moisture of the substrate are caused by runoff or direct ET (Using the volumetric water content [*VWC*] sensor).

Since the three roofs on *WaterShed* are different sizes—one has the green roof while the other two are impervious—we had to consider taking into account peak flow coming off the roof along with the slow release of water coming from the green roof after a storm. After some preliminary research of previous methods used for green roof runoff analysis, we concluded that a method had not been developed for a complete roof analysis both handling high-intensity storms, while capturing small quantities of runoff. Tipping buckets had a higher accuracy but for smaller quantities of water, which would be perfect for a lab-based scenario; however, they could not handle peak flows during average-sized storms. The goal was to develop a mechanism that measured peak flow and delayed discharge from the roof, by attaching a flume mechanism directly to a downspout relatively small in size. The development of the flume started with a box that would attach to the bottom of the downspout, made of the same galvanized aluminum material, and which housed a weir inside (V-notch that can relate height of water within the V to a given flow rate). A pressure sensor would record the water level as the runoff flowed through the V-notch. Traditionally, weirs have been used in much larger-scale applications (stream flow

analysis) compared to what was needed specifically for *WaterShed*. To start I looked into the design of the flumes and how they could be integrated unnoticeably into *WaterShed*'s design for peak flow rate data off the respective roofs. The V-notch weir equation was used (Eq. 2), which is traditionally used as a flow rate analyzer for an open channel stream (Moore, 1975).

$$Q = 4.28 * C * \tan\left(\frac{\theta}{2}\right) * (h + k)^{5/2} \qquad \textbf{(Eq. 2)}$$

Where:

Q Discharge *(cfs)*

C Discharge Coefficient *(d.u.)*

θ Notch Angle *(deg)*

h Head *(ft)*

k Head Correction Factor *(ft)*

(U.S. Department of the Interior, 1997)

Table 3.1 Storm Sizing Calculation for Flume.

Predicting flow rates through various angled V-notches given the respective roof sizes.

The V-notch angle (θ) is determined by the peak flow and desired height. A taller height

	Rain Depths for 24-Hour Storm Events					
	1 yr 24 hr		10 yr 24 hr		100 yr 24 hr	
	2.6 in		5.1 in		7.2 in	
Green Roof	0.0304	*CFS*	0.0596	*CFS*	0.0841	*CFS*
PV Roof	0.0386	*CFS*	0.0756	*CFS*	0.1068	*CFS*
Bathroom	0.0048	*CFS*	0.00943	*CFS*	0.0133	*CFS*

***Green Roof*:** 504.59 ft^2 (72,659.52 in^2) ***PV Roof*:** 640.65 ft^2 (92,253.60 in^2)

***Bathroom Roof*:** 79.89 ft^2 (11,505.46 in^2)

will allow the angle to be smaller resulting in a greater elevation change, which will produce

more accurate flow data. To start, calculations were completed to determine the peak flow coming off the roofs and the required angle of the V-notch, due to the different sizes and retention rates of the respective roofs. Table 3.1 shows the steps taken to determine what size storm the box angles could handle. We obtained information about rain depths associated with storm event years from the Maryland Stormwater Design Manual, specifically for Montgomery County (where the *WaterShed* site is located). The storm events were applied to the respective roof sizes and roof surface type which resulted in a predicted flow.

The calculated flow rate was then applied to equation 3, several standard angles, and the equation was solved for *h*. The angles were the dependent variable for this equation, as they determine the height of water level in the flume box, helping to ensure the size of the designed box would be tall enough to handle the storm's flow with the given V-notch angle. The angles for each box were adjusted until the height was within the previously determined dimension of the box. The final angles determined for the three flume boxes were: Green roof 50°, PV roof 70°, and bathroom roof 40°. Appendix F shows the detailed drawings for each of the flume boxes. The water would fill up to the bottom of the V-notch, which would act as the base height until a storm event occurred and then increase in height as runoff started. This base height would stay relatively close to the bottom of the V-notch between rain events due to no evapotranspiration (covered box), leaks within box eliminated, and no other inputs.

As the intensity of a storm increases, the overall height of water will increase within the box at a non-linear rate due to the V shape of the water outlet, letting a higher quantity of water exit during higher rainfall events, while being able to measure smaller events or lags in runoff more accurately. All the variables within the V-notch weir equation are constants except for the height of water, which is measured above the bottom of the V (baseline). The variables *K* and *C* are dependent upon the angle of the V-notch (calculation shown in Appendix C). In order to measure this the pressure transducer data must be subtracted by the baseline measurement (constant), which will give you the height above the V-notch, resulting in a flow rate. Figure 3.14 shows the various heights described here, while the head above the V-notch is the desired measured point needed and only available during storm events.

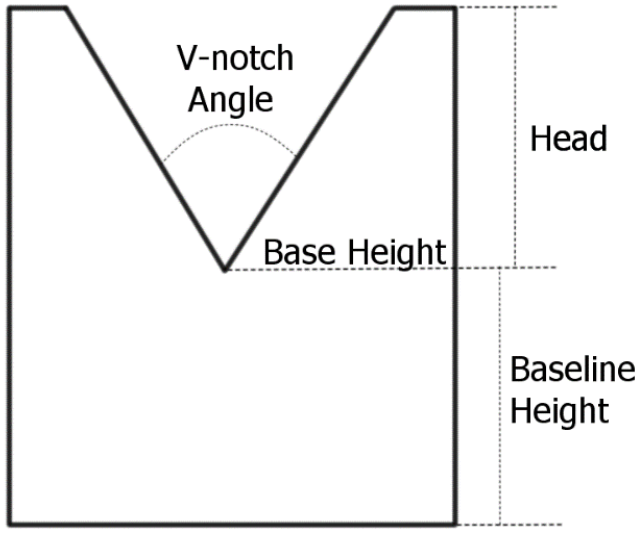

Figure 3.14 Labeled flume diagram.
One of these inserts per flume box, with the angle the only variable changing.

Design

For the *WaterShed* site we needed a box that would be able to attach to the gutters of the house itself, so the design of the box would allow the gutter to come into the box without losing any water. In Figure 3.15 the different sections of the box are displayed. The water entering the flume box would come from the gutter to the far left and contribute to the volume of water inside the box. The water would then flow under a baffle, which helps reduce the disturbance of the water as it flows through the V-notch, while allowing water to flow underneath. Once on the other side the rainwater has the opportunity to flow through the V-notch, depending on the rate of water entering the box. And the water level is determined by the pressure transducer at the bottom of the box, providing data for the overall flow equation.

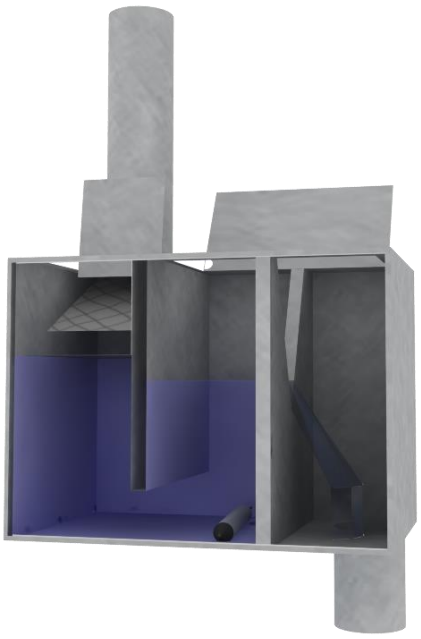

Figure 3.15 Flume rendering.
Cross-sectional view of flume showing back baffle and V-opening.

Flume Calibration

Due to irregularities between the sensors' water levels readings, a flow calibration was undertaken to ensure the height given by the pressure transducer corresponded to the correct flow rate coming through the V-notch. To accomplish this the water hose available onsite was set to various flow rates and put through the flume box itself. Table 3.2 shows the different flow rates achieved by the hose and the correction factor taken into account for each of the respective flume boxes.

We achieved the flow rate from the hose by slowly turning on the hose valve and measuring the flow rate at 8 different flows. Two timers measured the time it took to reach a volume of 1 liter within a measuring device (Figure 3.17). This took place a total of 3 consecutive times for the respective flow rates, and we averaged the 3 measurements. Table 3.2 and Figure 3.16 show these combined averages for each of the different hose flows.

Table 3.2 Flume Calibration Flow Rates.

Green roof flume box initial readings for flow rate after initial heights were recorded.

Sensor Height (mm)	Corresponding Flow (CFS)	Hose Flow (CFS)
168.7	-0.00238	0.009957
172.2	-0.00304	0.0096
145.8	-0.00037	0.00184
150.6	-0.00063	0.00272
156.6	-0.00109	0.00398
159.3	-0.00131	0.00457
163.4	-0.00179	0.00582
166.2	-0.00213	0.0065
y = -3.146 x + 0.0006		

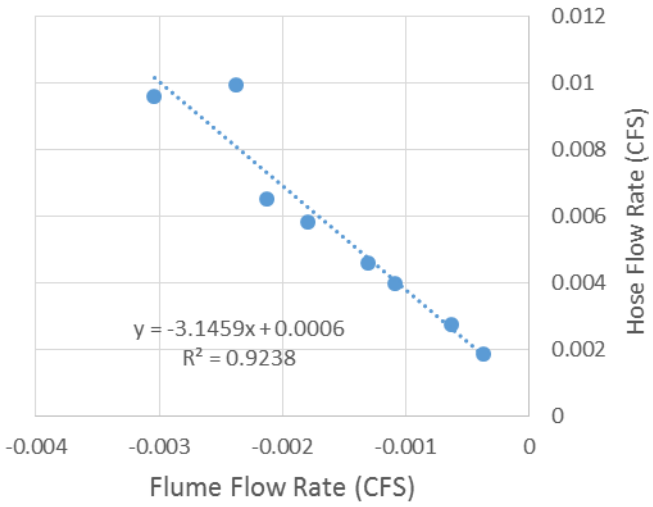

Figure 3.16 Linear regression calibration for flume Correction factors returned from this linear regression, which were used for equation 3.

Figure 3.17 Testing hose flow before flume calibration.

Once these correction numbers were determined for each flume, the correction multiplier and y-intercept were added to the respective flow rate equation for each of the flume boxes. This helped to improve the accuracy of the flow due to a variation within the water level sensor from the various flumes. Once these correction numbers were added another flow test was completed to validate that the values added were accurate, having a correlation of 90% or higher (results are found in Appendix H).

Water Balance Conclusion

Equation 1 is manipulated to solve for ET, as the other variables are easier to quantify during periods of precipitation. ET, of interest during times when it is not raining, can now be computed by using the change in storage over time (Marasco et al., 2014). The data become more accurate as the average time intervals become longer (greater than 7 days) because of small changes within the substrate that are hard to traditionally quantify (Allen et al., 1998).

ET_A was estimated from the soil depletion methods, which requires that P and RO are zero in *Equation 1*. RO was known to be zero when the flume was reading zero. This usually occurs within a few hours following the termination of a rain event.

3.3 Energy Balance Measurements

The energy balance of an ecosystem, such as a green roof, includes the shortwave and longwave radiation, sensible heat exchanged with the atmosphere, latent energy of evapotranspiration and conduction of heat through the substrate (Eq. 3). The attributes of an ecosystem (e.g., percentage of area covered by vegetation, leaf area index, leaf color) influence each of the energy flows in the energy balance. The latent energy associated with transpiration is typically a large part of the energy balance and major pathway for removing heat created by solar and longwave absorption.

$$R_n - G - \lambda ET - H = 0 \qquad \textbf{(Eq. 3)}$$

Where:

R_n	Net radiation
G	Soil heat flux
λET	Latent heat flux
H	Sensible heat

(Takebayashi and Moriyama, 2007)

At the *WaterShed* site the net radiation (R_n) was the sum of net shortwave and net longwave radiation, while soil heat flux (G) was measured directly within the green roof substrate, while ET was calculated through the water balance equation discussed in Section 3.2

or through a standard model. This leaves sensible heat (H), for which equation 2 can be solved to estimate (see Eq. 3b). Figure 3.18 helps to visually show these variables, while Figure 3.19 breaks down the net radiation variables.

$$H = R_n - G - \lambda ET \qquad \textbf{(Eq. 3b)}$$

The energy balance in Equation 3 assumes that the change in heat stored is negligible, which is justified over a 24-hour period because the change in heat stored is small in comparison to any of the individual flows during that period. Since H was not measured with any instrumentation, *Equation 3* was solved for H to derive *Equation 3b*.

Equation 3b will help understand how energy is used within a green roof itself, while seeing what benefit it contributes to the overall performance of the house (Allen, Pereria, and Raes, 1998). The energy balance equation looks at inputs coming into

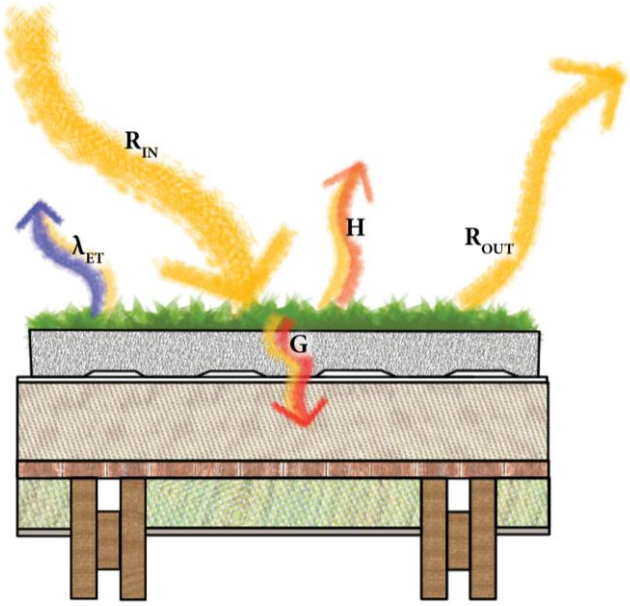

Figure 3.18 Visual flows of energy balance equation variables.

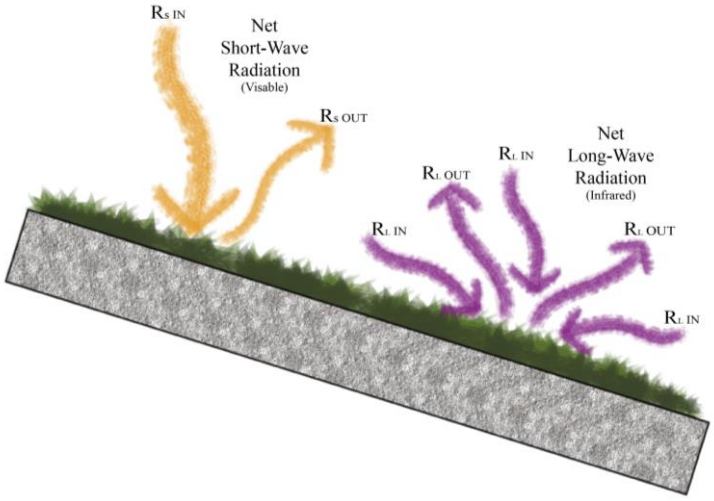

Figure 3.19 Net radiation illustration.

Downwelling radiation is entering the green roof, while upwelling radiation is leaving the green roof.

the system, solar and longwave radiation, while the other variables utilize the energy. (Specific instrumentation can be found in Appendix B). The net radiation sensor used took into account the sum between net shortwave and net longwave on the roof. For this research project net radiation and soil heat flux are measured at a 15-minute interval directly through Campbell Scientific instrumentation (Appendix B). We can calculate ET multiple ways depending on what variables are measured. The water balance is approach discussed in Section 3.2, of the traditional method for modeling ET rates with FAO (Food and Agriculture Organization of the United Nations) methods (Allen, Pereria, and Raes, 1998).

The FAO equation is based on the Penman-Monteith model and takes into consideration standard localized meteorological data, which are often obtainable but depend on site. In 1948 Penman computed this equation with the combination of the energy balance and mass transfer methods for the original open pan evaporation method, using local climatological data of sunlight, temperature, humidity, and wind speed. Over time this method was progressively developed, adding other variables including reference crop resistance factors (Allen, Pereria, and Raes, 1998). Empirical formulas have been developed around a crop reference, used to best represent ET of the desired crop. Many of these formulas have been tested in various conditions and locations in which the FAO Penman-Monteith was recommended as the standard method for defining reference ET in 1990 (Allen, Pereria, and Raes, 1998). This crop reference takes into account the resistance, crop height, crop roughness, reflection, ground cover, and rooting characteristics for different types of plants under the same normal environmental condition (Allen, Pereria, and Raes, 1998).

Penman-Monteith Equation:

$$ET_p = \frac{0.408\Delta(R_n - G) + \gamma \frac{Cn}{T+273}(e_s - e_a)u_2}{\Delta + \gamma(1 + C_d u_2)} \qquad \textbf{(Eq. 4)}$$

Where:

Δ	**Slope of saturation vapor pressure curve**		**kPa/°C**
	Dependent on temperature sensor	*°C*	
R_n	**Net radiation**		**W/m²**
	Net radiometer	*W/m²*	
G	**Heat flux density to the soil**		**MJ/m² day**
	Soil heat flux sensor	*W/m²*	
γ	**Psychrometric constant**		**kPa/°C**
	Dependent on atmospheric pressure	*kPa*	
Cn	**Numerator constant (depends on crop reference)**		**D.u.**
	Constant		
T	**Mean daily temperature**		**°C**
	Temperature sensor	*°C*	
e_s	**Mean saturation vapor pressure**		**kPa**
	Dependent on temperature sensor		
e_a	**Mean actual vapor pressure**		**kPa**
	Dependent on humidity	*%*	
u_2	**Mean daily wind speed**		**m/2**
	Wind speed/direction sensor	*m/s*	
C_d	**Denominator constant (depends on crop reference)**		**D.u.**
	Constant		

(Allen, Pereria, and Raes, 1998)

Appendix F contains supplemental information to support subcomponents and variables of the Penman-Monteith equation.

The Penman-Monteith equation (Eq 4) is traditionally analyzed for a 24-hour period by averaging the daily values of the various variables (Lovelli et al., 2008). We generally observe ET over longer periods of time to see overall trends vs. detailed performance for individual days. The variables used for the equation can sometimes be difficult to populate for various sites because of data resolution and availability. When planning the monitoring system installed in *WaterShed* at the final site parameters, contributors within the various equations, such as the

Penman-Monteith, were taken into consideration along with location and what interval was appropriate**.**

3.4 Green Roof Vegetation Assessment

To assess the green roof, measurements for both leaf area index (LAI) and percentage of vegetation cover were done during the data collection period. These assessments measure the biomass changes of the plants over time and can relate other site specific measured variables to these changes over time. The LAI is commonly used to measure the canopy density rather than simply area covered. A 1 m x 1 m square with 1-inch intervals was made, where we randomly selected 5 points within each quadrat to measure LAI. A point was selected by randomly selecting an *X* coordinate and a *Y* coordinate (Figure 3.20). At this coordinate a count was done for the number of leaves touching the object inserted through the media. Within each of the 9 zones on the roof (Figure 3.4), 5 points were chosen (from the randomly generated coordinates) per data period. This number was then divided by the measured area of the quadrat (1 m^2) to yield the zone LAI (number of leaves per area).

Figure 3.20 Grid pattern used for measuring LAI, 1m x 1m in size.

To assess percentage of cover of the roof, we took photographs of each quadrat within zone. We analyzed the pictures using a software called *ImageJ,* which enables the user to trim and crop an image and select a certain color spectrum to focus on an area of vegetation only. These color spectrums were determined by changing the hue, saturation, and brightness of pixels to select, agreeing upon thresholds that select the greatest area of vegetation. The software computes the pixel quantities for the total area and the area of vegetation, providing a pixel ratio, which represents percent cover (Carter and Butler 2008). This is a method used for other percent cover applications along with other analyses; methods can be found in Appendix E. Depending on the season the color spectrum of the canopy will change, which will determine which colors to analyze in the software.

3.5 Data Collection

The data collection period for this thesis was June 18 through September 15, 2014, which in part was dictated by when the data collection systems were installed. However, the data collection is ongoing so long term research can be conducted. For this thesis the data collection was stopped at midnight on September 15th.

4. Results and Discussion

4.1 Water Balance

Each of the 30 day periods during the data collection period received above average rainfall (Table 4.1). Daily precipitation events were mostly evenly distributed throughout each month with the exception of a relatively dry 2 weeks in late July (see Figures D.1–D.5 in Appendix). Since the substrate is 63.5 mm thick with an average porosity of 25%, the result is a 15.8-mm potential. Both organic matter and root density decreases the overall water storage, which contributes to the 25% porosity. Given the variability in rain events, the time between rain events is the biggest influence on how much of that 15.88 mm of rain is retained within the substrate. A significant amount of rain fell at the location during the summer compared to monthly averages in past years.

Table 4.1 Total Precipitation and Mean Daily Site Conditions.

Total	June 16–July 15	July 16-August 15	August 16-September 15	Average
Precipitation (mm)	154.94 (6.10 in)	130.8 (5.15 in)	112.27 (4.42 in)	398.02 (15.67)
Historical Precipitation (mm)	*88.65 (3.49 in)*	*73.66 (2.9 in)*	*97.28 (3.83 in)*	259.59 (10.22)
Mean Daily				
Total Precipitation Volume (m^3)	0.44	0.33	0.24	0.34
Runoff Volume (m^3)	0.40	0.31	0.21	0.31
% Retention	9.69%	7.01%	11.41%	9.37%
ET (mm/day)	0.27	0.19	0.24	0.23

This correlation shows that with a moisture increase the rate of ET also increases. This reduced rate of ET with lower water availability is crucial to note within the performance of the system. This can mostly be attributed to the Sedum plants and their ability to conserve water during periods of low available water and shift to higher consumption rates during times of high available moisture. When using models to predict ET, the performance of the plants and exposed soil is drastically influenced by not included variables of available moisture and vegetation conditions within the system. The plants have varying rates of transpiration, while the evaporation of moisture changes with exposure.

ET is highly dependent upon available moisture within the substrate for the plants in the system to utilize. The linear regression in Figure 4.1 shows the strong positive relationship (R-

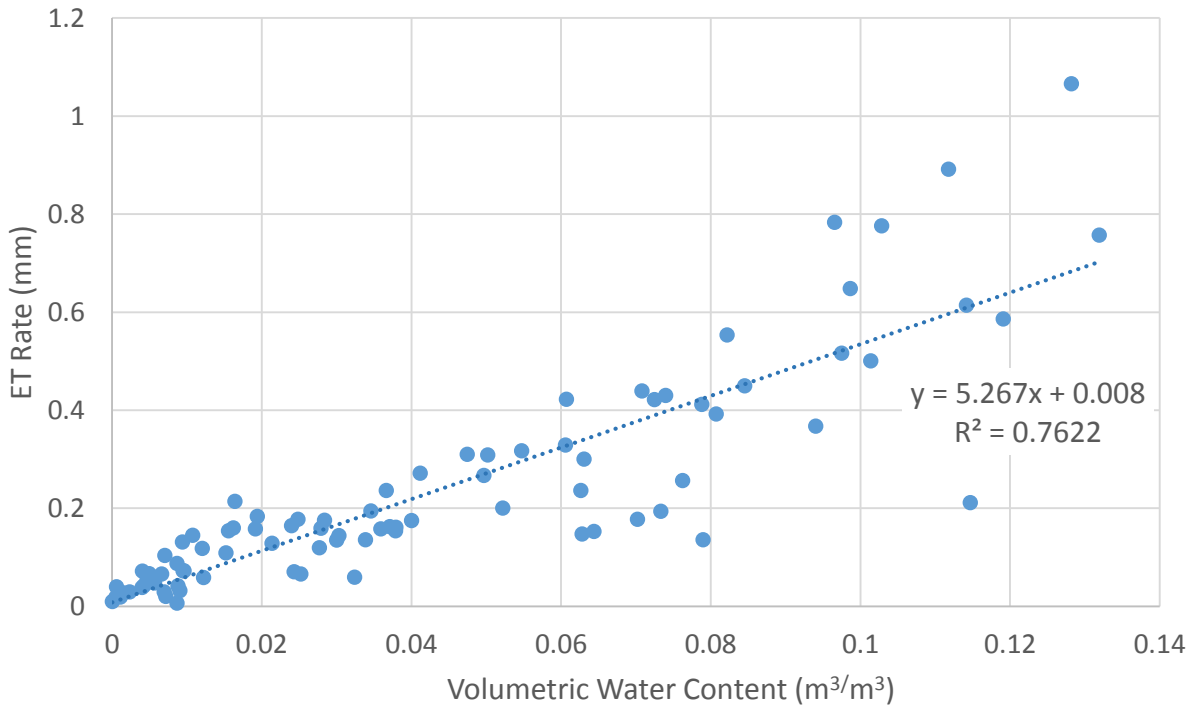

Figure 4.1 Effect of VWC on ET during data collection period.

Mean hourly correlation between available water and ET rate during entire data collection period. (Rain threshold applied.)

squared value of 0.77) between the moisture and ET rate. Previous studies have validated the correlation between lower ET rates and lower availability of soil moisture (Marasco et al., 2014). With *Watershed*'s thin green roof system, it was able to hold less moisture than a 100 mm thick extensive green roof, having an hourly ET rate of 6.4 mm/day during July, while *WaterShed's* green roof was around 4.49 mm/day. The higher average rate of ET is a result of more available moisture within the substrate.

Figure 4.2 shows an 11.5mm precipitation event on September 6, 2014, while the starting VWC average was 0.037 m^3/m^3, and 91 hours since the last rain event. During this event the green roof provided a 15 minute delay in runoff, a 44% reduction in peak flow, and a 1.5 hour runoff lag.

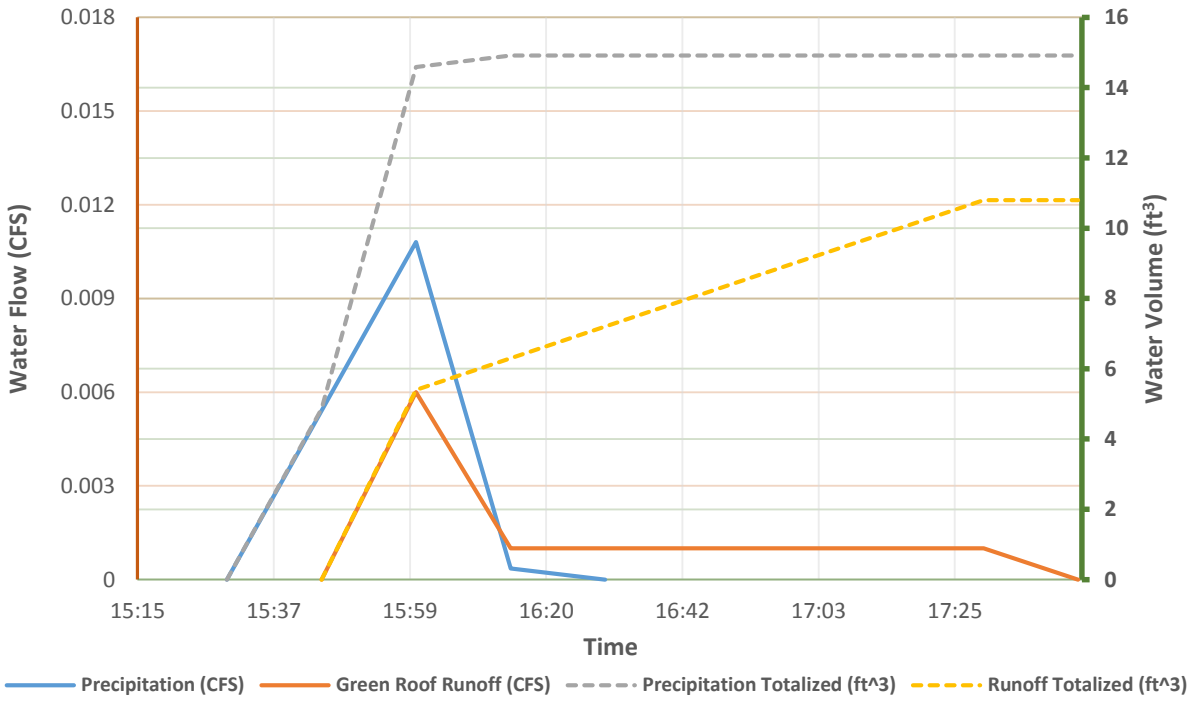

Figure 4.2 Hydrograph for the green roof runoff.

September 1, 2014, rain event -- 11.5 mm total Instantaneous runoff flow rates and totalized runoff volumes for one rain event, showing reduced peak flow and elongated runoff period after rain event.

Figure 4.3 shows the hydrograph from *WaterShed'*s green roof during an 11.5-mm rain event collected by the flume weir. The rainfall lasted for an hour. This retention rate is highly dependent upon the soil thickness, and slope, with *WaterShed*'s thin tray system having minimal storage capacity. The retention rate is also influenced by antecedent conditions, where the roof's substrate could be more susceptible to accept moisture during precipitation if dry compared to times when the substrate is close to saturation. Figure 4.3 shows a rain event that occurred on September 1, being 21.5 hours since the last rain event and with the average VWC reading before precipitation started 0.078 m^3/m^3. The rain lasted around 45 minutes. If the green roof started out with a higher volumetric water content there would be an overall lower total retention, due to lower moisture retention cavities. While if the volumetric water content were to start

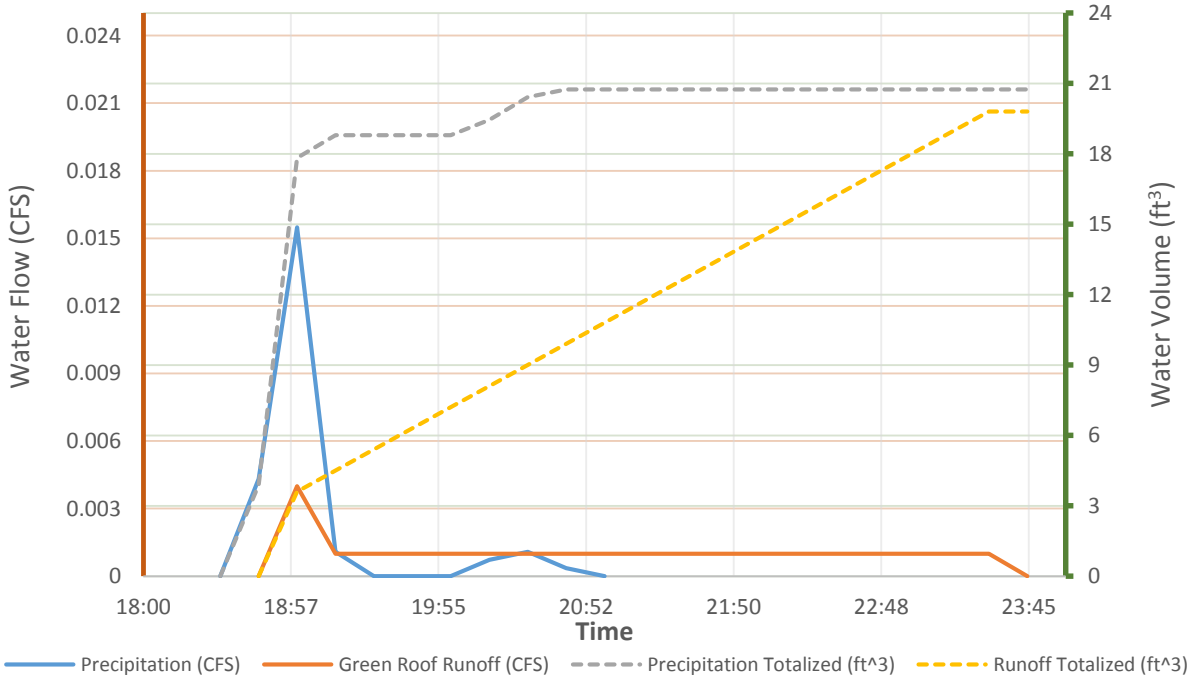

Figure 4.3 Hydrograph for the green roof.

September 6, 2014, rain event -- 16.25 total. Runoff flow rates and totalized runoff volumes for one rain event.

lower around 0, there would be a greater demand within the moisture retention cavities to be filled, resulting in an overall larger retention.

During the rain event, the green roof provides a 15-minute delay in runoff, a 67% reduced peak flow, and a 5-hour runoff lag, while only sustaining a 4.5% runoff retention. This rain event's intensity may have caused more water to become instantaneous runoff due to a pooling effect on the roof. The starting volumetric water content was around 0.078 m^3/m^3. Although the total retention was only 4.5%, the reduced peak flow is a great indicator that the rainwater was absorbed, coinciding with the long runoff lag.

Since the total retention is much lower than on thicker roofs, the anticipated goal of this thin system includes short-term retention in order to dry out before the next storm event. With this being said, the green roof is managing the peak flow vs. reduction in overall rainwater volume. This can provide feedback that every green roof and installation are different, given their different hydrologic performance.

4.2 Flume Results

Using a new method for measuring runoff we wanted to see the correlation between the data collected from the flume and the soil depletion method collected with the VWC sensors. We compared these methods for several storm events (Figure 4.4). Based on the R-squared value of 0.51 there is a correlation between the two runoff-measuring techniques. In comparison to a perfect correlation (1:1 line shown) on average the flume underpredicted during times of low precipitation, while overpredicting during times of high rainfall in comparison to the soil depletion method. Because of flume calibration issues the rainfall events measured by the flume are limited to these 11 storm events for this thesis. The 11 storms are shown in Table 4.2. With this lower accuracy during times of lower precipitation, the pressure transducer sensor may not

be as accurate with it not picking up smaller changes in water level during the lag period. Future analysis of the flume data along with further soil depletion data collection is recommended for a more transparent understanding of the flume performance during the rain events. Alternatively, it could be that the soil depletion method over predicted runoff for small events, under certain conditions, following the cessation of precipitation, soil depletion can be due to runoff and ET. If ET was large, then the *RO* estimate by soil depletion would overestimate *RO*.

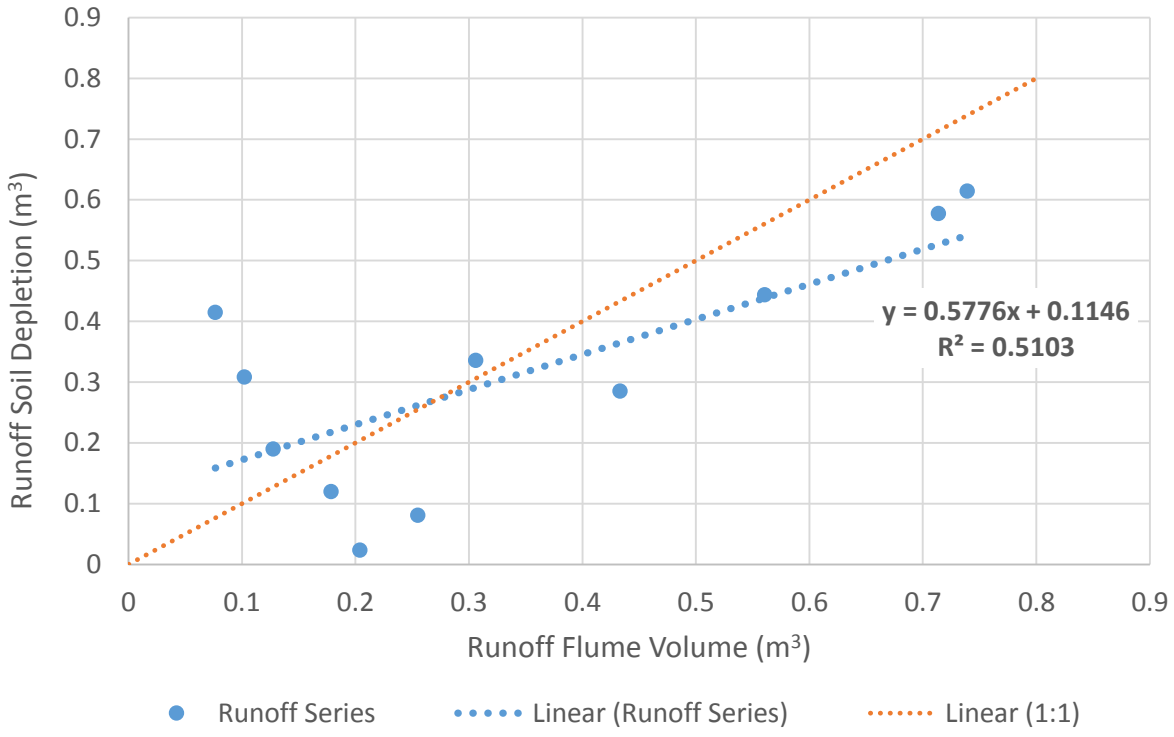

Figure 4.4 Linear correlation between flume runoff data and change in soil moisture.
A total of 11 storms recorded between 8/21/2014 – 9/13/2014.

When using soil depletion methods for ET_A a threshold had to be established based around precipitation events and the measured runoff from the flume, providing a timestamp feedback to other analysis. This threshold took into consideration 11 rain events, averaging the total time from when precipitation stopped to when runoff stopped (Table 4.2). This threshold was averaged to get a stronger average threshold to use for previous rain events when using the soil depletion method. The average threshold consists of an 88.6-minute (rounded to 1.5-hour) window after the last recorded precipitation, allowing this averaged time stamp to be an indicator for the separation of runoff and ET_A representation. Previously, during this average 1.5-hour time period after the rain, the soil depletion within the substrate was not known to be contributing to the total runoff or ET_A.

Table 4.2 Runoff Lag Flume Measurements.

Timestamp	**Runoff Lag (min)**
8/21/2014 18:30	15
8/22/2014 16:45	60
8/23/2014 9:00	90
8/23/2014 13:45	120
8/31/2014 18:15	15
9/1/2014 15:45	75
9/1/2014 23:30	105
9/2/2014 16:30	180
9/2/2014 23:15	105
9/6/2014 18:45	165
9/13/2014 11:00	45
Overall Average	88.6

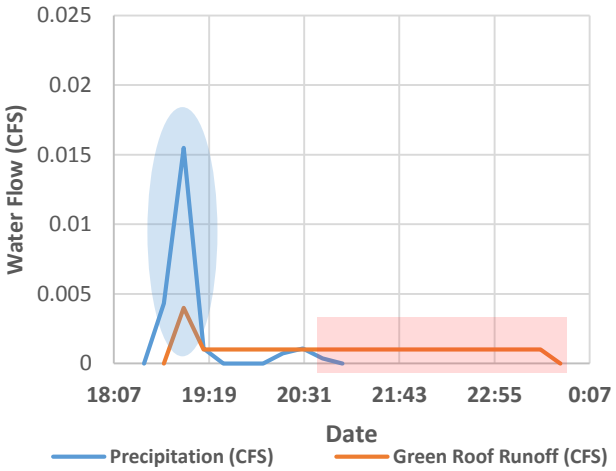

Figure 4.5 Rain event hydrograph.

Red box represents lag period between time rain stops and runoff is last recorded due to green roof short-term retention. Blue circle represents reduced peak runoff flow.

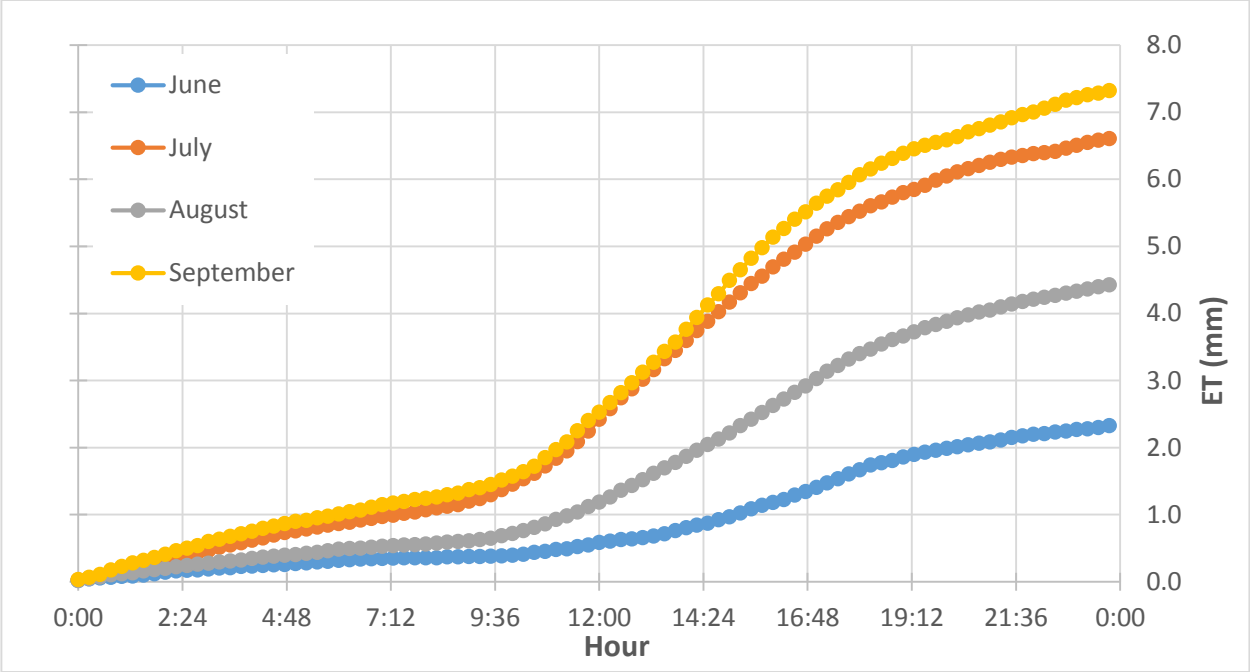

Figure 4.6 Mean cumulative daily ET for each month.

ET_A is shown on a 24-hour average monthly basis in 15-minute intervals in Figure 4.6. Previous studies have found the summer average ET_A rate to be 3.68 mm/day (Marasco et al., 2014) with *Watershed*'s being 0.23 mm/day (both using a K_C reference value of 1). The Marasco study took place in Manhattan, NYC, where an unirrigated 10-cm (3.94-in) extensive flat green roof planted with sedum and native plants was monitored to estimate ET rates. In comparison to the Marasco study (Table 4.3) *WaterShed*'s average ET_A rates was significantly lower and varied month to month. In comparison to *Watershed*'s monthly cumulative ET, the ET rates differ given the experimental conditions. Because of *WaterShed*'s thin soil green roof and its inability to retain significant long-term rainfall, these fluctuations in available moisture did happen more regularly compared to the fluctuations in the 4-inch growing media used in Marasco's study, along with the sloped roof. It can be noted that the *WaterShed* site received a

higher average precipitation during this data collection period (Table 4.3), while the mean precipitation value was not provided for the Marasco study.

Table 4.3 ET Rate Comparison.

Monthly Averages of ET (mm/day) *(Marasco et al., 2014)

	June	**July**	**August**	**September**
Previous Study*	4.2	3.45	4.8	2.3
WaterShed	0.11	0.29	0.19	0.31

4.3 Sloped Roof Contribution

With the given slope of *WaterShed*'s installed green roof, the retention rate moving up the elevation of the slope was predicted to be different because of gravity acting on the moisture as it is being pulled further down the substrate towards the bottom of the roof. This moving moisture would provide additional moisture to these middle and bottom zones. The top would have a lower retention volume compared to both the middle and bottom sections, while the bottom would always have the highest retention volume as a result of available water flowing down the roof. Figure 4.7 shows a summarized detailed view of the soil moisture, during August 31st – September 16th, 2014, while Figure D.4 in Appendix D shows the fluctuations throughout the entire data collection period.

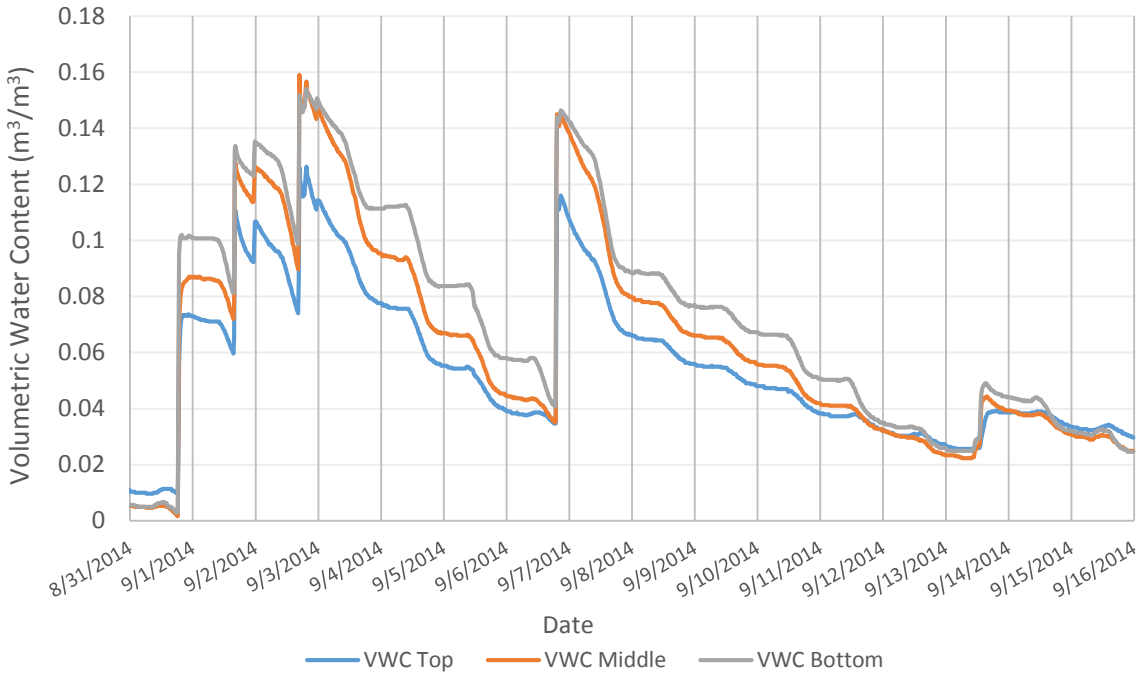

Figure 4.7 Stored moisture throughout slope of roof.

The different stored moisture averages moving up the elevation of the roof, while diurnal cycles (major vertical grid lines represent midnight) are mimicked by all the levels, having a higher decrease rate in stored water mid to late day.

During the time period shown in Figure 4.7 the trend is as follows: after rain events, which can be noted at the large positive peak in all 3 VWC zones, the lower elevation has the highest moisture content, followed by the middle and top elevations, respectively. After about a day after the rain event soil moisture is depleted mainly due to ET. Each zone exhibits a similar pattern of decline in VWC because ET is responding to similar ambient conditions. As the plants continue to utilize the available water within the substrate, they will reach a stress point that causes their normal consumption to change, influencing the plants physical processes. At this point the moisture within the substrate is harder for the plants to utilize, resulting in a slower decrease throughout the day or a lower peak of ET during the day. Since the top zone has the

lowest quantity of water it experiences the side effects of lower available water before the other two zones. At a certain period after the rain event all three zones get close to the same available moisture, given sedum's adaptation to conserving water when available water is low. It can also be noted that directly after a storm event the available moisture within the top is substantially lower than within the middle and bottom, which share comparable levels immediately after storm events.

The variability among the top, middle, and bottom zones represents the overall influence the slope has on the moisture retention within the substrate. Figure 4.8 shows the overall 9 zones' standard deviation compared to the available moisture, while Figure 4.9 shows the 9 zones broken up into top, middle, and bottom.

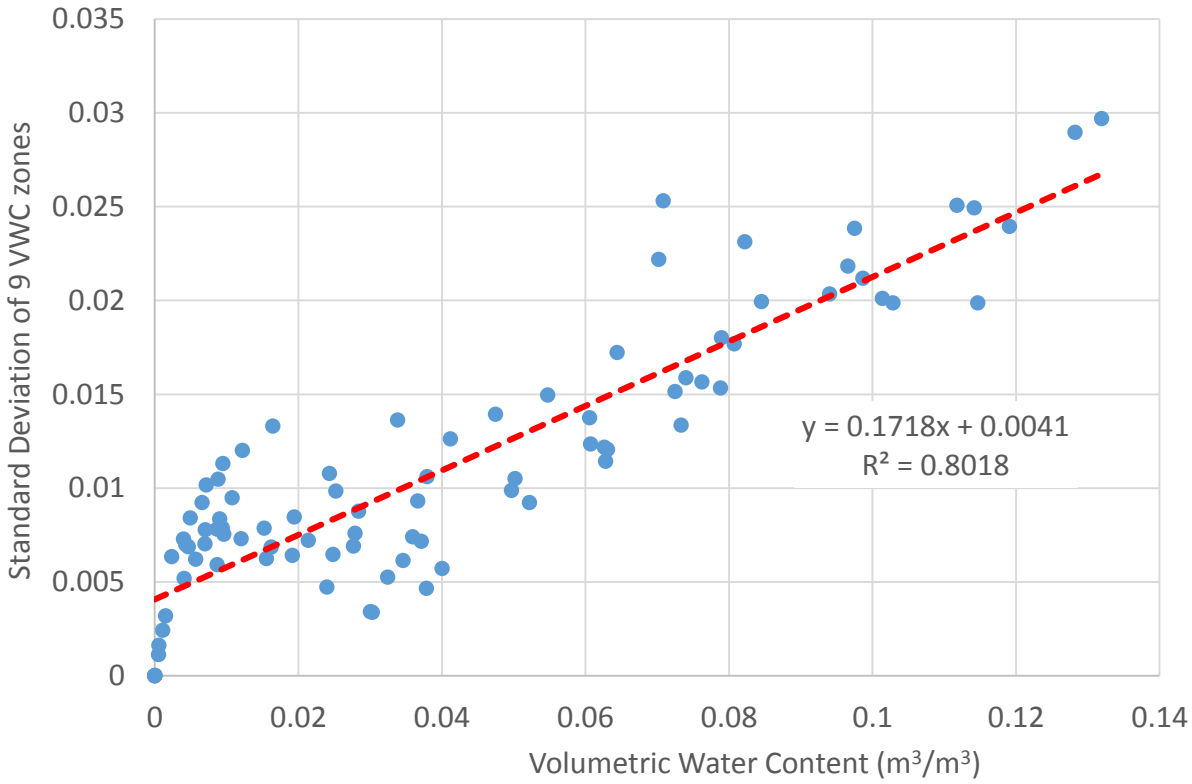

Figure 4.8 Mean daily soil moisture of all 9 zones within green roof compared to the standard deviation among the zones, influenced by the roofs slope.

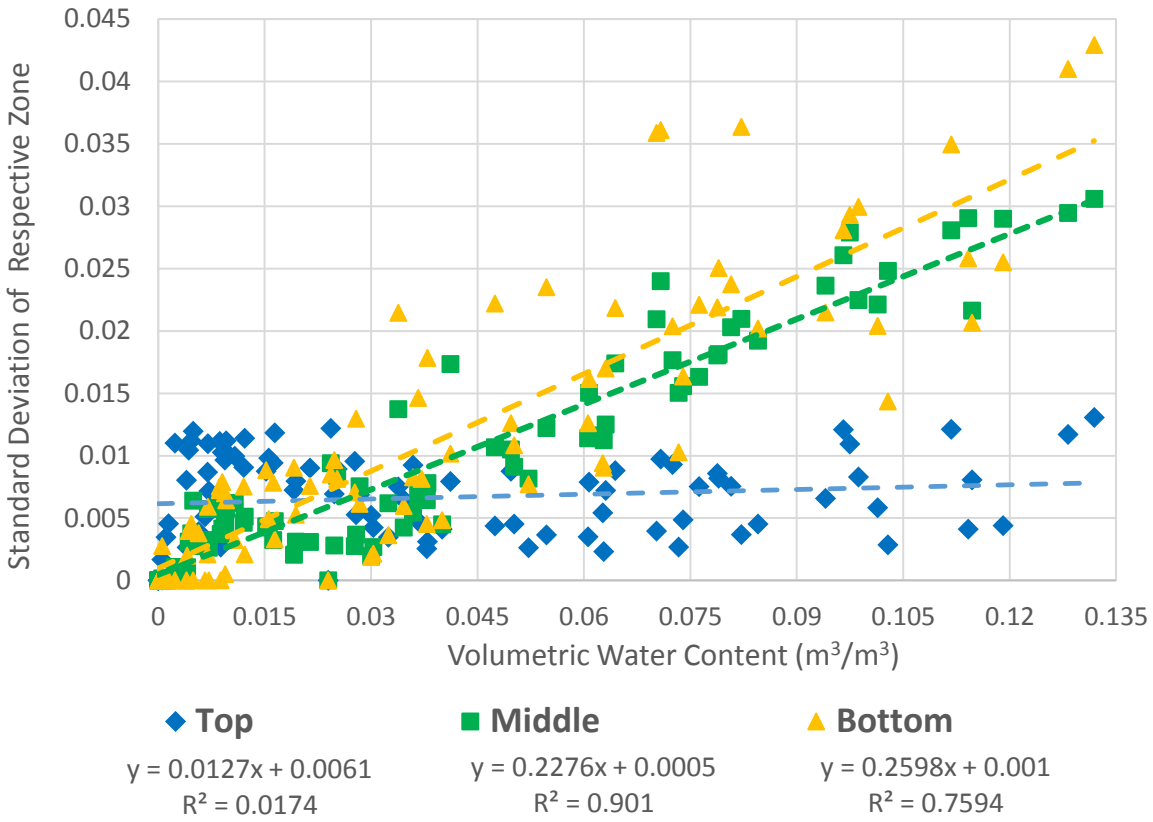

Figure 4.9 Mean daily soil moisture compared to standard deviation of the respective 3 elevations up the slope of the green roof.

Unlike Figure 4.8, Figure 4.9 breaks up each zone to see the influence slope may have. Figure 4.9 illustrates the influences of slope, given the bottom has a greater potential to receive water from the other two zones, corresponding to the varying VWC data in Figure 4.7. The slopes of the trend line relate the available moisture within the substrate to the variation from the average. The bottom trend line has the steepest slope, followed closely by the middle, with the top having a very low slope. The steeper slopes have more fluctuation due to more available moisture flowing down the roof slope, while the lower sloped trend line shows less variation.

4.4 Net Radiation

The installed radiometer automatically calculated the longwave and shortwave coming into and reflecting off the green roof system. The net radiation was the sum of the incoming shortwave and longwave minus the sum of the reflected shortwave and emitted longwave. Figure 4.10 gives an example of the typical amount of shortwave, net shortwave and difference during a 7 day period. The energy that is considered net radiation is energy input to the green roof, contributing to ET, latent heat flux, sensible heat flux, and soil heat flux (Equation 4). Table 4.4 and Figure 4.11 summarize the energy balance for the green roof. In this case the soil

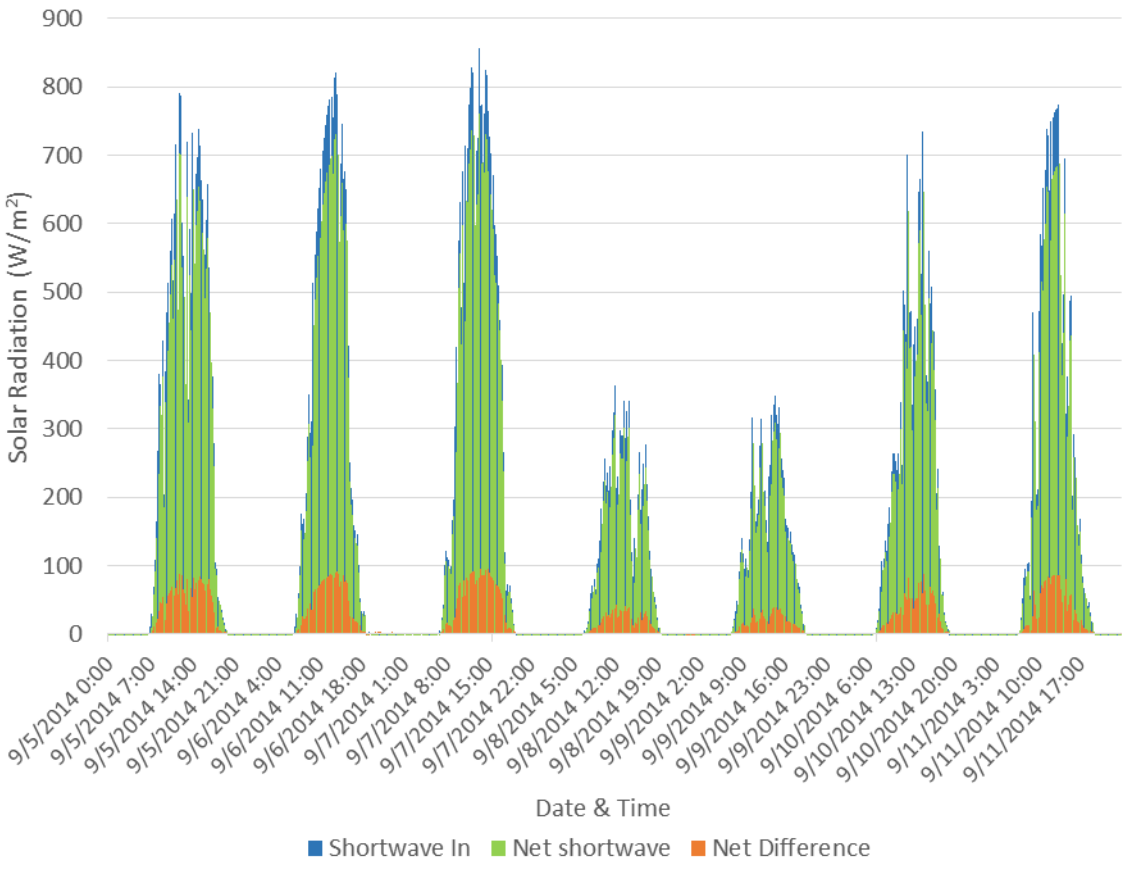

Figure 4.10 Solar radiation experienced by green roof on WaterShed. Net difference represents the energy input of the green roof system.

heat flux is positive when heat is leaving the system to enter the atmosphere and negative when heat is transferred through the system to the roof.

Table 4.4 Mean Daily Energy Balance Equation Variables.

Mean Daily	June/July	July/August	August/September	Average	% Radiation
Net Radiation [W/ m^2]	119.90	109.03	99.16	108.25	
Latent Heat Flux [W/m^2]	6.53	6.18	5.99	6.29	5.7 %
Soil Heat Flux [W/m^2]	-2.81	-1.55	-0.39	-1.28	1.1 %
Sensible Heat [W/ m^2]	115.56	104.02	93.54	103.22	93.2 %

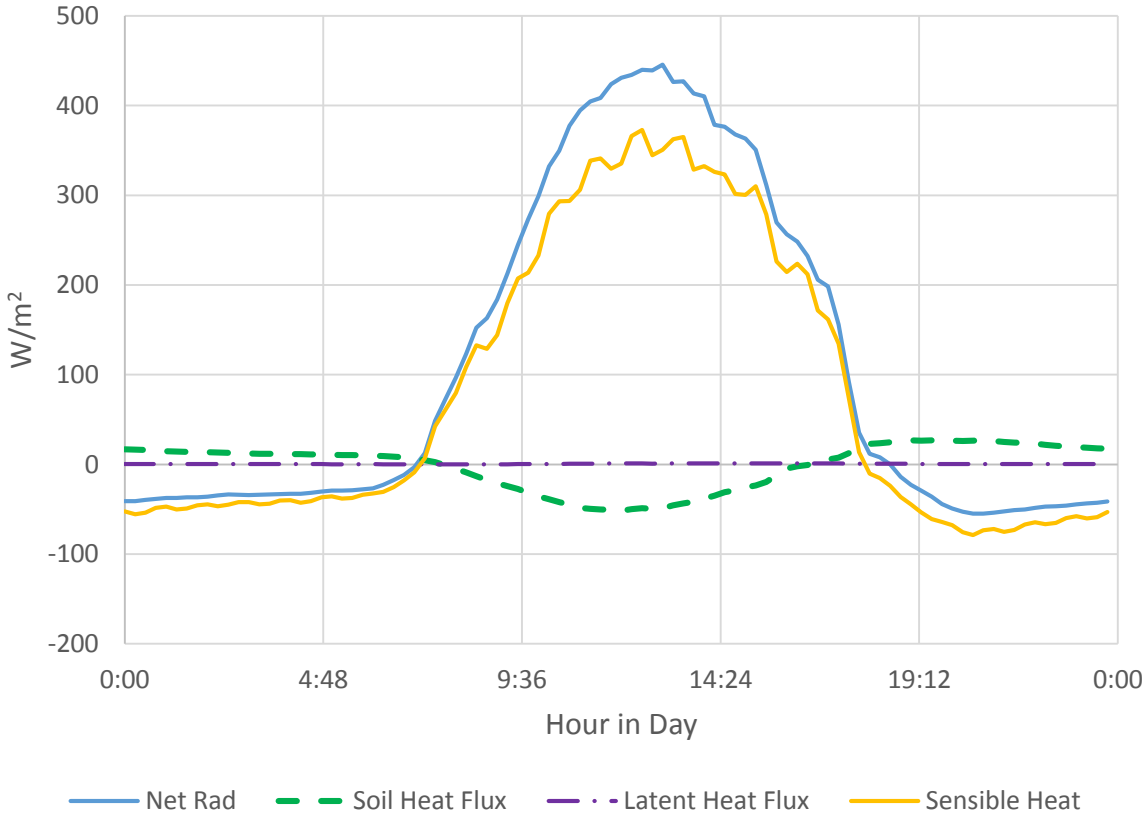

Figure 4.11 Mean 24-hour energy budget for the summer

(June 18 – September 15, 2014)

Due to low measured levels of ET, the Latent energy is not noticeable in this graph. Appendix J provides individual energy balance variables graphed with appropriate scale.

This energy budget graph helps to show the average flux of energy within the green roof system on a 24-hour basis. Because sensible heat is an important variable to model, it is highly influential on the net radiation energizing the system, followed by the consumption of energy through heat transfer through the media to the roof (soil heat flux) and consumption by the plants used through ET processes (latent heat flux). Other studies have found the maximum sensible heat flux to be around 360 W/m^2, while it can get as low as 2 W/m^2 depending on angle of roof and variety of plants within the system (Takebayashi and Moriyama, 2007). This sensible heat value is important to calculate, as it helps to feed back to the reduction in ambient temperature of the surrounding area caused by the application of the green roof.

4.5 Plant Performance

On average we performed bi-weekly sampling to determine the percent cover and leaf area index (LAI) of the green roof. The data were collected within the nine zones of the green roof, corresponding to the sensor locations. Table 4.5 and Figure 4.12 show LAI during the collection periods.

Table 4.5 LAI Measurements from Green Roof.

	Zone 1	Zone 2	Zone 3	Zone 4	Zone 5	Zone 6	Zone 7	Zone 8	Zone 9
6/26/2014	1.6	2.2	1.6	1.6	2.2	1.2	1.8	0.8	0.8
7/10/2014	2.6	2.4	2.4	2.4	2.6	1	1.4	1.8	1.6
7/25/2014	0.4	0.4	1.4	2.4	1.6	2	1.4	0.6	0.4
8/22/2014	1.4	0.8	0.6	1.4	0.6	0.2	1.8	0.6	1.6
9/5/2014	1.8	0.4	1.2	0.8	1.2	3	1.6	0.8	1.6
9/18/2014	1.8	1	1	0.6	1	1.6	0.6	1.2	1.6

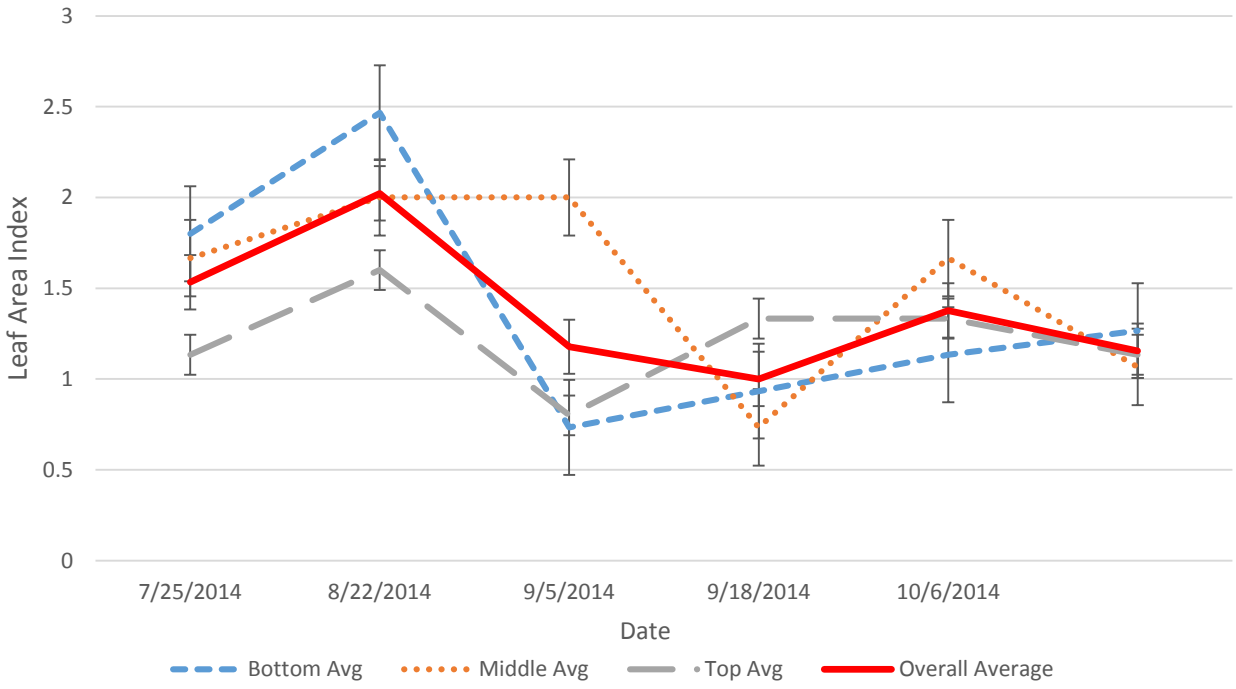

Figure 4.12 LAI trend from different elevations in slope and overall average.

With this data set over the course of 3 months, the LAI had no significant trends within the elevation of the slope of the green roof. The overall trend peaked during mid-August, while the lowest recorded measurement occurred in early September.

For the percent cover each data collection period Table 4.6 and Figure 4.13 display the percent cover data from the 9 zones. Overall the different zones follow the same trend over time. Percent cover depends on the geographical region where the roof is located. This could result in a margin of variability between data sets, given the poor health of the plants initially.

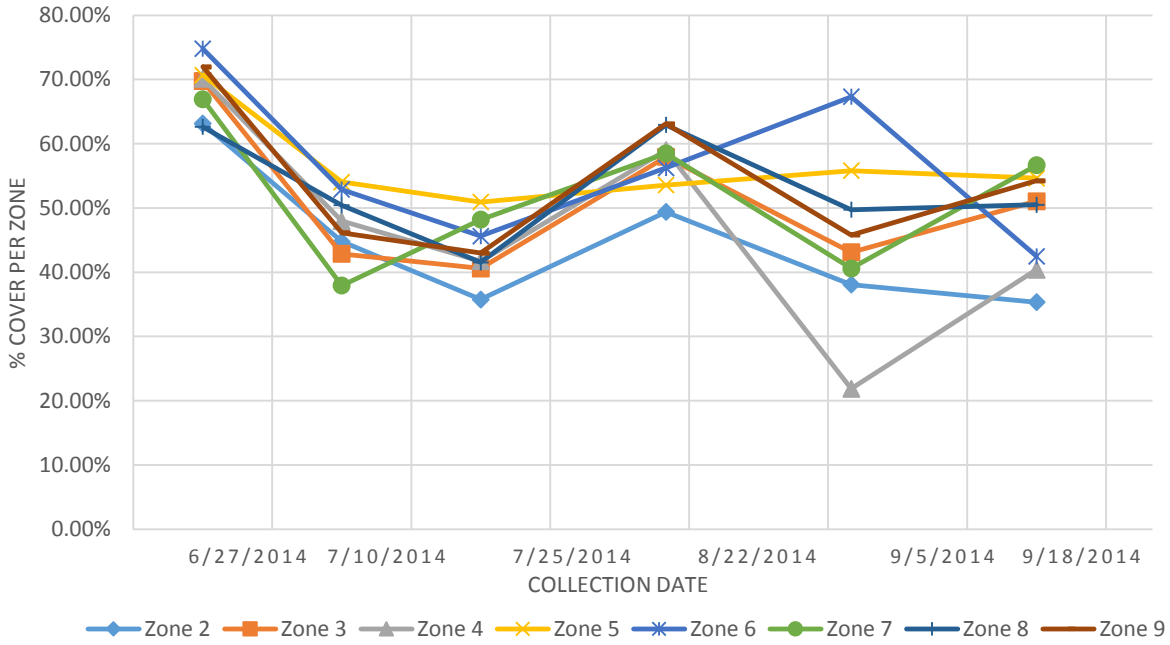

Figure 4.13 Green roof individual zone percent cover.

The percent cover trend throughout the data collection period is mostly similar for all 9 zones, with one exception occurring during the 8/22 collection day (outliers within zones 4 and 6).

Table 4.6 Percent Cover Measurements from Green Roof.

	Zone 1	Zone 2	Zone 3	Zone 4	Zone 5	Zone 6	Zone 7	Zone 8	Zone 9
6/18/2014	61.7%	63.1%	69.7%	70.1%	70.7%	74.8%	66.9%	62.6%	72.0%
6/27/2014	46.7%	44.8%	42.9%	48.0%	54.0%	52.9%	37.9%	50.4%	46.2%
7/10/2014	40.9%	35.8%	40.6%	41.7%	50.9%	45.6%	48.2%	41.5%	43.0%
7/25/2014	51.8%	49.4%	57.9%	59.0%	53.6%	56.2%	58.5%	62.9%	63.1%
8/22/2014	41.0%	38.1%	43.1%	21.9%	55.8%	67.3%	40.6%	49.7%	45.8%
9/5/2014	45.2%	35.3%	51.0%	40.4%	54.6%	42.5%	56.6%	50.5%	54.2%
9/18/2014	49.4%	29.8%	44.4%	47.0%	54.3%	36.1%	58.5%	57.2%	62.7%

To compare these vegetated measurements with the conditions the plants were experiencing requires a comparison to available moisture within the substrate. Figure 4.14 shows the individual zone's VWC during the data collection period. The trend during the data collection period is not due to soil moisture levels, as June showed relatively low soil moisture, while percent cover was the highest overall recorded. The first peak in VWC occurred in late July (7/27), when the plants' second peak took a few weeks longer to react (8/22).

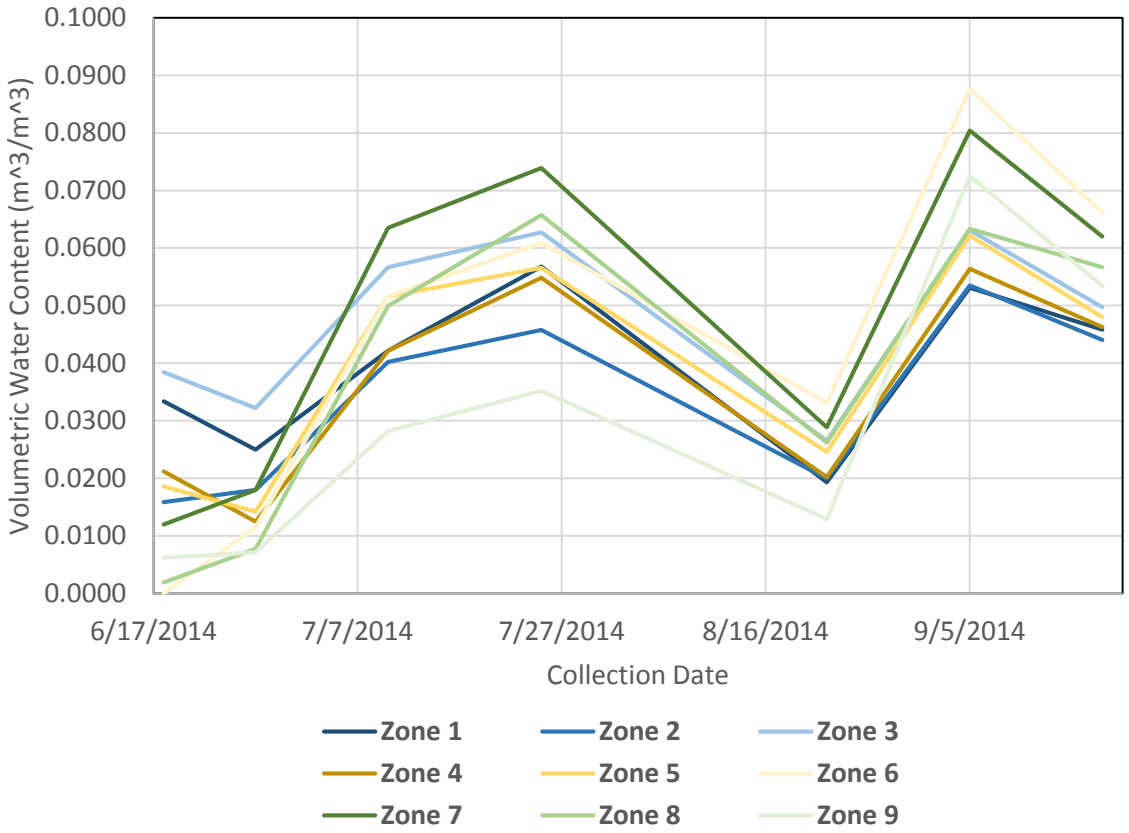

Figure 4.14 Green roof VWC for each zones going up the slope of the roof.

Overall, a trend with available moisture and plant cover can be noticed with plant response time taken into consideration. Figure 4.15 provides the direct correlation between the percent cover and average VWC between data collection periods. Overall, with the relatively poor canopy coverage the performance of the system is not tightly correlated to percent soil

moisture. However, this wide correlation is important to note given the higher frequencies of wet and dry periods due to the thin growing media and consumption through ET over time. This will take longer to analyze giving the plants time to recover to full functionality. When looked at independently some of the zones exhibited a stronger correlation than others, although additional data would improve the quality of this analysis (Appendix I). Because of plant response time and a low collection interval for plant performance the trend will be hard to perceive with this short data collection interval. The slope and thin-soil growing media are major contributors to this difficulty, given the high fluctuation rates of available moisture. This analysis will have to be examined for longer periods of time.

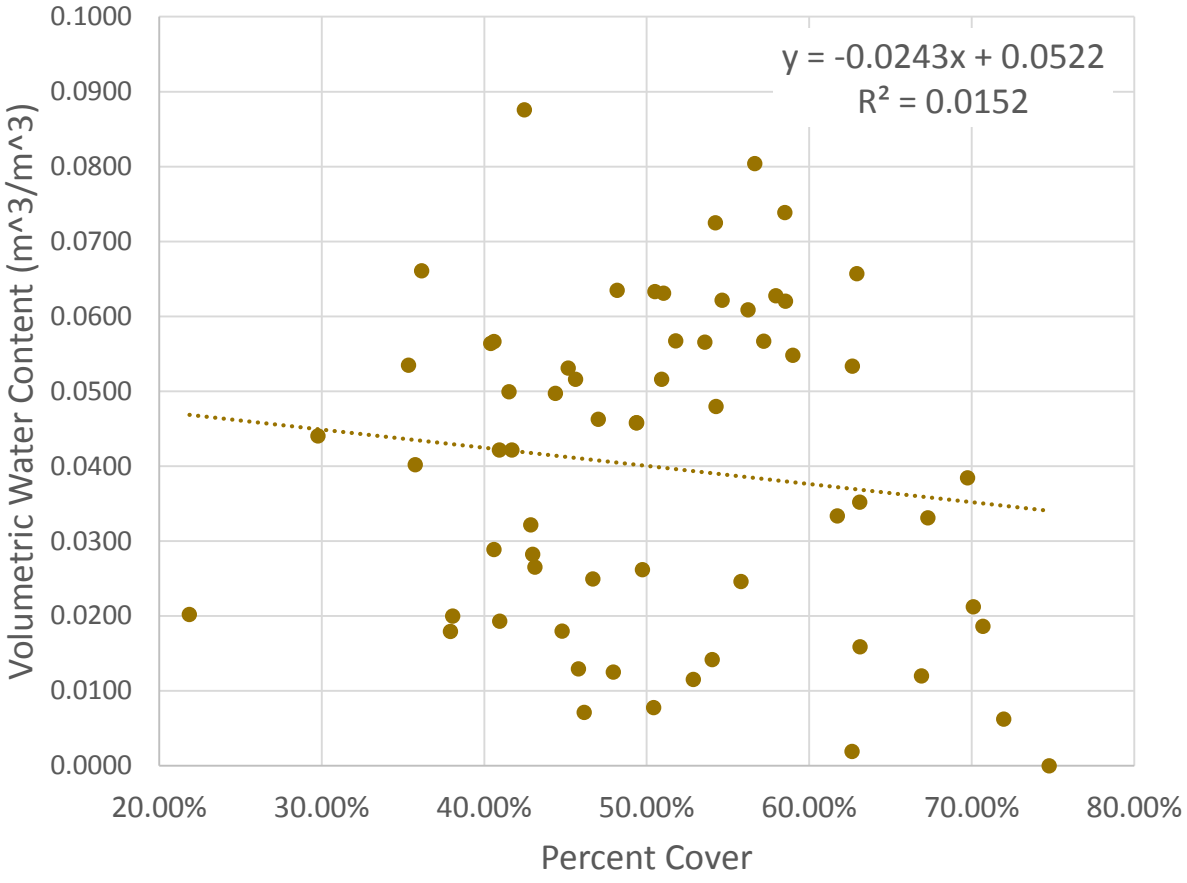

Figure 4.15 Overall soil moisture and percent cover correlation.

4.6 ET Measured vs. Predicted

The traditional method for ET_P of a green roof (Penman-Monteith equation) was analyzed at different intervals using the 15-minute data collected onsite, providing a direct comparison to the ET_A, measured by change in stored water, over time (Figure 4.16). Over the course of the data collection period these two indicators of ET_P fluctuated with over- and underestimating in comparison to ET_A. The ET_P model was consistently between 60 and 130 W/m^2 during times between rain events (ET occurring during this time is minimal, while having no direct method for measurement in this thesis), with minimal fluctuation. In comparison ET_A drastically increases during times following precipitation and decreases at a diminishing rate between rain events due to reduced moisture availability. If we observe the mean ET_P model over longer periods of time (as is traditional), the two methods have a stronger correlation. But during times with higher resolution, intervals have too much variability, making the two methods incomparable.

Since the VWC sensors within the substrate are providing data for the soil depletion, this presumably more accurately represents water usage within the green roof system at a higher resolution. The different mean time intervals for the two variables returned drastically different ET values given the amount of fluctuation that occurs with 15-minute data. Although all of the data frequencies (hourly, daily, and weekly) resulted in ET_P overpredicting ET_A, the correlations were drastically different (Figure 4.17 – 4.19). This is an important aspect to note, given the resolution the data is analyzed results in a different ET prediction when assuming the soil depletion method is ET_A.

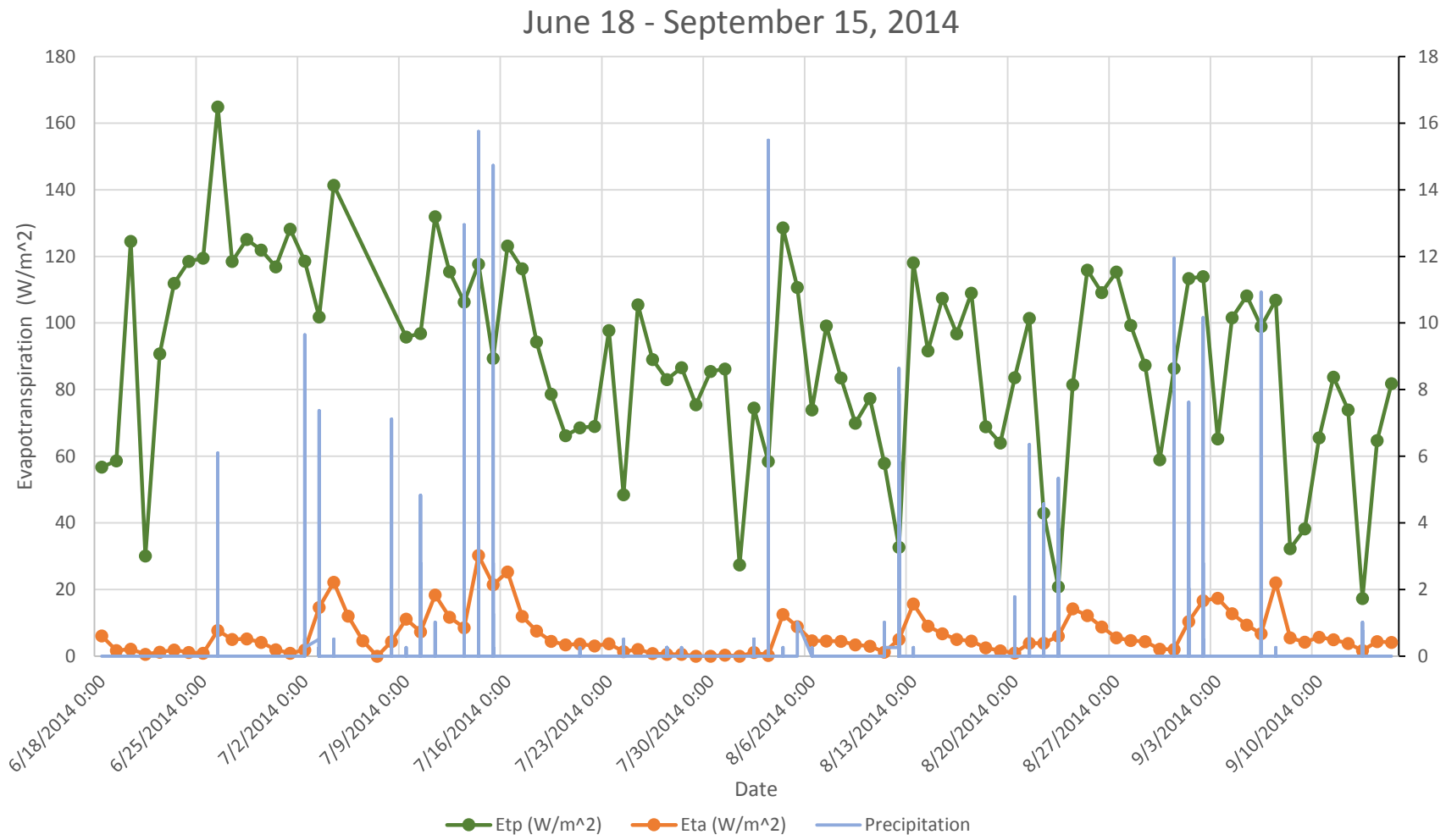

Figure 4.16 Mean daily ET_P, ET_A, and precipitation.

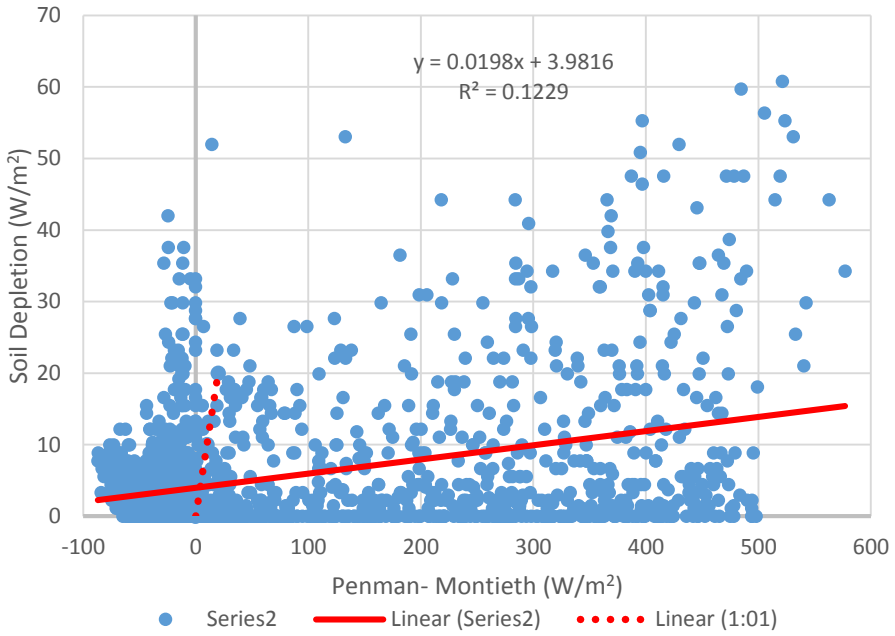

Figure 4.17 Hourly ET_P vs. ET_A comparison.

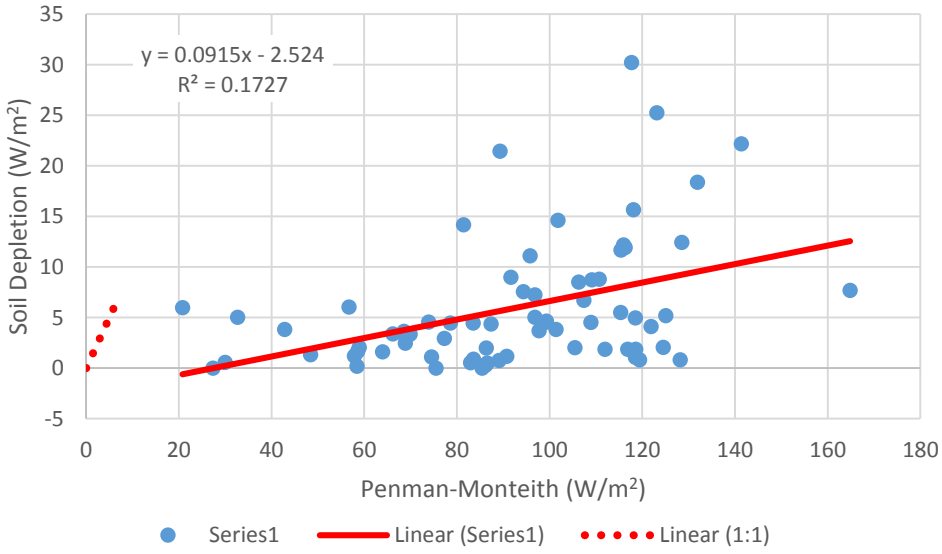

Figure 4.18 Daily ET_P vs. ET_A comparison.

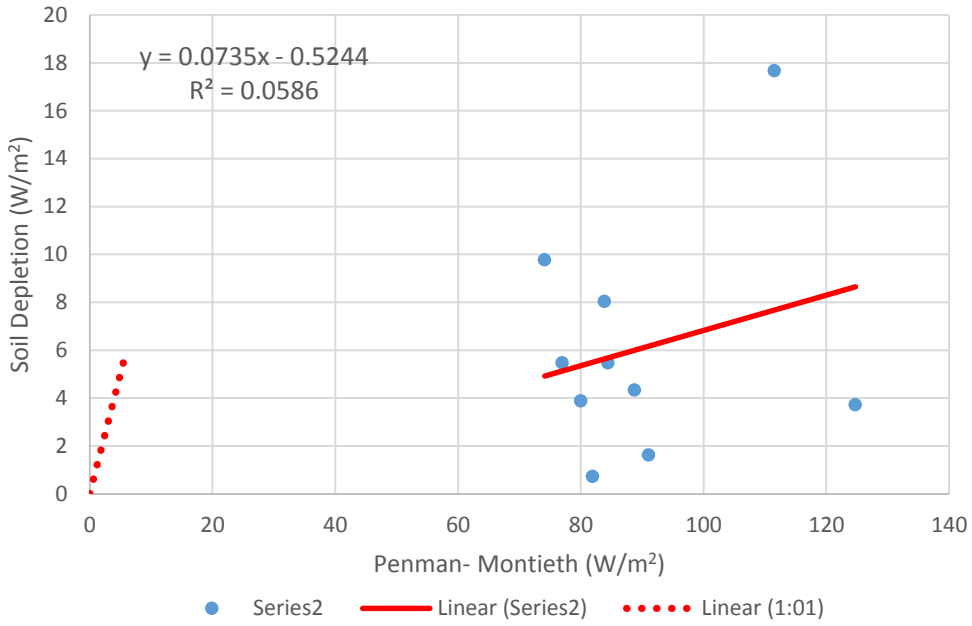

Figure 4.19 Weekly ET_P vs. ET_A comparison.

Although soil moisture is not a parameter in the Penman-Monteith model, soil moisture is an important aspect that drastically influences ET rates. However, as shown in Figure 4.16, ET_A is directly related to the availability of soil moisture for this thin, sloped green roof. Thus, it is imperative that caution be used when applying the Penman-Monteith model to green roofs because they can often be water-stressed.

Since the green roof was not irrigated the variability of available water changed dramatically during the data collection period. This was mostly done to mimic the natural cycle a mature green roof would experience in the mid-Atlantic region and resulted in a few extreme dry periods during mid to late July. The Penman-Monteith model is not responsive to available substrate moisture, only surrounding conditions. Studies have shown that as a result of average monthly variations in weather conditions, the Penman-Monteith energy model shows a comparative underestimation of ET. Other parameters would have to be taken into

consideration, as the equation shows no variation in soil moisture (Marasco et al., 2014)**.** Although these models do average out over longer periods of time, the fluctuations are important in performance using higher resolution data. We can conclude with the data collected that the Penman-Monteith does not accurately predict ET in its original form. We believe this analysis helps show how a system operates under normal weather conditions considering the different stress types which are experienced within the averaged longer periods of observation for modeling ET. The ET_A measured through the soil depletion method helps to show these drastic performance changes over the periods of available to low available moisture within the substrate.

Additional variables can be added to the Penman-Monteith equation to better predict ET, giving a K_C and K_S values. K_C or Crop Coefficient is a multiplier that helps to account for specific plant species differences within ET modeling, given different plant performances. To take into consideration the available water, K_S is an adjustment for systems that are less than well-watered conditions (Starry, 2013). Since the original Penman-Monteith equation was intended for a well-watered system with tall fescue like grass, these variables would help to mimic more of a green roof system, reducing the overall predicted ET values. This would be a possible next step in comparing the Penman-Monteith model to actual measurements of the green roof.

4.7 Overall Comparison

Pulling the model's data together and analyzing it as one during the data collection period has revealed a trend. Figure 4.20 shows the mean water balance over a 24-hour period with the precipitation and various models. This helps to display the average throughout a 24-hour period within the data collection period. Two graphs were produced; Figure 4.20 shows the data from the models not taking into account the precipitation threshold, while Figure 4.21 applies the rain

threshold, gathered from the flume runoff data. The left axis represents energy for the solar net radiation, ET_P, and ET_A. The numbers that are positive represent energy consumption by the plant's transpiration, while negative numbers reveal times when the substrate is gaining moisture

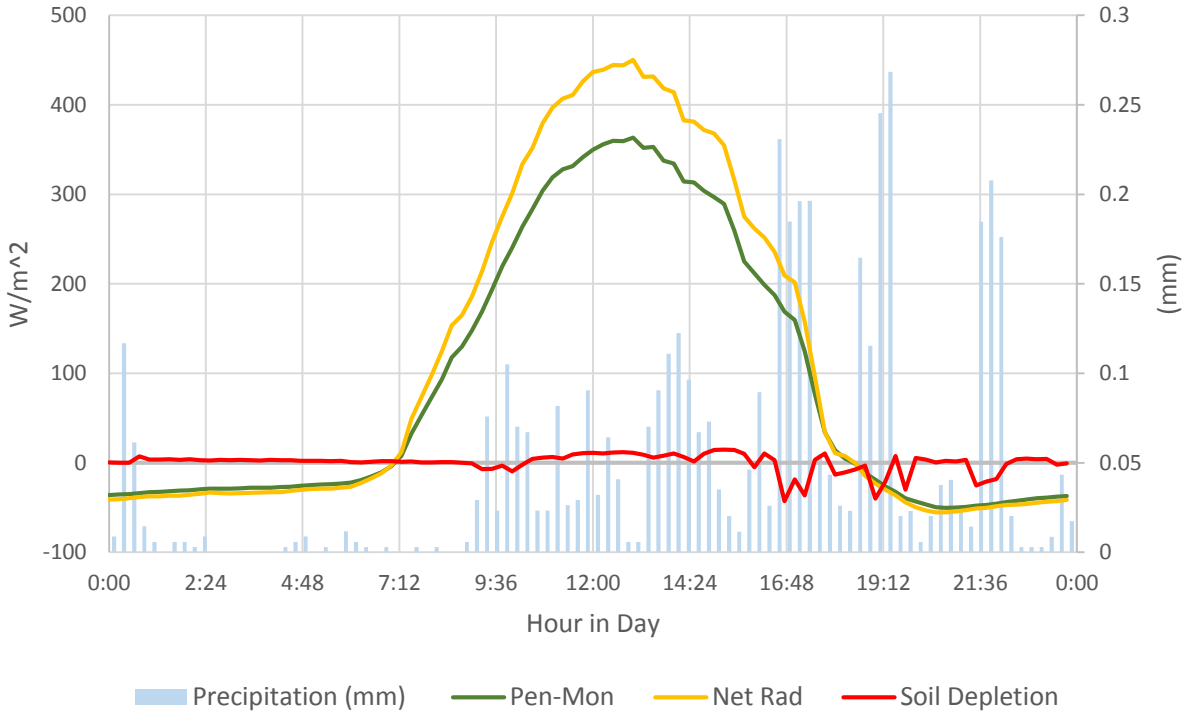

Figure 4.20 Hourly average conditions over the data collection period.
(No rain threshold applied to data.)

caused by precipitation or dew at night. The net radiation line appears in the comparison to provide the average available sunlight during this data collection period. The Penman-Monteith model can be noted to follow the same trend throughout the 24-hour period, while the change in storage of the green roof is following the trend during periods when the average precipitation is low.

Since the precipitation does skew the change in substrate moisture a precipitation threshold was established to eliminate times when it rained. Traditionally, the threshold

eliminates data for a 6-hour window after the last precipitation data are collected. For the application at *WaterShed* we were able to measure runoff from the roof and specifically tell when runoff or ET caused change in storage of the substrate. Table 4.2 in Section 4.1 shows the runoff values for the various storms taken into consideration. We took the average time from the recorded rain events to obtain the projected time after the precipitation stopped to account for runoff. The average from the storms taken into consideration was 88.6 minutes. The average was used to get a much larger dataset, not limiting the analysis to just times when the flume data was collected. This threshold was applied to the change in storage (for the entire data collection period) and anytime during precipitation and 88.6 minutes after precipitation stopped was taken out, since this was a known period when the roof was not losing moisture due to ET.

Figure 4.21 shows the 24-hour average with the precipitation threshold, where it is now easier to see the trend throughout the period when the negative values of change in storage are taken out.

It can now be noted that the trend throughout the day is shifted to the right for the change in storage compared to the Penman-Monteith model. Several interpretations of this can be established. First, since the roof is sloped with a slight northern exposure, the whole roof could be affected less by the net radiation compared to other variables including temperature and wind speed. Second, the availability of moisture within the substrate was much greater closer to the end of the day compared to the beginning as a result of precipitation events occurring mostly after 1 pm on average. In different time comparisons of both ET_P and ET_A (Figure 4.16), the trend is that after times when available moisture is high from precipitation the change in storage is much higher than the predicted ET**.** The plants now utilize moisture within the substrate at a

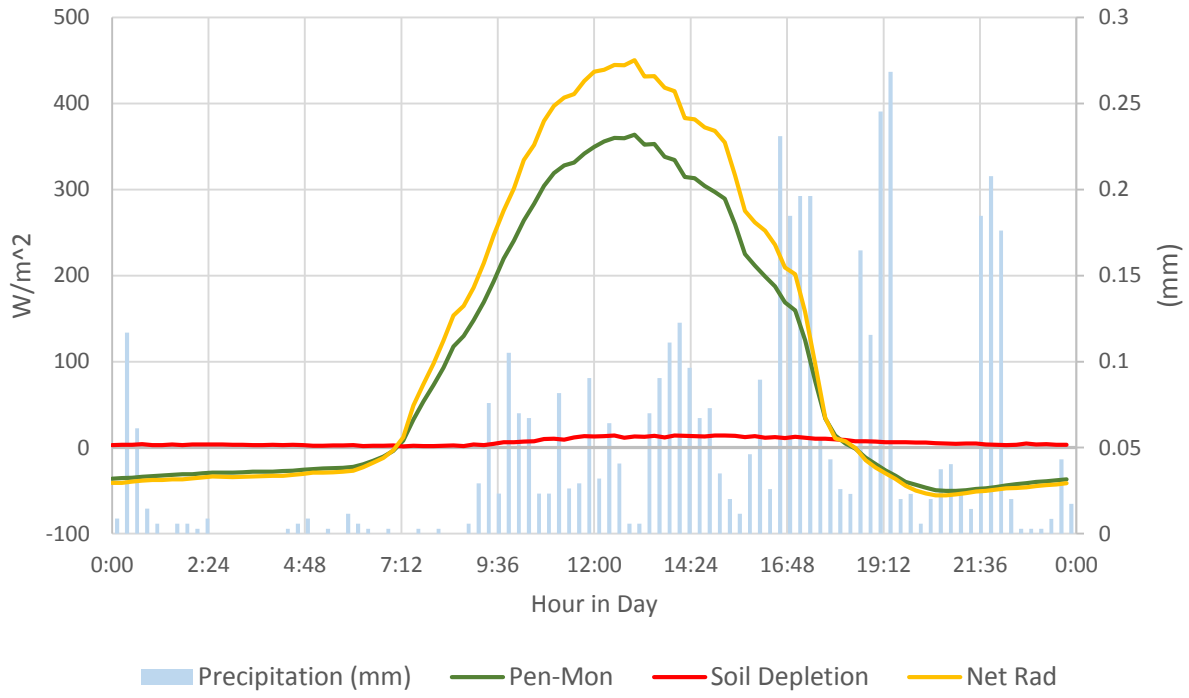

Figure 4.21 24-hour ET predictions during data collection period.
(Rain threshold applied.)

decreasing rate as the time from the last rain event increases. This is mostly caused by stress to the plants in the form of reduced available water. Sedum plants can tolerate times with reduced available moisture, resulting from plant characteristic adaptations (i.e., facultative CAM: C_3/C_4 to CAM adaptations). Given the mean precipitation is greatest during the last third of the day this could account for the shifted soil depletion, as it is easier for plants to utilize the stored water. With this higher energy consumption during periods when moisture is present, the discussion of irrigation can be brought up, in helping to manage the available energy within the system by plant process rather than heat transfer through the roof. Since the roof's substrate is thinner, presenting more fluctuations of wet and dry periods, irrigation can help reduce the time the plants are stressed between rain events, allow radiant energy to be used in ET process vs. absorbing through substrate, and improve the biomass production rate. Figure 4.22 shows the

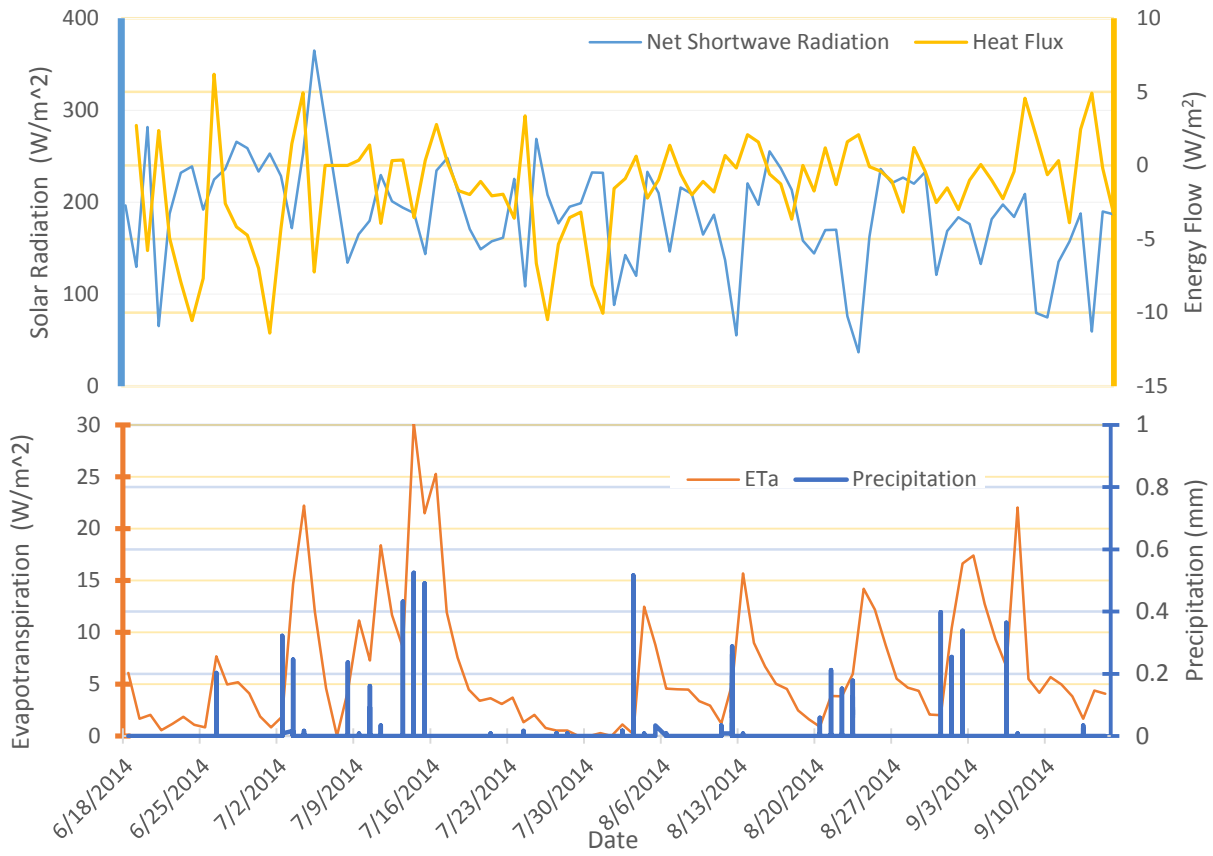

Figure 4.22 Water and energy flux within the green roof.

Relationship between stored moisture within the substrate and energy flux within the green roof. During times of high stored moisture (7/15/2014), the heat flux is close to -1 W/m^2, while time of low stored moisture (7/30/2014), the heat flux is around -8 W/m^2.

relationship between the energy flux and stored moisture within the substrate during the data collection period. This observation informs the summer conditions of wet and dry periods, while longer data collection through seasonal differences can help draw a stronger conclusion.

Previous studies conducted on a bigger application have used generic thresholds to predict when the cutoff is for the change in storage. The application here utilizes the runoff from the same roof where the other data is being collected. This allows for a more precise turning point for when the roof is using the rainwater or contributing to overall roof runoff.

The discussion of irrigation can be brought up for a thin, sloped system like this, given the durations of dry periods within the data collection period. Since the plants did not have

available water the energy they would otherwise be utilizing is now transferring through the roof to the building structure. If water was present, it would be helping to reduce this thermal heat transfer. During the time periods when the VWC was under 0.05, the ET_A rates were slowing down, given the plants were now in a stressed condition, allowing for the energy to otherwise be absorbed into the growing media. During these periods of low moisture if irrigation is applied, the energy balance could benefit. Given the set-up of *WaterShed's* site the rainwater eventually stored in open air cisterns could act as a water source for this process, reducing the overall need for potable water. The water limiting energy performance analysis would need to compare longer sets of data, and look more closely at the temperature gradient through the green roof layers.

5. Summary and Conclusion

With applications of green roofs becoming more widespread in residential sloped conditions, it is crucial to understand how these systems perform develop performance standards. The slope characteristics and thin-soil media can be seen to have a major influence on retention rates within the substrate, providing greater available moisture at the bottom of the slope compared to the middle and top zones. It cannot be distinguished which variable (slope vs. soil thickness) has a bigger influence, thus future research is needed for independent control for each factor. The green roof contributes to stormwater management by reducing the peak flow and elongating the runoff time, however the total retention in the green roof is small. Nonetheless, *WaterShed's* green roof reduces the peak flow which helps to relieve stress to natural systems downstream. This lower total retention is important to note, helping to show all the various types of green roofs and installation characteristics that influence the overall performance. The reduced rainwater retention within the soil media increases plant stress and can reduce the building's performance over time by increasing heat flux through the soil and into the buildings roof material. The Penman-Monteith model was not able to estimate ET for the sloped, thin soil media green roof studied. The main reason that P-M could not estimate ET was because it assumes unlimited soil moisture, which was not the case for our green roof. Thus, application of PM to estimate ET on green roofs should proceed with caution if soil moisture availability is questionable. Analyzing ET at a higher resolution with *Watershed's* installed monitoring system resulted in major differences between ET_A and ET_P, as no consideration was given to water availability within the substrate. Given moisture within the substrate is the driving force for ET, this variable is imperative in predicting the overall performance of the roof relative to plant

functionality. Future manipulation of the equation would have to take this into account when examining ET with a higher resolution for sloped, thin-soil green roofs.

As the data collection continues at *WaterShed* Sustainability Center, plant performance and ET will continue to undergo analysis in comparing the conditions of the green roof**.** Attributes like LAI and percent cover determine the plant density of the sedum canopy. This unique performance of the thin and sloped systems has revealed no significant quantities of rainwater retained, rather stored short-term and drained out of the system over a longer period of time by gravity. This stormwater management feature is important within our overall BMP system, but should be categorized and awarded differently than thicker green roofs. Depending on the installation goal, this thin green roof application can help reduce flow in streams and surrounding waterways during peak intensities of storms, releasing the water slowly over a period of time after the rain stops – ultimately influencing other variables like plant performance and survivorship, and overall energy transfer. This conclusion helps to bring the performance of this sloped, thin soil green roof system together, while providing information for a platform for other comparisons to other green roof types and their performance goals.

Appendices

Appendix A: Sedum Overview

Sedum Background:

This section provides supplemental information for the sedum plants used on *WaterShed's* green roof. The trays which held the growing media and sedum plants were grown at a local nursery and delivered mature, as the plants were selected during the growing season prior to delivery.

Zone: 3 – 9
Height: 3 – 5 inches
Spread: 5 – 9 inches
Bloom Time: May to June
Attracts: Butterflies when in bloom
Description: Dense foliage with small linear-oblong leaf structure, dark green, turning reddish brown for fall and winter.
Source: http://www.jeeperscreepersusa.com/SEDUM-album-Coral-Carpet_p_63.html

Figure A.3 Sedum album "Coral Carpet"

Zone: 4 – 9
Height: 3 – 5 inches
Spread: 12 – 18 inches
Bloom Time: August to September
Description: Wedge-shaped leaf structure is medium green during growing season, turning a deep burgundy in fall for overwintering.
Source: https://www.gardenerdirect.com/buy-plants-online/570/Sedum-Stonecrop/Sedum-spurium-Dragons-Blood-Dragons-Blood-Stonecrop

Figure A.4 Sedum spurium "Dragon's Blood"

Zone: 3 – 9
Height: 3 – 5 inches
Spread: 12 – 18 inches
Bloom Time: May to June
Attracts: Butterflies when in bloom
Description: Unique medium-green leaf color with reddish-tinged margins.
Source:
http://commons.wikimedia.org/wiki/File:Sedum_spurium_'tricolor'.jpg

Figure A.5 Sedum spurium "Tricolor"

Zone: 3 – 11
Height: 3 – 5 inches
Spread: 15 – 18 inches
Bloom Time: May to June
Attracts: Butterflies when in bloom
Description: Blue-gray leaf color ranging to light greens and yellows during fall and winter.
Source: http://www.onlineplantguide.com/Plant-Details/3668/

Figure A.6 Sedum relexum "Blue Spruce"

Zone: 5 – 8
Height: 3 – 5 inches
Spread: 12 – 24 inches
Bloom Time: June to August
Description: Ground cover, yellow-leaved cultivar with reddish-orange tips in autumn.
Source: http://www.whiteflowerfarm.com/l038220-product.html

Figure A.7 Sedum rupestre "Angelina"

Zone: 3 – 9
Height: 3 – 5 inches
Spread: 12 – 18 inches
Bloom Time: May to June
Attracts: Butterflies when in bloom
Description: Dense foliage, with narrow needlelike structures, deep green to red tips in fall and winter.
Source:
http://www.netherlandbulb.com/index.cfm?fuseaction=bulbs.plantDetail&plant_id=7209

Figure A.8 Sedum sexangular "Utah"

Appendix B: Monitoring System Sensor Details

Monitoring System Background:

This section provides supplemental information for the monitoring system installed on *WaterShed*. The various sensors listed below were selected based on the desired parameters needed for either energy or water balance models.

Table B.1 Green roof datalogger sensor details.

Green Roof Sensor Type	Sensor Description	Brand	Model #	Qty.	Scan
Vegetation Temp	Apogee Infrared Radiometer	Campbell	SI-111	3	5 sec
Under-Tray Temp	Thermocouple Probe	Campbell	109-L	3	5 sec
EPDM Surface Temp	Apogee Infrared Radiometer	Apogee	SI-111	2	5 sec
Net Radiation	4-Component Net Radiation Sensor	Hukseflux	NR01-L	1	5 sec
Soil Heat-Flux	Soil Heat Flux	Hukseflux	HFP01-L	2	5 sec
Soil Moisture & Temp	Water Content Reflectometer Plus	Campbell	CS655-L-DS	9	5 sec
Total roof runoff	Pressure Transducer (SDI-12)	Campbell	CS451-L	1	20 sec

Table B.2 PV roof datalogger sensor details.

PV Roof Sensor Types	Sensor Description	Brand	Model #	Qty.	Scan
Panel Surface Temp	Surface-Mount Thermocouple Probe	Campbell	110PV-L	3	5 sec
Exposed Roof Temp	Infrared Radiometer	Apogee	SI-111	2	5 sec
Shaded Roof Temp	Infrared Radiometer	Apogee	109-L	3	5 sec
Total roof runoff	Pressure Transducer (SDI-12)	Campbell	SI-111	1	5 sec
Net Radiation	4-Component Net Radiation Sensor	Hukseflux	NR01-L	2	5 sec

Table B.3 Weather station datalogger sensor details.

Weather Station Sensors	Sensor Details	Brand	Model #	Qty.	Scans
Radiation	Hukseflux Pyranometer	Hukseflux	Lp02-L	1	10 sec
Rain Gauge	Hydrological Services	HS	TB4MM-L	1	10 sec
Temperature & Humidity	Temperature Probe	Campbell	CS215-L	1	10 sec
Water/Soil Temperature	Temperature Probe	Campbell	109-L	1	10 sec
Leaf Area Wetness	Devices Leaf Wetness Sensor	Decagon	LWS-L	2	10 sec

Appendix C: Calculations

Calculation Background:

This section provides supplemental information for quantifying retention of green roof for runoff, weir runoff equation (Equation 3), and Penman-Monteith ET model (Equation 6).

Roof Footprint: Upscaling for Total Runoff Volume

WR Area: 77.26 sq. ft (7.177 sq. m)

GR Area: 311.99 sq. ft (28.98 sq. m)

Total Area: 389.25 sq. ft (36.16 sq. m)

P: Precipitation

GR Thickness: Depth of green roof soil 2.5 in (0.064 m)

GR Rain In: Rainwater that has fallen on green roof footprint

WR Rain In: Rainwater that has fallen on white roof footprint

Total Roof Runoff: Volume of water entering gutter system from entire roof

$$P\ [mm] * \frac{1\ [m]}{1000\ [mm]} = P[m] \quad \textbf{(Eq. C.1)}$$

$$\Delta\ Storage\ \left[\frac{m^3}{m^3}\right] *\ (GR\ thickness\ [m] * GR\ Area\ [m^2]) = GR\ Retention\ [m^3] \quad \textbf{(Eq. C.2)}$$

$$(P\ [m] * GR\ Area\ [m^2]) = GR\ Rain\ [m^3] \quad \textbf{(Eq. C.3)}$$

$$(P\ [m] * WR\ Area\ [m^2]) = WR\ Rain\ [m^3] \quad \textbf{(Eq. C.4)}$$

$$(GR\ Rain\ In\ [m^3] - GR\ Retention\ [m^3])\ +\ WR\ Rain\ In\ [m^3]\ \ = Total\ Roof\ Runoff\ [m^3] \quad \textbf{(Eq. C.5)}$$

The series of equations above are used to quantify the total amount of rainwater coming off the green roof using the volumetric water sensors in the soil of the green roofs to predict retention rates. First precipitation is converted from millimeters to meters (Eq. C.1). The

measured retention rate uses the depth of the soil media and area of the green roof to upscale the predicted volume change to the entire green roof area (Eq. C.2). The total available rainwater falling on the system determines the green roof footprint input (Eq. C.3). Due to incomplete coverage of the roof footprint with the green roof, the white roof area would act as pure runoff to the total runoff (Eq. C.4). The difference between the green roof total input and retention are added to white roof runoff to return total runoff entering gutter system (Eq. C.5). We utilized this method for each storm event to quantify the total storm storage within the substrate, which reduces overall runoff volume.

Weir Equation: *C* and *K* equations

The variables C (Discharge Coefficient) and K (Head Correction Factor) are based on the angle previously chosen for the weir. For the application on *WaterShed*, the C and K values are reported in Table C.1.

$$C = 0.607165052 - 0.000874466963\,\theta + 6.10393334\text{x}10^{-8}\,\theta^2$$

$$K\,(ft) = 0.0144902648 - 0.0003395535\,\theta + 3.29819003\text{x}10^{-6}\,\theta^2 - 1.06215442\text{x}10^{-8}\,\theta^3$$

Table C.1 Values of C and K for *WaterShed*'s flume weir runoff boxes.

	Angle of v-notch	C value	K value
Bathroom	40°	0.5722	0.0055
PV roof	70°	0.5786	0.0032
Green roof	50°	0.5787	0.0044

Predicted ET Equation

$$ET_p = \frac{0.408\Delta(R_n - G) + \gamma\frac{Cn}{T+273}(e_s - e_a)u_2}{\Delta + \gamma(1 + C_d u_2)}$$

The potential ET (ET_p) [mm/day] based on selected reference crop, calculated every 15 minutes from onsite data collection and predetermined constants. Assuming well-watered crop.

Slope of saturation vapor pressure curve (Δ) [kPa/°C] was calculated monthly using the average temperature collected during the same period onsite, using the following equation:

$$\Delta = \frac{2504\ exp^{\left(\frac{17.27\,T}{T+237.3}\right)}}{(T+237.2)^2}$$ (Zotarelli et al., 2013)

Net radiation (R_n) [MJ/m^{2}day] : was automatically collected onsite and averaged over the 15-minute data interval. The program took the sum between the calculated incoming net radiation and the outgoing net radiation. The various mean time stamps used the 15-minute data. Figure C.1 helps to show what component of the sensor (Up/Down) corresponds to the labeled data (In/Out) for both short and longwave.

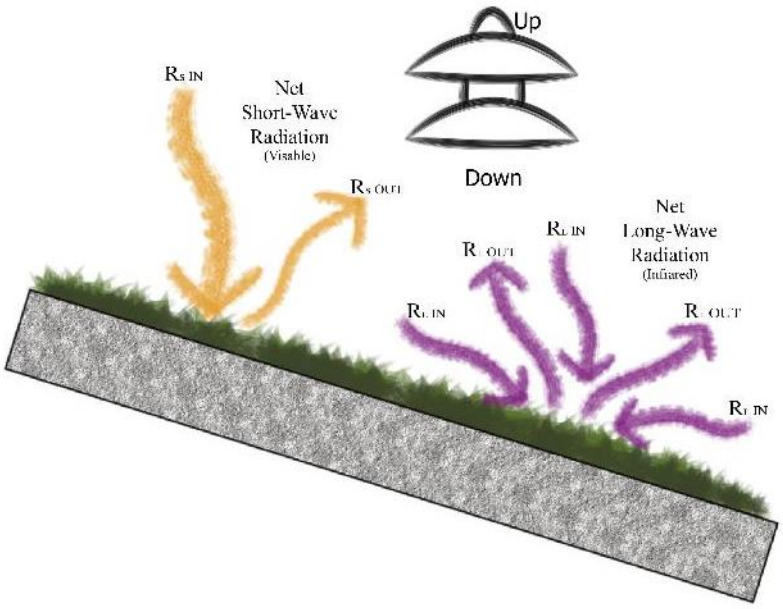

Figure C.1 Net radiation breakdown of In/Out longwave and shortwave radiation.

Heat flux density in soil (G) [MJ/m^{2}day] was collected onsite automatically from two locations over the 15-minute data collection period. The average of the two sensors was used to eliminate slope influences on heat flux. The heat flux data are usually neglected due to

long-term averages (Frevert and Schwab, 1966), but analyzing on a higher resolution made measuring the variable necessary**.**

$$R_n = R_{ns} - R_{nl} \quad \text{(Zotarelli et al., 2013)}$$

The psychrometric constant (γ) [kPa/°C] was calculated once, based on the following equations:

$\gamma = .000665\,P$, where P is the mean average atmospheric pressure [kPa] (Frevert and Schwab, 1966).

$$P = 101.3\left(\frac{293\ \ 0.0065z}{293}\right)^{5.26}$$

where *z* is the weather station elevation above sea level [m]. (Fangmeir, 2006)

The calculated P for *WaterShed* was 99.44 kPa, with the elevation of 153 m above sea level.

Cn is a constant, determined by a crop reference (grass), with the value being 900 per hour or 37.5 per 15 minute (Frevert and Schwab 1966).

Cd is another constant, determined by the crop reference, with a given value of 0.34 no matter the time interval (Frevert and Schwab 1966).

Temperature (*T*) [°C] data were collected automatically onsite every 15 minutes. Sensor was approximately 18 inches off the roof surface. Humidity was also collected with this sensor

Mean saturation vapor pressure (e_s) was calculated from the following equation (Frevert and Schwab, 1966):

$e_s = 0.6108^{\left(\frac{17.27\,T}{T+237.3}\right)}$, where T is air temperature [°C]. (Zotarelli et al., 2013). e_s was calculated on a 15-minute interval, using the onsite temperature collection.

The mean actual vapor pressure (e_a) was calculated using the relative humidity collected onsite in the following equation:

$e_a = Ue_s$, where U is relative humidity [%], e_s is saturated vapor pressure, with the mean being calculated every 15 minutes.

The *average wind speed* (u_2) [m] is measured with the onsite weather station, averaged over the 15-minute collection interval.

Conversions within ET prediction model (Zotarelli et al., 2013):

Latent Heat Flux Conversion: $ET_p \left[\frac{mm}{day}\right] * 2.45 \left[\frac{MJ}{m^2\ day}\right] = \lambda ET \left[\frac{MJ}{m^2\ day}\right]$

Energy Conversion: $\lambda ET \left[\frac{MJ}{m^2\ day}\right] * \frac{1\ W}{0.0864 \left[\frac{MJ}{m^2}\right]} = ET \left[\frac{W}{m^2\ day}\right]$

Appendix D: Environmental Conditions

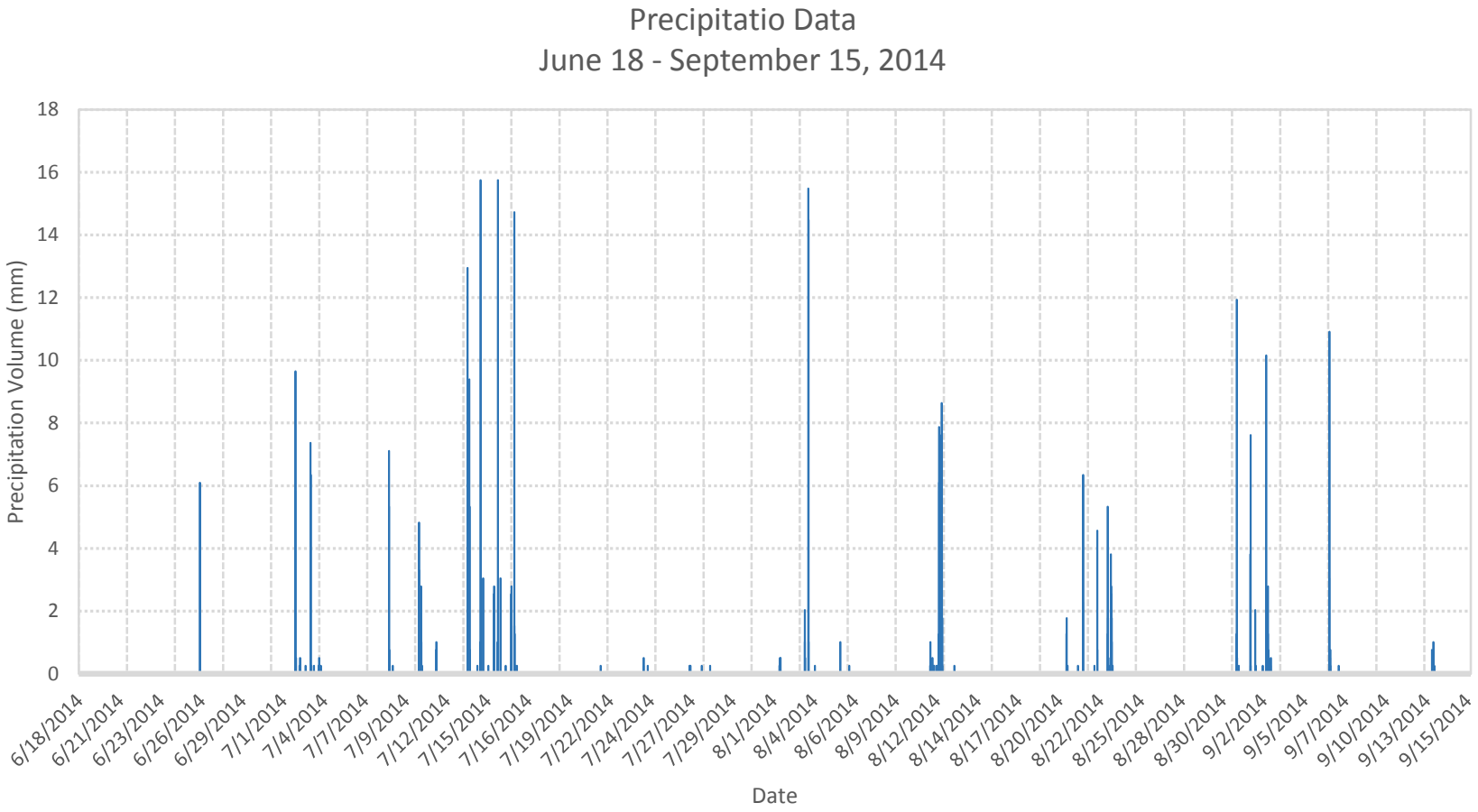

Figure D.1 Precipitation data (15 min data).

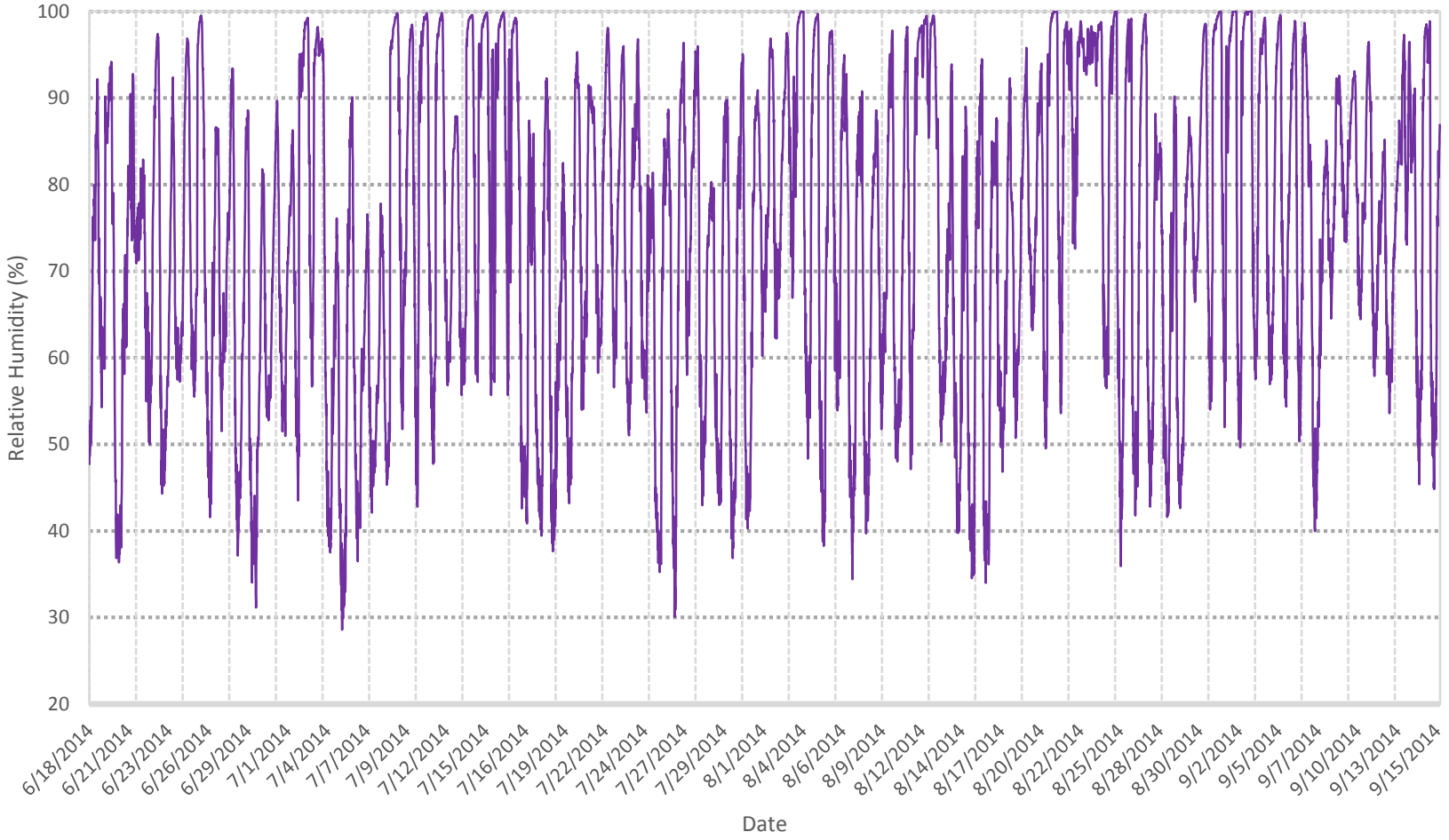

Figure D.2 Relative humidity data (15 min data).

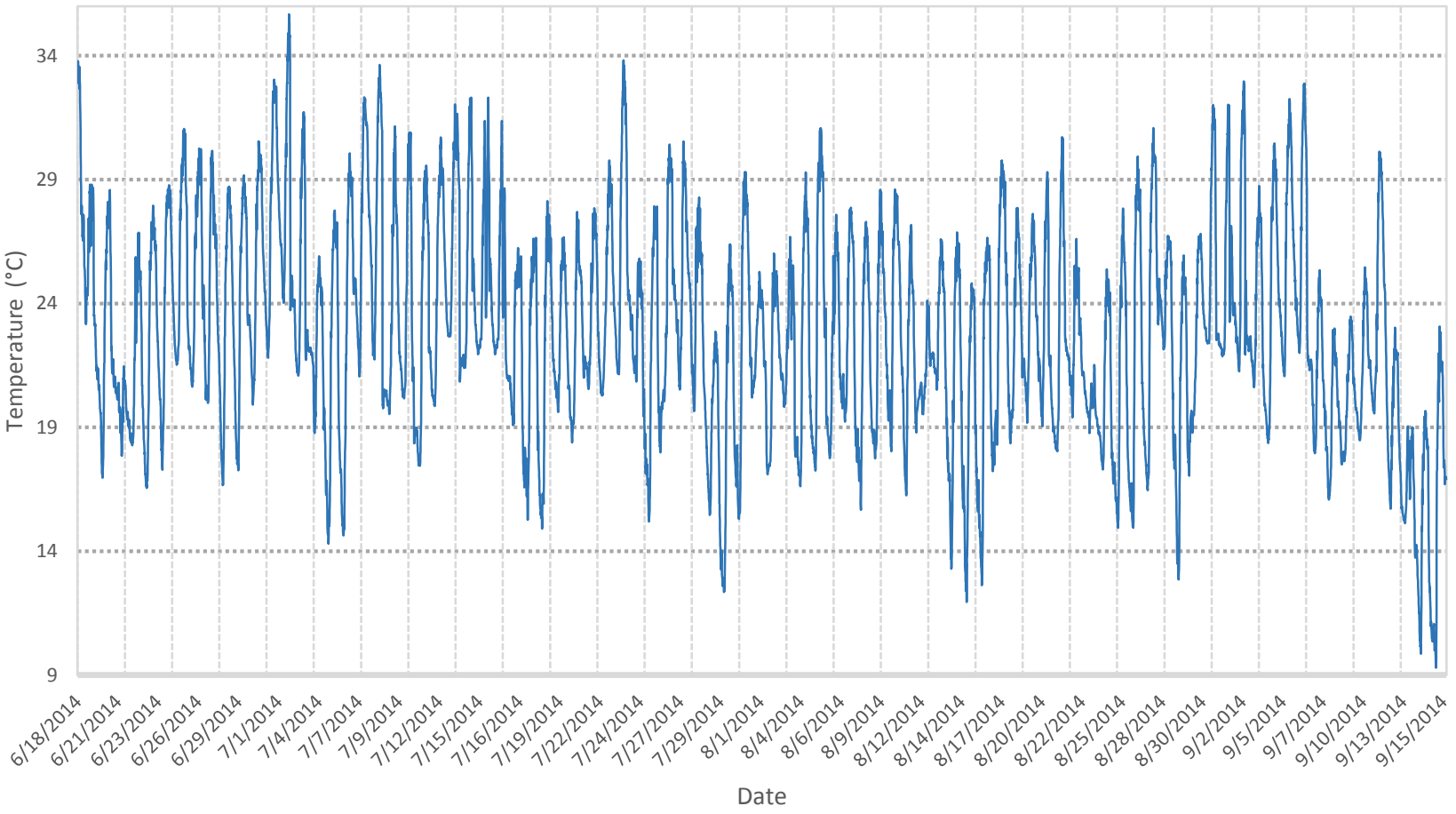

Figure D.3 Temperature data (15 min data).

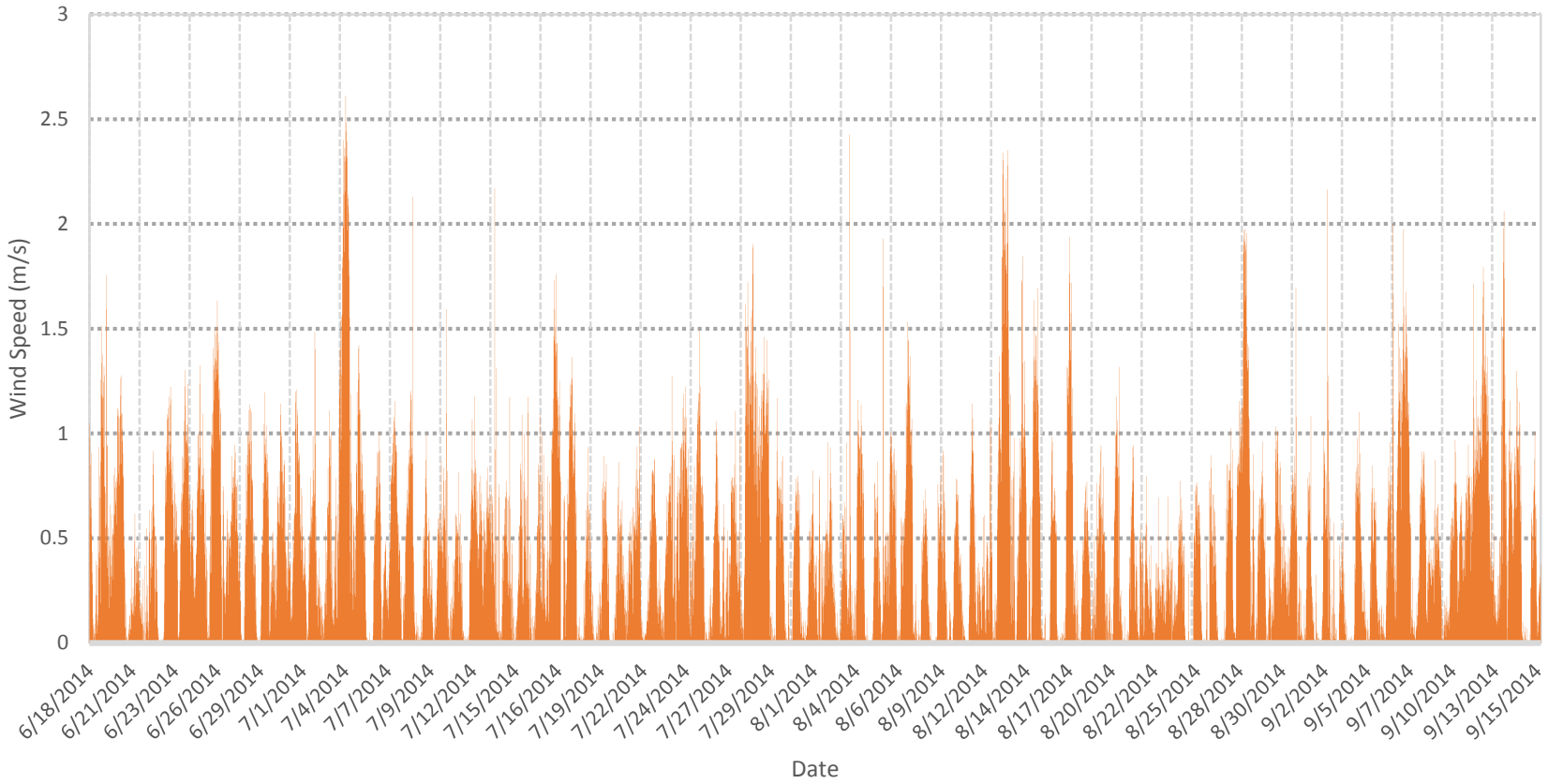

Figure D.4 Wind Speed data (15 min data).

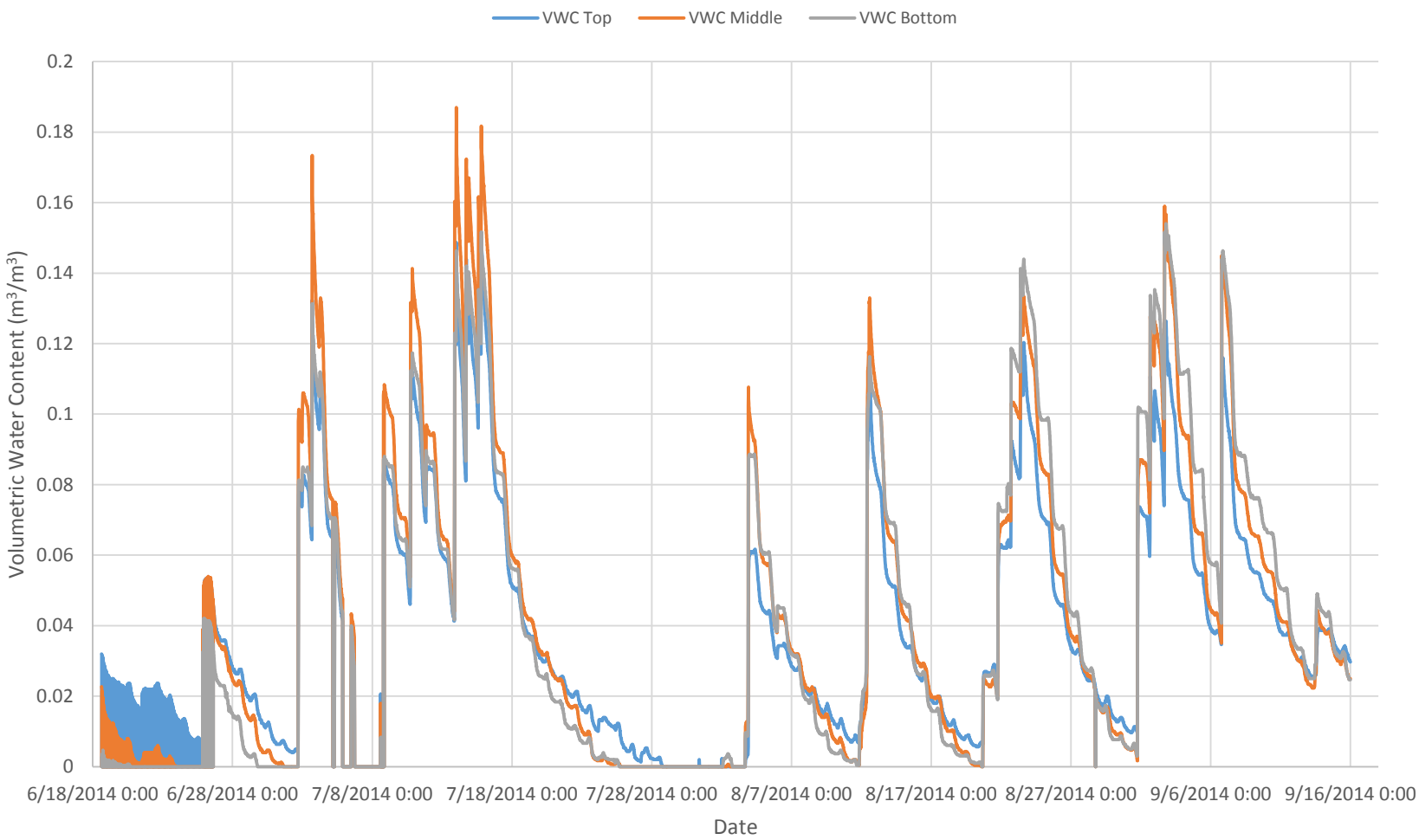

Figure D.5 Soil depletion data (15 min data).

Appendix E: Methods for *ImageJ* Software

Calculation Background:

This section provides supplemental information for processing green roof pictures to achieve a percent cover number. The steps below rely on the *ImageJ* software, which can be downloaded from the following link: http://imagej.nih.gov/ij/download.html

Once software is downloaded open the desired picture of the area needed to be analyzed: **File > Open > 'file'**

Crop the designated area you want analyzed by using a polygon tool in the top toolbar. End polygon by clicking on first point.

To erase outside pixels select **Edit > Clear Outside**

Select **Image > Crop** to get new image cropped to the canvas size.

Select **Save image as** to obtain separate images of cropped area and plant area for future reference

At this point with the area still selected take a measurement of the entire area by selecting **Analyze > Measure (Ctrl + M)**

This will bring up a table with the file name and pixel count. Other variables can be added but for this application the pixel count is all that is needed.

Adjust the color threshold of the image by selecting **Image > Adjust > Threshold**

Once the threshold window appears ensure the settings are in the HSB Color mode at the bottom, with the rest of the settings as follows:

Hue: 0 – 100
Saturation: 46 – 255
Brightness: 1 – 255
Default threshold method
Threshold color: Red (overlay)
Dark background selected

Click **Select** at bottom of Threshold window and select vegetation

To select vegetation by itself, right click on the image and select **Properties > Edit > Erase outside**

The vegetation should be the only thing left. At this point take a new measurement by selecting **Analyze > Measure or (Ctrl + M)**, which will populate a new pixel count of just the vegetation. **"Save As"** this image as well for future reference.

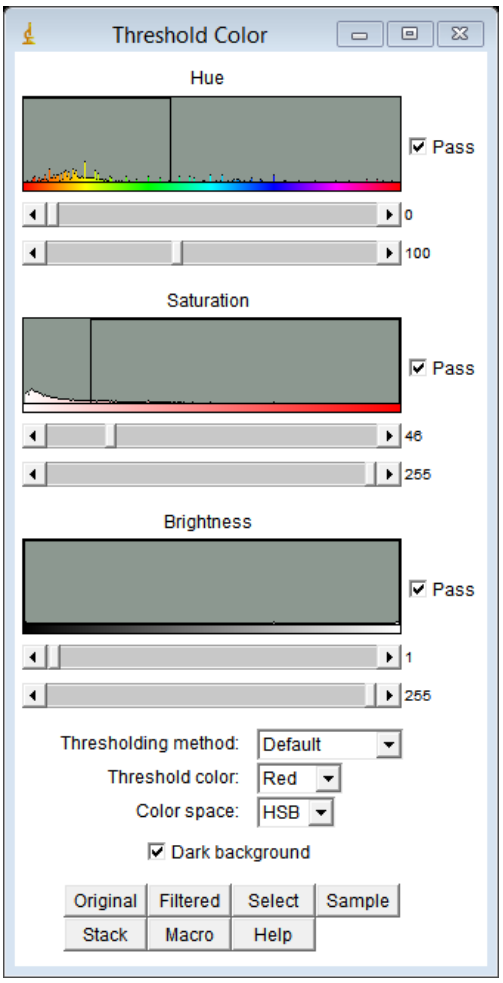

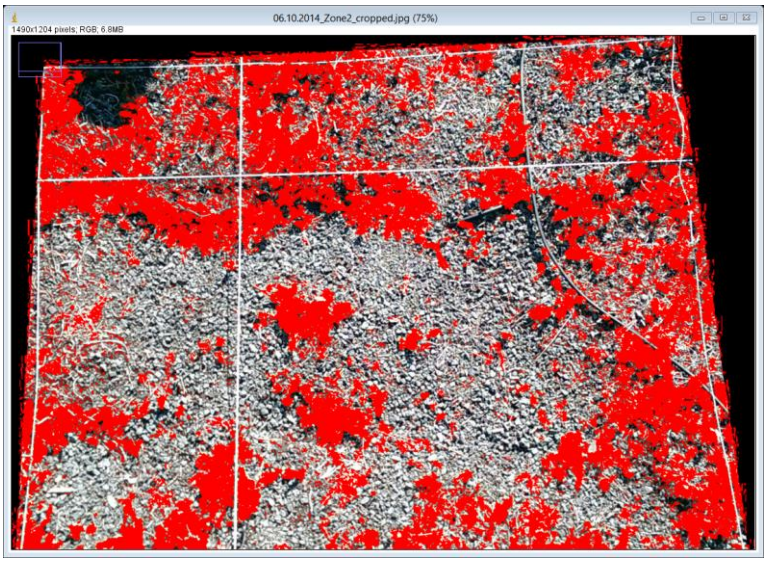

Figure E.1 Threshold set to only select vegetation within respective zone of green roof.

Appendix F: Percent Cover Image Details

Percent Cover Details Background:

This section provides visual results for the percent cover of the green roof using *ImageJ* software (Discussed in Appendix E).

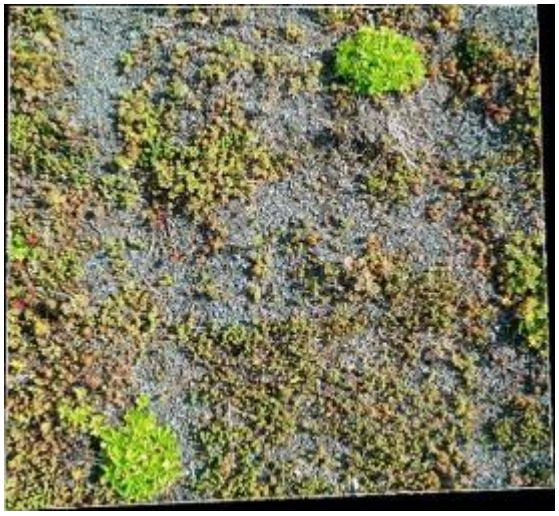

Selected Vegetation Only

Selected Vegetation Only

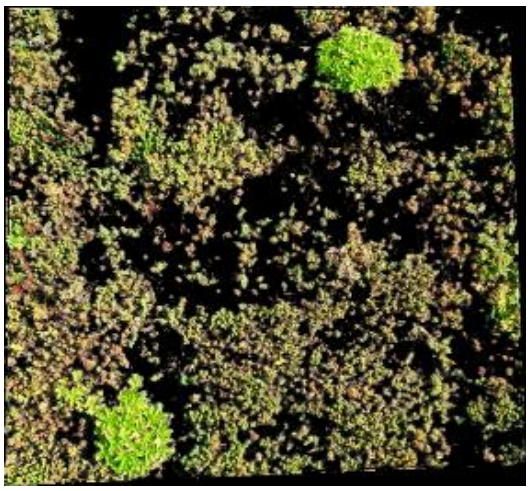

Zone 1 – 6/18/2014

$$\frac{(Vegetation\ Pixels)}{(All\ Pixels)}\frac{1{,}006{,}562}{1{,}630{,}630} = 61.73\ \%$$

3 Months Later

Zone 1 – 9/18/2014

$$\frac{(Vegetation\ Pixels)}{(All\ Pixels)}\frac{724{,}638}{1{,}468{,}133} = 49.36\ \%$$

Appendix G: Flume Detailed Drawings

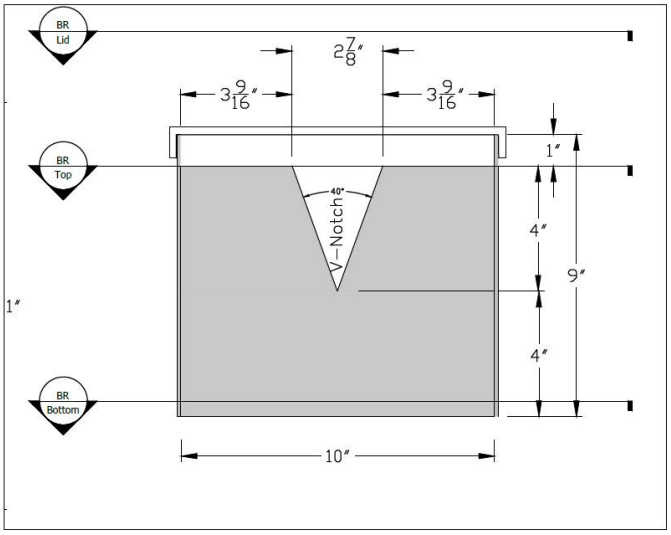

Bathroom Runoff
Flume Details

Feb. 19, 2014
Contact: Scott Tjaden

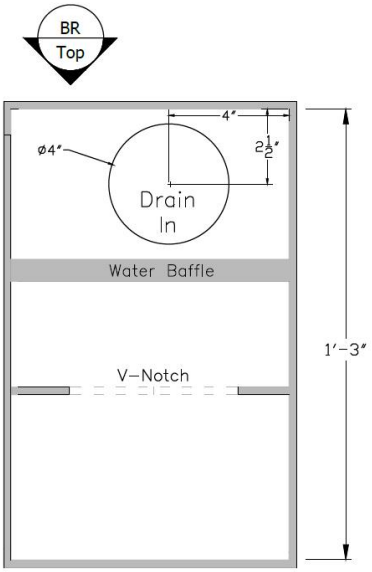

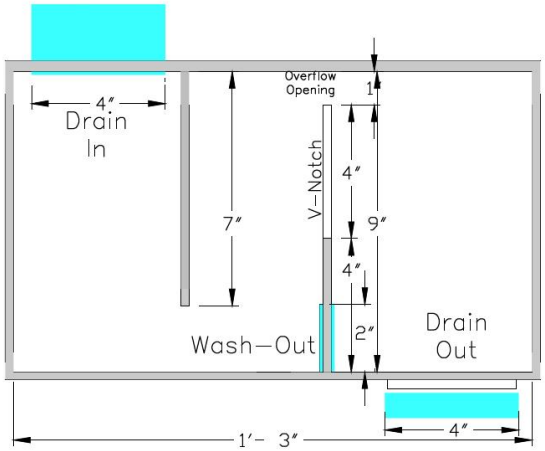

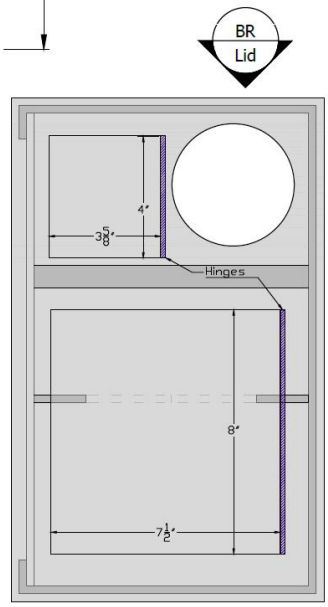

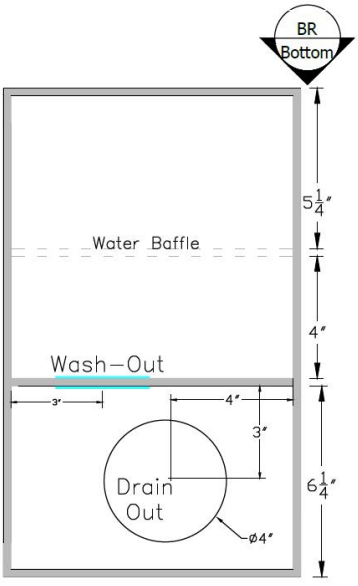

Green Roof Runoff Flume Details

Feb. 19, 2014

Contact: Scott Tjaden

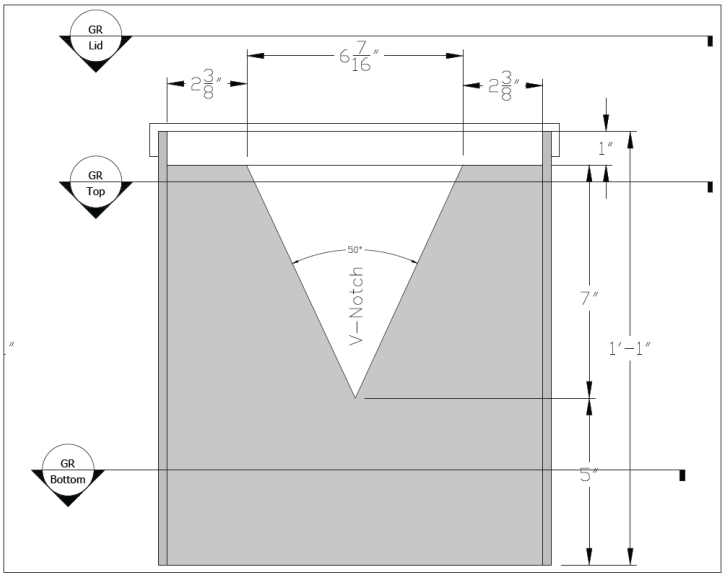

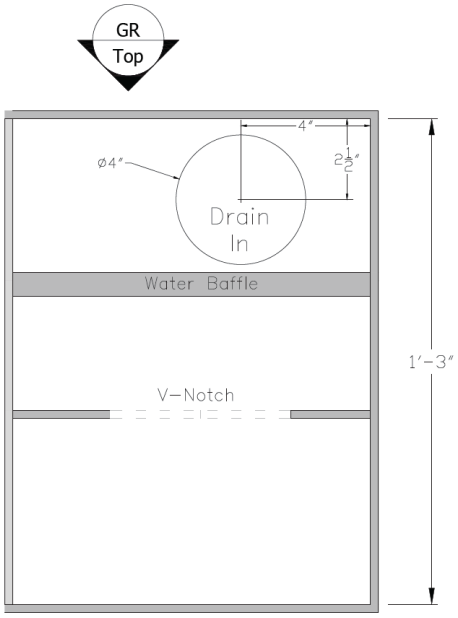

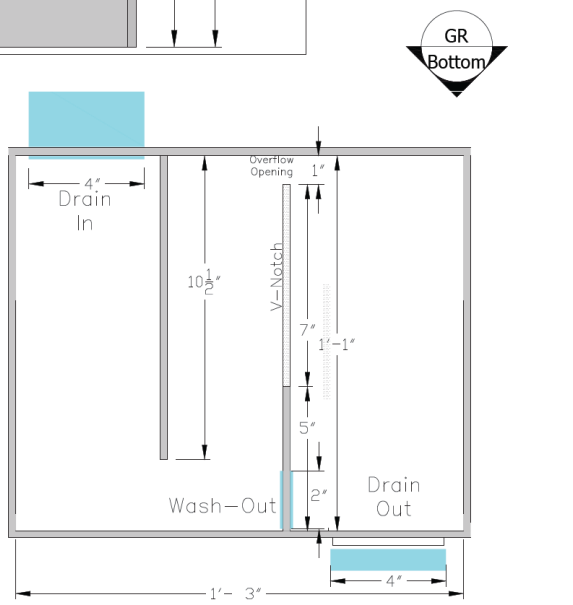

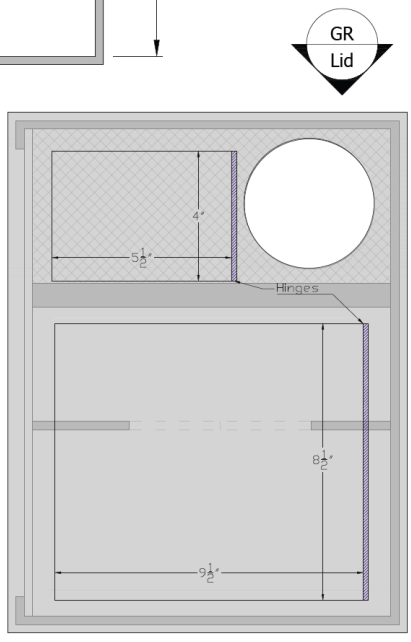

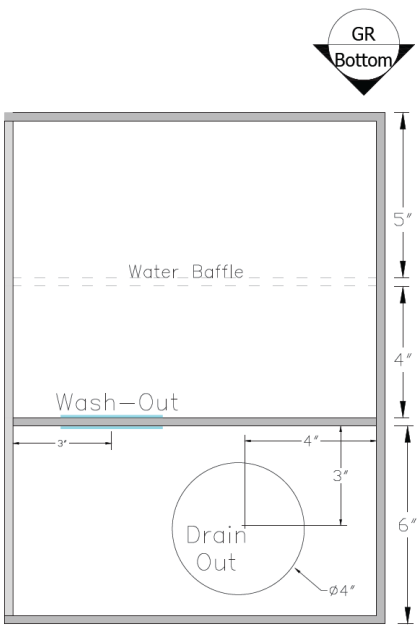

PV Roof Runoff Flume Details

Feb. 18, 2014

Contact: Scott Tjaden

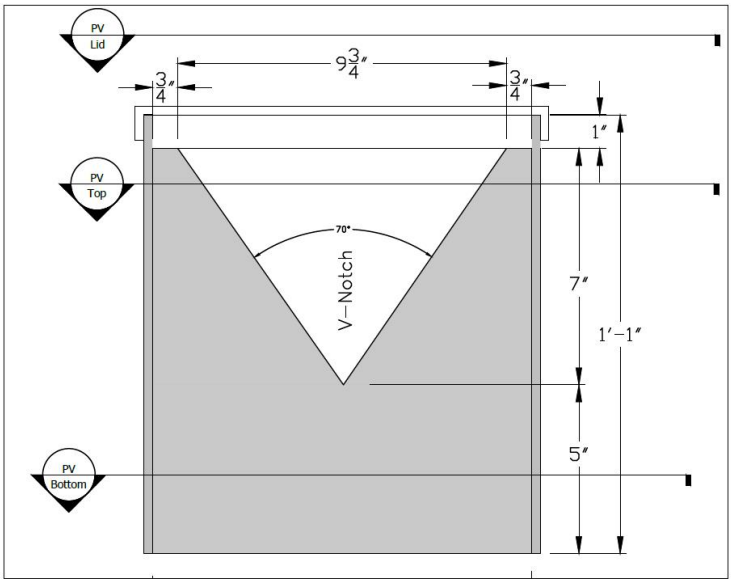

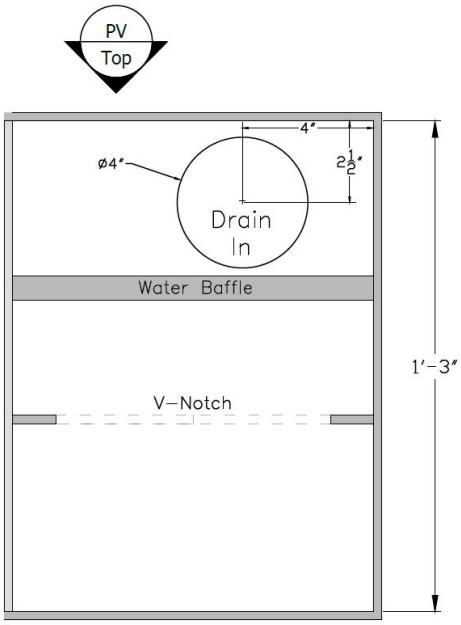

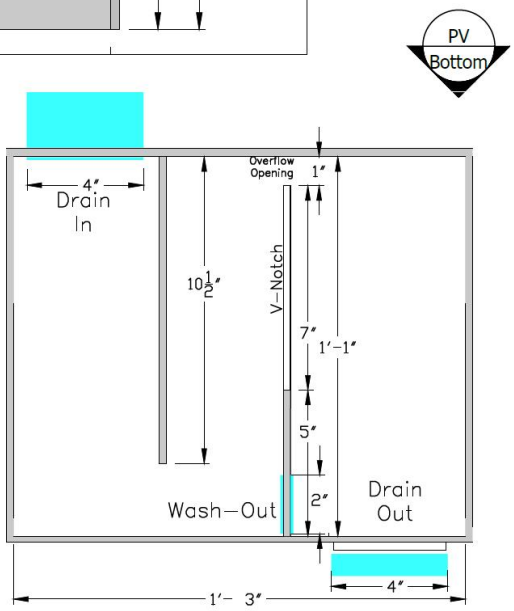

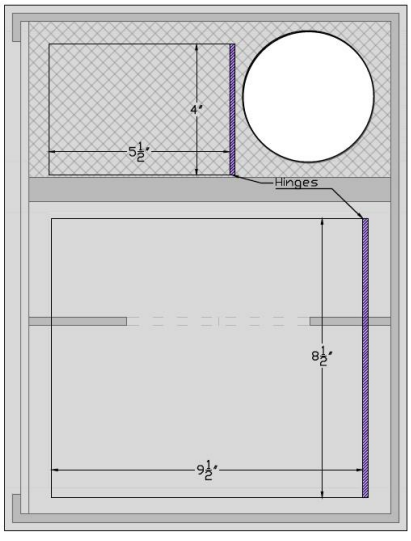

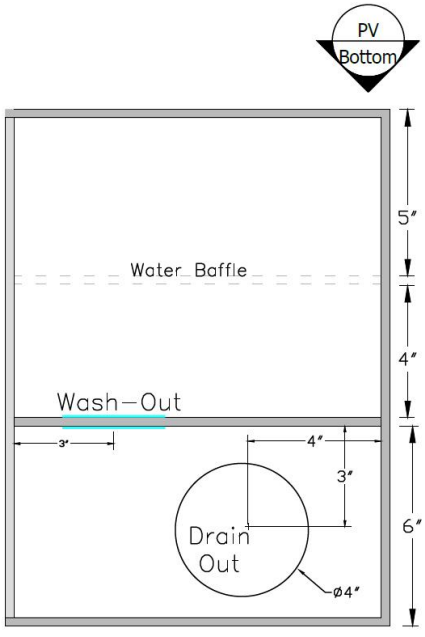

Appendix H: Flume Calibration

Flume Calibration Background:

This section provides the direct measurements made to calibrate the flume sensors installed on *WaterShed* to get runoff rates and volumes. The equations populated by the correlation were used as the calibration number in the weir equation (Equation 2).

Table H.1 Bathroom flume.

Sensor Height	Bathroom Sensor	Hose Flow
162.4	0.00924	0.0096
134.5	0.00191	0.00184
139.7	0.0028	0.00272
145.1	0.00393	0.00398
148.8	0.00484	0.00457
151.9	0.00578	0.00582
145.7	0.00239	0.0065
y = -2.8185 x + 0.0005		

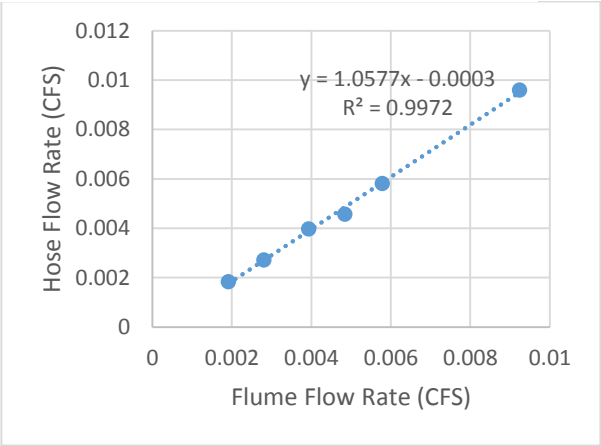

Figure H.1 Bathroom flume correlation and calibration curve.

Table H.2 PV flume calibration.

Sensor Height	PV Sensor	Hose Flow
181.5	0.012	0.0096
156.7	0.0039	0.00184
161.2	0.0048	0.00272
168.5	0.00654	0.00398
171.4	0.00764	0.00457
174.5	0.00872	0.00582
y = -2.8185 x + 0.0005		

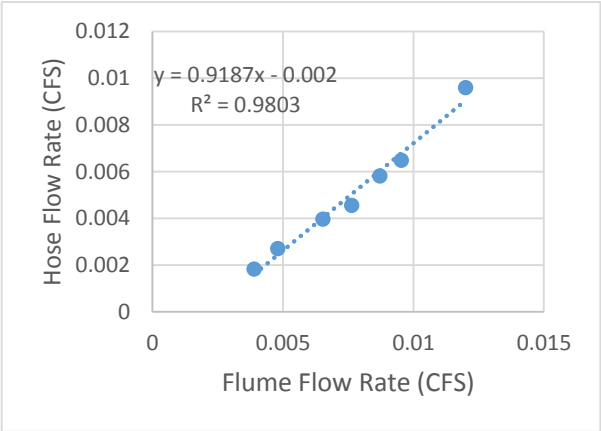

Figure H.2 PV flume correlation and calibration curve.

Table H.3 Green roof flume calibration.

Sensor Height	Green Roof Sensor	Hose Flow
168.7	-0.00238	0.009957
172.2	-0.00304	0.0096
145.8	-0.00037	0.00184
150.6	-0.00063	0.00272
156.6	-0.00109	0.00398
159.3	-0.00131	0.00457
y = -2.8185 x + 0.0005		

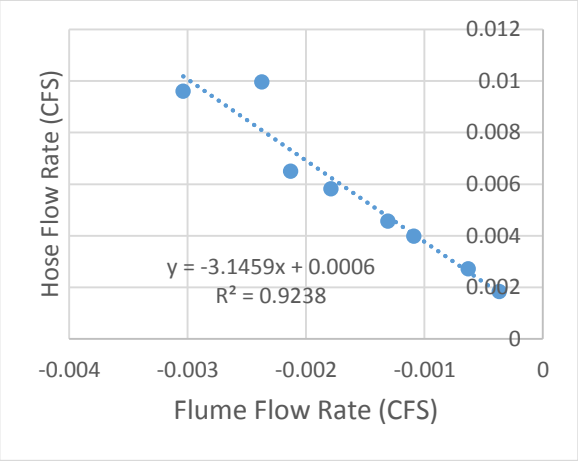

Figure H.3 Green roof flume correlation and calibration curve.

Figure H.4 Flow calibration using given flow rate from hose coming into the system.

Figure H.3 Flow calibration: Note V-notch and height of water, dependent on water flow rate coming into the system behind back baffle.

Appendix I: Individual Zone VWC vs. Percent Cover

VWC vs. Percent Cover

Background:

This section provides the individual correlations for each VWC sensor on the green roof. These VWC sensors are varied among the 3 zones, top, middle, and bottom (sensors depicted in Figure I.1).

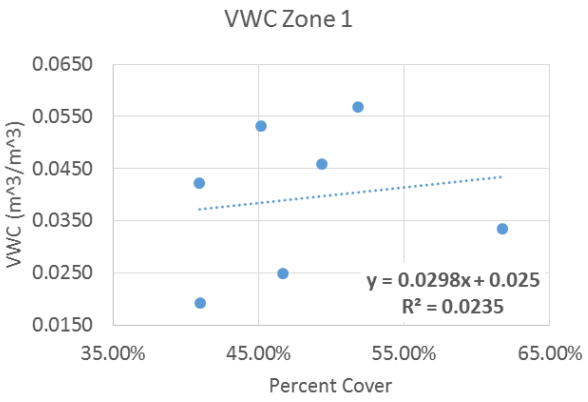

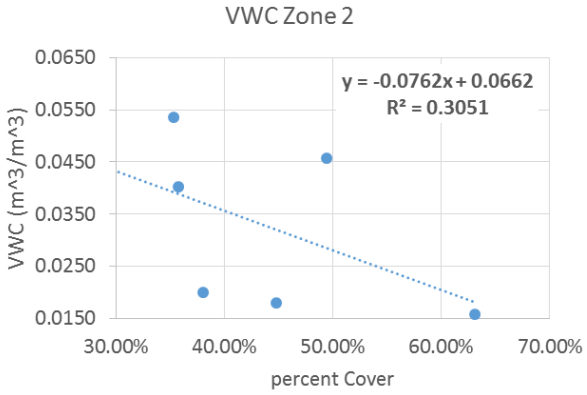

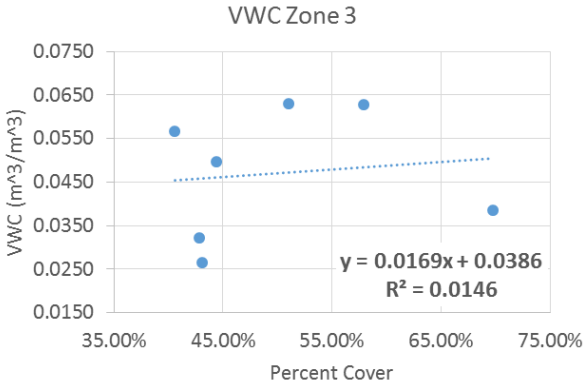

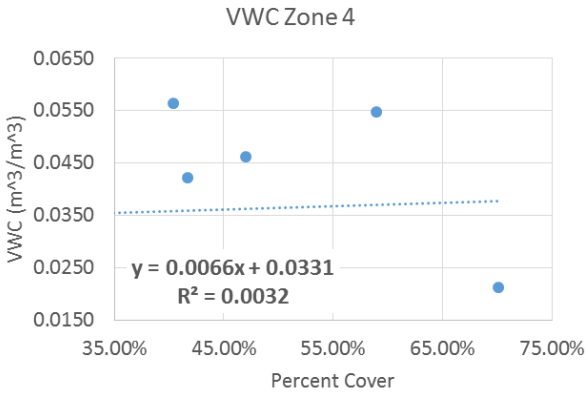

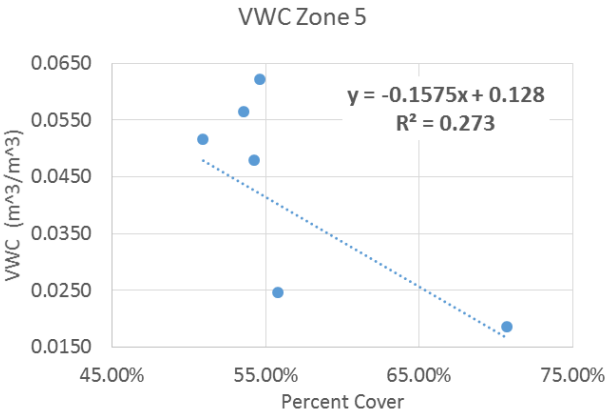

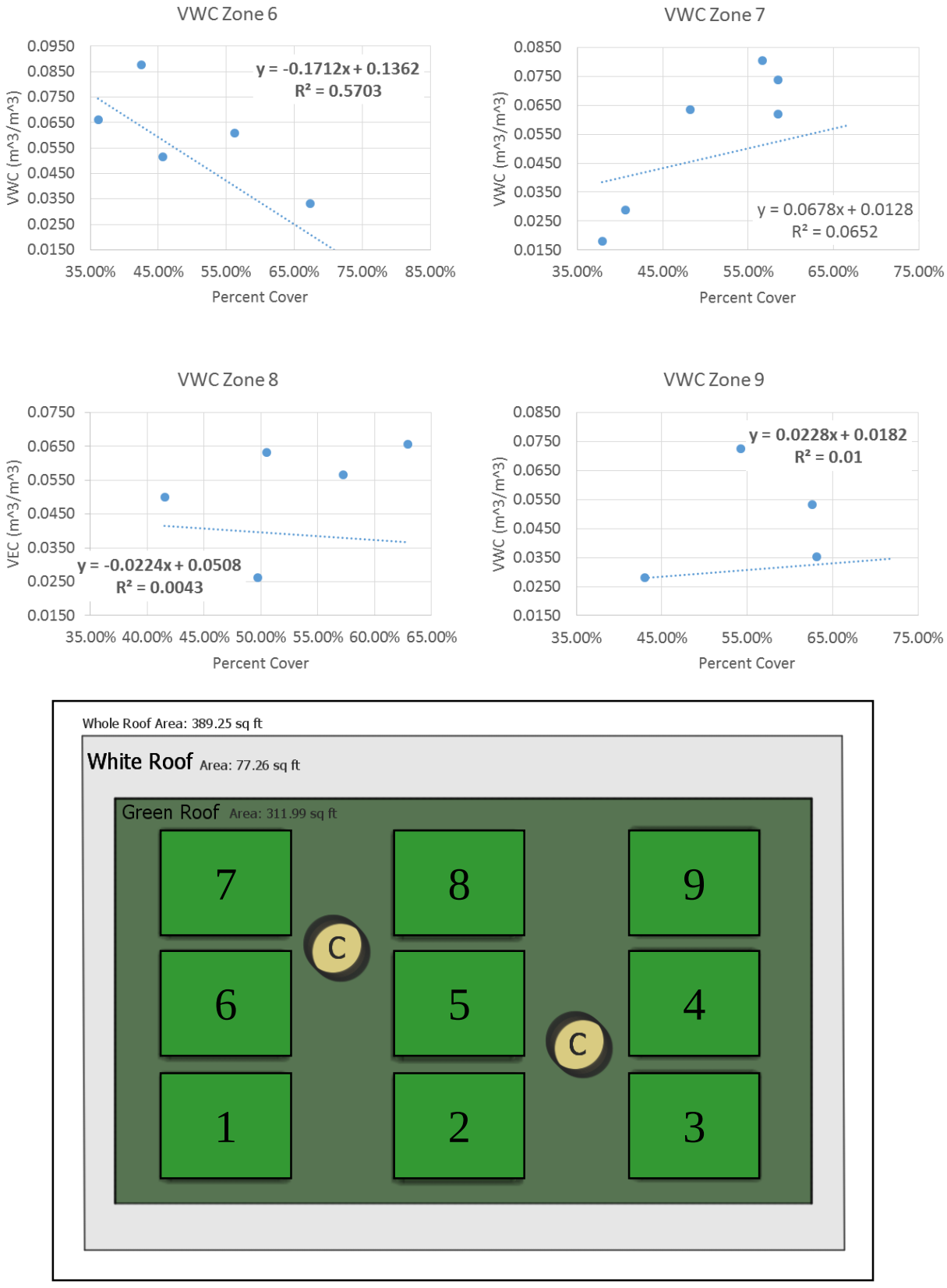

Figure I.1. Layout of VWC sensors, corresponding to the numbered zones

Appendix J: Energy Balance Graphs

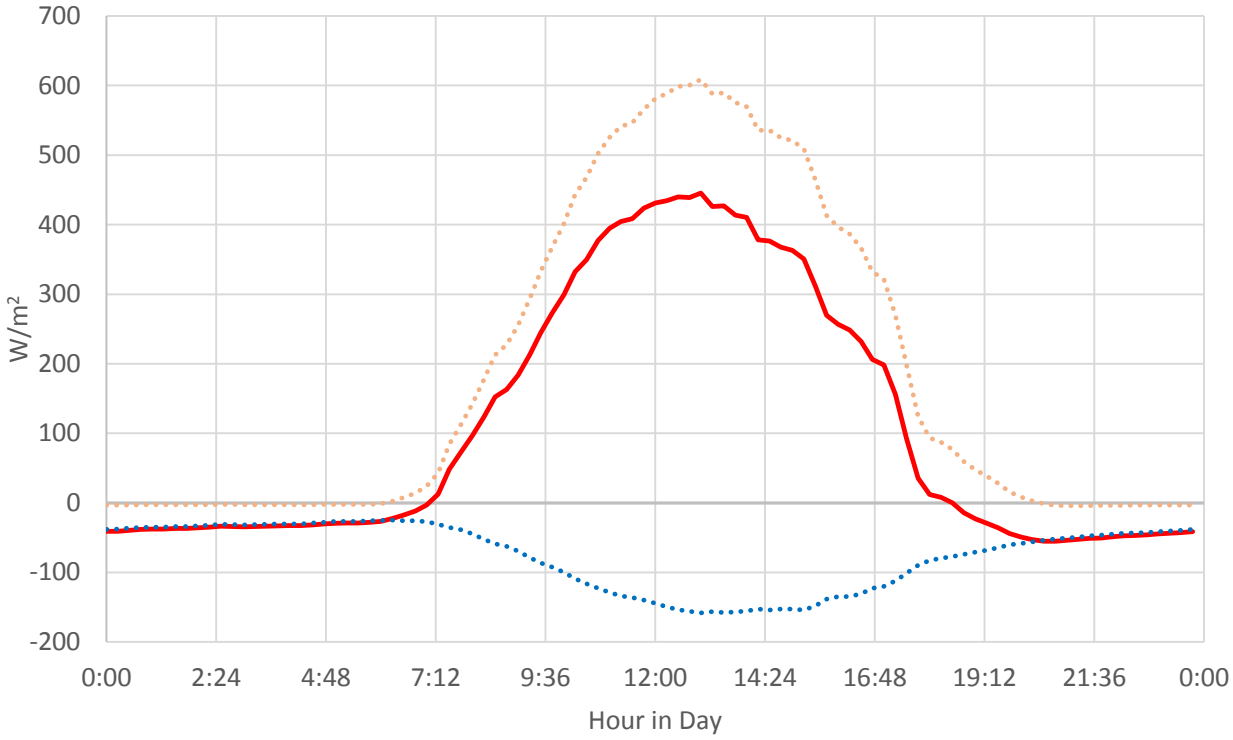

Figure J.1 Mean 24-hour net radiation variables: long and shortwave radiation.

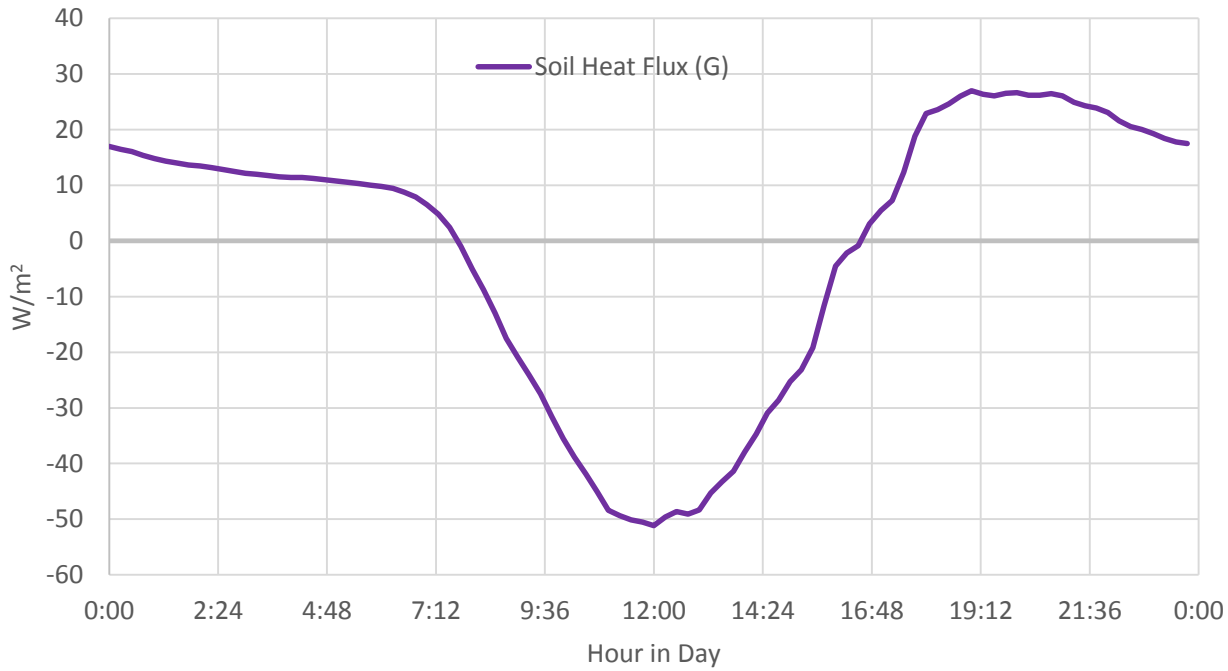

Figure J.2 Mean 24-hour soil heat flux: negative value represents energy gain, while positive represents energy loss

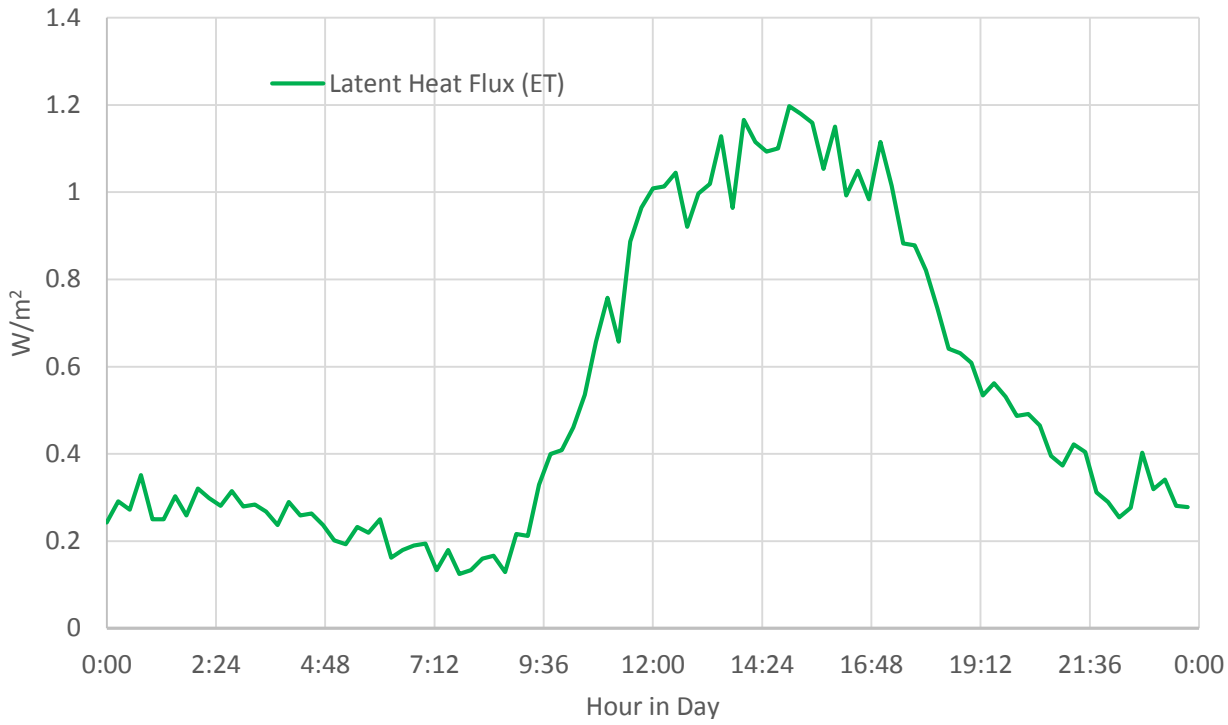

Figure J.3 Mean 24-hour latent heat data.

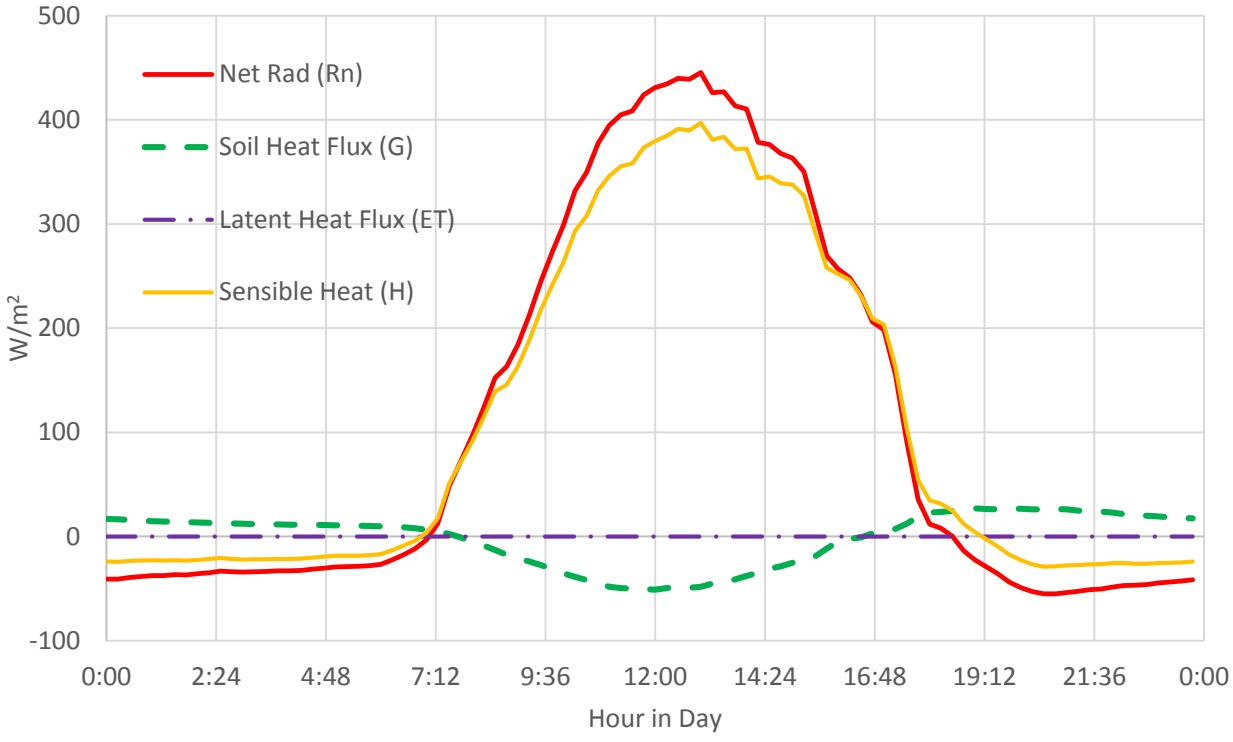

Figure J.4 Mean 24-hour overall energy balance.

Glossary

Blackwater: Effluent water draining from the toilet and kitchen sink within the house.

Evapotranspiration (ET): The vaporization of water through direct evaporation from wet surfaces, plus the release of water vapor by plants through leaf pores (transpiration). ("Climate and Weather Terms Glossary," 2014)

Field Capacity: Maximum amount of water stored within the substrate, held against the force of gravity.

Greywater: Effluent water draining from the dishwasher, bathroom sink, shower, and washing machine.

Leaf area index (LAI): A relationship to the plant's leaf coverage compared to visible ground.

Rain event: A period of precipitation determined by a rain gauge installed onsite, determining the start and stop times of an event occurring.

Roof runoff: Determined by the measured runoff in the flumes attached to the 3 downspouts on *WaterShed*, resulting in a flow rate from the respective roofs.

Runoff: Determined by the start and stop times of the rain gauge, while allowing a 6-hour window after the last precipitation event.

Stormwater: Water that accumulates due to precipitation.

Stormwater retention: The absorption of rainwater within the substrate of the green roof; substrates can absorb a finite amount of this liquid for use during times between rain events.

Bibliography

Allen, G.A., L.S. Pereria, D. Raes, and M. Smith. 1998. “Crop Evapotranspiration: Guidelines for Computing Corp Water Requirments.” *FAO Irrigation and Drainage Paper*, no. No. 56: 300. http://www.fao.org/docrep/x0490e/x0490e00.htm.

Carter, Timothy, and Colleen Butler. 2008. “Ecological Impacts of Replalcing Traditional Roofs with Green Roofs in Two Urban Areas.” *Cities and the Environment* 1 (2): 1–17.

Chesapeake Program, Bay. 2014. “Chesapeake Bay Executive Order.” http://executiveorder.chesapeakebay.net/.

“Climate and Weather Terms Glossary.” 2014. http://www.wrcc.dri.edu/ams/glossary.html#E.

Cook-Patton, Susan C, and Taryn L Bauerle. 2012. “Potential Benefits of Plant Diversity on Vegetated Roofs: A Literature Review.” *Journal of Environmental Management* 106 (October): 85–92. doi:10.1016/j.jenvman.2012.04.003.

Cushman, J C, and A M Borland. 2002. “Induction of Crassulacean Acid Metabolism by Water Limitation.” *Plant, Cell and the Environment* 25: 295–310.

D’Orazio, M., C. Di Perna, and E. Di Giuseppe. 2012. “Green Roof Yearly Performance: A Case Study in a Highly Insulated Building under Temperate Climate.” *Energy and Buildings* 55 (December): 439–51. doi:10.1016/j.enbuild.2012.09.009.

Davis, Allen P, William F Hunt, Robert G Traver, and Michael Clar. 2009. “Bioretention Technology : Overview of Current Practice and Future Needs.” *Journal of Environmental Engineering* 135, 3 (March): 109–18.

Durhman, Angela K, D Bradley Rowe, and Clayton L Rugh. 2006. “Effect of Watering Regimen on Chlorophyll Fluorescence and Growth of Selected Green Roof Plant Taxa” 41 (7): 1623–28.

Fangmeir, Delmar D. 2006. *Soil and Water Conservation Engineering, Fifth Edition*. New York: Thomas Delmar Learning.

Frevert, Richard K, and Glenn O Schwab. 1966. *Soil and Water Conservation Engineering*. New York: Wiley.

Gensler. 2011. *WaterShed At the University of Maryland, Inspired Innovation*.

Hathaway, A M, W F Hunt, and G D Jennings. 2008. “A Field Study of Green Roof Hydrologic and Water Quality Performance.” *American Society of Agricultural and Biological Engineers* 51 (1): 37–44.

He, Zhuangxiang, Allen P Davis, and F.ASCE. 2011. “Process Modeling of Storm-Water Flow in a Bioretention Cell.” *Journal of Irrigation and Drainage Enginering*, no. March: 121–32.

Hilten, Roger N. 2005. “An Alaysis of the Energetics and Stormwater Mediation Potential of Green Roofs.” University of Georgia.

Hucker, Delegate. 2012. *House Bill 987*. Maryland: House Bill. http://mgaleg.maryland.gov/2012rs/bills/hb/hb0987e.pdf.

Kubba, Sam. 2010. *LEED Practices, Certification, and Accreditation Handbook*. Burlington, MA: Butterworth-Heinemann/Elsevier.

Lovelli, S., M. Perniola, M. Arcieri, a.R. Rivelli, and T. Di Tommaso. 2008. “Water Use Assessment in Muskmelon by the Penman–Monteith ‘one-Step’ Approach.” *Agricultural Water Management* 95 (10): 1153–60. doi:10.1016/j.agwat.2008.04.013.

Marasco, Daniel E, Betsy N Hunter, Patricia J Culligan, Stuart R Ga, and Wade R Mcgillis. 2014. “Quantifying Evapotranspiration from Urban Green Roofs : A Comparison of Chamber Measurements with Commonly Used Predictive Methods.” *Environmental Science & Technology*, no. 78: 10273–81.

McLennan, Jason. 2008. *The Living Building Challenge: In Pursuit of Tree Sustainability in the Built Environment*. http://phipps.conservatory.org/_pdfs/general-resources/lbc-v1.3.pdf.

MDE. 2000. *Construction Specifications for Sand Filters, Bioretention and Open Chanels*.

Montgomery County Government. 2012. *Residential Energy Conservation Code*. Rockville, MD. http://permittingservices.montgomerycountymd.gov/DPS/pdf/ResidentialEnergyConservationCode.pdf.

Moore, P.R. 1975. “Measuring Flow of Small Streams: Use of a Portable Wier.” *The Journal of the Auckland Unversity Field Club* 21: 147–52.

Northern American Insitution, Manufacturers Association. 2014. “How Much Insulation Should Be Installed.” http://www.naima.org/insulation-knowledge-base/residential-home-insulation/how-much-insulation-should-be-installed.html.

Oberndorfer, Erica, Jeremy Lundholm, Brad Bass, Reid R. Coffman, Hitesh Doshi, Nigel Dunnett, Stuart Gaffin, Manfred Kohler, Karren K. Y. Liu, and Bradley Rowe. 2007. “Green Roofs as Urban Ecosystems : Ecological Structures , Functions , and Services.” *BioScience* 57 (November): 823–34.

Perini, Katia, Marc Ottelé, a.L.a. Fraaij, E.M. Haas, and Rossana Raiteri. 2011. “Vertical Greening Systems and the Effect on Air Flow and Temperature on the Building Envelope.” *Building and Environment* 46 (11): 2287–94. doi:10.1016/j.buildenv.2011.05.009.

"Rebates, Resources and Financial Incentives: Green Roofs." 2014 http://www.montgomerycountymd.gov/DEP/water/green-roofs.html.

Santamouris, M., C. Pavlou, P. Doukas, G. Mihalakakou, A. Synnefa, A. Hatzibiros, and P. Patargias. 2007. "Investigating and Analysing the Energy and Environmental Performance of an Experimental Green Roof System Installed in a Nursery School Building in Athens, Greece." *Energy* 32 (9): 1781–88. http://linkinghub.elsevier.com/retrieve/pii/S036054420600329X.

Starry, Olyssa. 2013. "The Comparative Effects of Three Sedum Species on Green Roof Stormwater Retention." University of Maryland.

Takebayashi, Hideki, and Masakazu Moriyama. 2007. "Surface Heat Budget on Green Roof and High Reflection Roof for Mitigation of Urban Heat Island." *Building and Environment* 42 (8): 2971–79. http://linkinghub.elsevier.com/retrieve/pii/S0360132306001752.

U.S. Department of the Interior, Bureau of Reclamation. 1997. *Water Measurement Manual : A Guide to Effective Water Measurement Practices for Better Water Management*.

U.S. Environmental Protection Agency, (EPA). 2014. "U.S. EPA and Department of Energy, Energy Star Website." www.energystar.gov.

Wolf, Derek, and Jeremy T. Lundholm. 2008. "Water Uptake in Green Roof Microcosms: Effects of Plant Species and Water Availability." *Ecological Engineering* 33 (2): 179–86. http://linkinghub.elsevier.com/retrieve/pii/S0925857408000438.

Zinzi, M., and S. Agnoli. 2012. "Cool and Green Roofs. An Energy and Comfort Comparison between Passive Cooling and Mitigation Urban Heat Island Techniques for Residential Buildings in the Mediterranean Region." *Energy and Buildings* 55 (December): 66–76. doi:10.1016/j.enbuild.2011.09.024.

Zotarelli, Lincoln, Michael D Dukes, Consuelo C Romero, Kati W Migliaccio, and T Kelly. *Step by Step Calculation of the Penman−Monteith Evapotranspiration (FAO−56 Method) 1*.